Elucidating the role of GBA in the pathology of Parkinson's disease using patient derived dopaminergic neurons differentiated from induced pluripotent stem cells.

A thesis submitted for the degree of

Doctor of Philosophy

Hilary Term 2014

by

Hugo José Ribeiro Fernandes

St Cross College

University of Oxford

Abstract

Heterozygous mutations in the glucocerebrosidase (*GBA*) gene represent the most common risk factor for Parkinson's disease (PD), a disease in which midbrain dopaminergic neurons are preferentially vulnerable. However, the mechanisms underlying this association are still unknown, mostly due to the lack of an appropriate model of study. In this thesis, we aimed at elucidating the role of heterozygous *GBA* mutations in PD using a specific human induced pluripotent stem cell (hiPSC)-based model of disease.

First we developed a protocol for the efficient differentiation of hiPSCs into dopaminergic cultures, and extensively characterized the derived dopaminergic neurons which expressed multiple midbrain relevant markers and produced dopamine. Next we screened a clinical cohort of PD patients to identify carriers of *GBA* mutations of interest. Using for the first time hiPSCs generated from PD patients heterozygous for a GBA mutation (together with idiopathic cases and control individuals) we were able to efficiently derive dopaminergic cultures and identify relevant disease mechanisms. Upon differentiation into dopaminergic neuronal cultures, we observed retention of mutant glucocerebrosidase (GCase) protein in the endoplasmic reticulum (ER) with no change in protein levels, leading to upregulation of ER stress machinery and resulting in increased autophagic demand. At the lysosomal level, we found a reduction of GCase activity in dopaminergic neuronal cultures, and the enlargement of the lysosomal compartment in identified dopaminergic neurons suggesting a decreased capacity for protein clearance.

Together, these perturbations of cellular homeostasis resulted in increased release of α-synuclein and could likely represent critical early cellular phenotypes of Parkinson's disease and explain the high risk of heterozygous *GBA* mutations for PD.

Declaration

Except where acknowledgment is made, all the work described in this thesis was performed by the author at the University of Oxford. The work reported in this thesis has not been submitted for any other degree in this or any other university or institute of learning.

Acknowledgements

I would like to express my gratitude to a vast number of people that direct and indirectly contributed to the development of this thesis.

In first place I would like to thank Richard for giving me the opportunity to join his lab to carry out the work described in this thesis. For being a supportive and concerned supervisor, and for having to deal with my occasional negativity towards science. An important word of appreciation also goes to Francis for his helpful advice and to all our collaborators mentioned in this thesis that were involved with this work. In particular, I am very thankful to Sally Cowley for her constant advice and help with the stem cell work and to Jane Vowles for being so patient and incredibly helpful in the generation of iPS cells.

I would like to thank also all my lab colleagues (some of which I can now call friends) that have demonstrated enormous patience and kindness to deal with me over the last 4 years. I have no idea how they did it without going crazy. Without wanting to go too much into detail there are a few people that I need to highlight. Liz, for all her support, guidance, advice and interesting chats over the last four years. All her patience and kindness is difficult to put into words. To Brent, for being an incredibly helpful and friendly person, and for all the support and advice over the last three years, inside and outside the lab. To Lara and Tara for all their massive support and guidance since the first day I joined the lab – I know I can be a bit annoying sometimes. To Matt and Max for the interesting and entertaining conversations we have had, mostly around pubs. Of course, to all the pubs in Oxford which helped in this adventure.

Many people from outside the lab also had an important role over the last four years, all of which will remain nameless. I had the pleasure of meeting really interesting people, some of which I now can call friends, and to keep in touch with some good old important friends. You all know who you are, and you also made this possible. To all the friends that although being far away, are always very important and present.

A very special thanks to Alison for being such an amazing person, friend and companion over the last few years. You surely helped me immeasurably in this adventure and I am a very lucky person to have you by my side.

To my family for their support. Although these last few years haven't been easy, without you I wouldn't be here. Thanks for everything.

To the friends I haven't seen for a long time, and to those for whom it is now too late to see again. I am sorry I wasn't around more often.

Publications and Presentations arising from this work

Hartfield, E.M., Yamasaki-Mann, M., **Ribeiro Fernandes, H.J**., Vowles, J., James, W.S., Cowley, S.A., and Wade-Martins, R. (2014) Physiological Characterisation of Human iPS-Derived Dopaminergic Neurons. *PLoS ONE*, 9, e87388

Hartfield, E.M, **Fernandes H.J.R.**, Vowles J., Cowley, S.A. and Wade-Martins, R. (2012) Cellular Reprogramming: a new approach to modelling Parkinson's disease. *Biochemical Society Transactions*, 40, 1152-7

Ribeiro Fernandes, H., Hartfield, E.M. Badger J., Vowles, J., Evetts, S., Talbot, K., Hu, M, Cowley, S., James, W., Wade-Martins, R. Dual proteostasis effect of heterozygous GBA mutations in Parkinson's Disease, using human induced pluripotent stem cells derived from patients. *(Selected oral presentation) Society for Neuroscience Meeting 2013. San Diego, USA, 2013*

Ribeiro Fernandes, H., Hartfield, E.M., Vowles, J., Evetts, S. Vargas-Caballero M., Talbot, K., James, W., Hu, M, Cowley, S., Wade-Martins, R. Elucidating the role of lysosomal dysfunction in the pathology of Parkinson's disease using human adult induced pluripotent stem cells derived from patients. *(Selected poster presentation) International Society for Stem Cell Research, 10th Annual Meeting, Yokohama, Japan, 2012*

Ribeiro Fernandes, H., Hartfield, E.M., Vowles, J., Evetts, S., Talbot, K., Hu, M, Cowley, S., James, W., Wade-Martins, R. Elucidating the role of GBA in the pathology of Parkinson's disease using human induced pluripotent stem cells derived from patients. *(Selected oral presentation) Society for Neuroscience Meeting 2011. Washington DC, USA, 2011*

Table of contents

Contents

List of Figures

List of Tables

Para ti Zé, Padrinho,

Enjoy every moment as it was your last,

because one day it will.

Chapter 1

Main Introduction

1.1 Parkinson's disease

Parkinson's disease (PD) was first described by James Parkinson in 1817 in the monograph entitled *An Essay of the Shaking Palsy* and is the second most common neurodegenerative disease after Alzheimer's disease (AD) in the developed world. Although PD can be diagnosed at any age, the prevalence increases in proportion with the population age. While 3% of cases are diagnosed under the age of 50 years (Shulman et al., 2011), a rapid increase in PD incidence is observed after the age of 60 years (Benito-León et al., 1998). The disease affects over 1% of the population over the age of 60 years, which rises to nearly 5% by the age of 85 years (Shulman et al., 2011) and affects over 10 million people worldwide (Badger et al., 2014). PD is a chronic, slow progressive disorder, with a median age of onset of 60 years, and a mean duration of 15 years from diagnosis to death (Katzenschlager et al., 2008; Lees et al., 2009). The prevalence and impact of PD in society is expected to rise dramatically, due to the increased aging of populations, and the number of patients worldwide expected to double by 2030 (Surguchov, 2013). PD is also associated with a high economic impact on public services and on individuals, with the costs increasing with age and disease severity, related to direct medical treatment, hospitalisations and nursing home

care (Kowal et al., 2013). In 2003, the costs associated with PD were estimated to be almost £600,000,000 per annum in the UK alone (Findley et al., 2003), while in 2010 the economic burden of PD in the US exceeded $14 billion (Kowal et al., 2013). Altogether, future generations will urge for better diagnostic tools and novel therapies to halt PD progression.

1.1.1 Pathology of PD

PD is mainly characterized by progressive degeneration of dopaminergic neurons in the substantia nigra pars compacta (SNpc) in addition to the accumulation of intracytoplasmic protein aggregate inclusions, named Lewy bodies (LB), in the remaining surviving neurons. α-synuclein is the main component of these protein aggregates and has also been found accumulated within neuronal processes in deposits named Lewy neurites (Dickson et al., 2009). SNpc dopaminergic neurons project mainly to the striatum (Shulman et al., 2011). Loss of these neurons ultimately results in the loss of dopaminergic innervation in the striatum, leading to reduced striatal dopamine levels. The defining clinical manifestations of PD are motor including tremor, muscle rigidity, and bradykinesia (slowed movement). These manifestations are directly linked to dopaminergic striatal loss and develop when dopamine concentrations in the motor region of the striatum (posterior putamen) falls below 60–70% of normal levels (Rodriguez-Oroz et al., 2009).

Recent findings have shown that PD has a broader impact on patients' quality of life, including non-motor symptoms such as hyposmia, sleep disturbances, constipation, depression and anxiety (Rodriguez-Oroz et al., 2009), some of which may develop up to 20 years prior to motor manifestations (Shulman et al., 2011). Furthermore, α-synuclein pathology has been found to be widespread throughout the peripheral and central nervous systems, affecting multiple non-dopaminergic cell types (Braak et al., 2003). These

observations resulted in a proposed staging system for the progression of PD, Braak staging, with a caudal to rostral progression of pathology (Braak et al., 2003). The Braak staging model supports the relevance of earlier non-motor PD symptoms in early disease, since the pattern of Braak earlier stages matches with the proposed pre-motor symptoms: olfactory structures (hyposmia), enteric nervous system (constipation) and lower brainstem (sleep disturbances) (Braak et al., 2003; Shulman et al., 2011). In addition, α-synuclein pathology in the SNpc is only observed at the later stages, stage 3 onwards. Furthermore, all vulnerable brain regions in this system are closely interconnected, supporting this proposed propagation of the pathologic process underlying PD (Braak and Del Tredici, 2008). Overall, PD diagnosis is only currently possible at a late stage of the disease when over 60% of dopaminergic neurons in the SNpc are already lost (Shulman et al., 2011). This increases the pressure for the development of better diagnostic tools, to allow neuroprotective therapies to be applied at earlier stages of the disease progression.

1.1.2 Treatment options for PD

Despite extensive research over the last decades, efficient treatment strategies are still lacking for PD. Available therapies are primarily symptomatic, and there is yet no treatment to stop or reverse the disease progression, rendering PD an irreversible and incurable disease (Corti et al., 2011). Introduced in the late 1960s, levodopa (L-DOPA), a dopamine precursor capable of crossing the blood brain barrier, is still the most effective treatment for the management of PD symptoms. Although motor symptoms respond well to this dopamine replacement therapy during initial treatment (Shulman et al., 2011), prolonged usage leads to the development of further motor impairments and dyskinesias (Bekris et al., 2010). Other available pharmacological methods include dopamine agonists that mimic the action of

dopamine, anticholinergics that help control tremor and rigidity, amantadine which increases dopamine release and blocks dopamine reuptake, and monoamine oxidase inhibitors to prevent dopamine degradation (Bekris et al., 2010; Surguchov, 2013). In more advanced stages of disease and in cases of severe motor complications, surgical methods can be employed, mostly via deep-brain stimulation (DBS) of the subthalamic nucleus (Shulman et al., 2011). However, DBS is not suitable for all patients, and the disease will continue to progress. Overall, although some available therapies prolong life expectancy and help symptoms management, none has yet efficiently been show to halt or reverse the degenerative progression of PD (Shulman et al., 2011).

1.1.3 The etiology of PD

The etiology of PD is unknown and likely multifactorial, resulting from complex interactions between genetic and environmental factors (Lesage and Brice, 2009). In the past, environmental factors were believed to be the predominant cause of PD. In the early 1980s, accidental intravenous injection of 1-methyl-4-phenyl-1,2,3,6-tetrahydropyridine (MPTP) by drug addicts who believed they were injecting 1-Methyl-4-phenyl-4-propionoxypiperidine (MPPP), resulted in the development of acute Parkinsonian symptoms in those individuals (Langston et al., 1983). Since then, other environmental factors have been explored, including exposure to high levels of the pesticides rotenone (Betarbet et al., 2000) and paraquat (Manning-Bog et al., 2002), which have been shown to induce Parkinsonian symptoms in rodents, and to increase the rate of α-synuclein fibril formation (Uversky et al., 2001b). Epidemiological studies have also supported the hypothesis that pesticide exposure is associated with a higher risk of PD as there is a higher incidence of PD in agricultural areas (Di Monte, 2003). Metals such as iron and copper have also been proposed as environmental

toxic factors for PD. This was based on the discovery of accumulation of these metals in PD brains (Dexter et al., 1989) and their ability to interact with and to modify α-synuclein (Uversky et al., 2001a), the major component of Lewy bodies. Furthermore, the effects of pesticides and metals were also proposed to be synergistic (Uversky et al., 2002). However, likely due to the complexity of these analyses, no definitive conclusions have been made to confirm these environmental factors as triggers of PD (Di Monte, 2003; Corti et al., 2011). Inversely, other environmental factors have been proposed to be protective for PD. Cigarette smoking has been proposed to be inversely associated with the risk of developing PD (Sugita et al., 2001; Tanner et al., 2002), while caffeine consumption was also associated with a lower incidence of PD (Ross et al.; Ascherio et al., 2001; Liu et al., 2012b; Palacios et al., 2012).

Although historically considered an idiopathic disease without genetic origin, this view has changed dramatically over the last two decades due to major developments and successes in genetic analysis. Massive technological developments in this field led to a better understanding of the underlying causes of several human pathologies. In the case of PD this led to the identification of multiple Mendelian loci, a common high-risk variant and many common low-risk variants (Hardy, 2010). Despite this, PD, like many other adult neurodegenerative diseases, is still viewed primarily as idiopathic. However, since the motor phenotypes in both genetic and idiopathic PD patients can be almost identical, many argue that they likely share common mechanisms and pathways of the disease, justifying the focus of research on less common genetic forms of PD (Hirsch et al., 2013). In fact, so far, the understanding of the molecular mechanisms involved in PD pathogenesis has been elucidated mostly by the study of monogenic forms of the disease.

Previous epidemiological methods have underestimated the genetic contribution to PD, with genetic variants initially identified in PD patients with a familial history now being

detected in apparently idiopathic PD cases (Shulman et al., 2011). Some epidemiological studies suggest that 10–30% of PD patients have a family history of the disease, and report a two- to seven-fold increase in the relative risk of PD in first-degree relatives (Bekris et al., 2010; Shulman et al., 2011). Others suggest that approximately half of the attributable risk of PD has already been identified by genetic analysis, and that this risk proportion is likely to increase with future genetic developments (Hardy, 2010).

1.1.3.1 Evidence for a genetic basis in PD

Overall, multiple genes have been implicated in PD (Table 1). Initial linkage analysis in families with multiple affected individuals have led to the identification of highly penetrant but rare genetic variants associated with PD, while modern genome-wide association studies (GWAS) performed in large numbers of PD patients have discovered more common susceptibility loci (of modest effect) involved in PD. Lastly, next-generation sequencing technologies are currently offering new insights into the identification of further genetic variability that might be relevant for PD.

Table 1 Summary of genes proposed to be associated with PD.

Gene	Gene Locus	Inheritance	Identification
SNCA	4q21	AD	Linkage Analysis/GWAS
LRRK2	12q12	AD	Linkage Analysis/GWAS
Parkin	6q25-q27	AR	Linkage Analysis
PINK1	1p36	AR	Linkage Analysis
DJ-1	1p36	AR	Linkage Analysis
ATP13A2	1p36	AR	Linkage Analysis
PLA2G6	22q13	AR	Linkage Analysis
FBX07	22q12-q13	AR	Linkage Analysis
EIF4G1	3q27	AD	Linkage Analysis
GIGYF2	2q37	AD	Linkage Analysis
GBA	1q21	Risk	GWAS/Candidate Gene
MAPT	17q21	Risk	GWAS
HLA-DRA	6q21	Risk	GWAS
GAK	4p16	Risk	GWAS
RAB7L1	1q32	Risk	GWAS
BST1	4p15	Risk	GWAS
VPS35	16q11	AD	Next-generation sequencing
DNAJC13	3q22.1	AR	Next-generation sequencing
DNAJC6	1p31	AR	Next-generation sequencing
SYNJ1	21q22	AR	Next-generation sequencing
HTRA2	2p12	AD	Candidate gene approach
UCHL1	4p14	AD	Candidate gene approach
NPC1	18q11	AD	Candidate gene approach
SMPD1	11p15	AD	Candidate gene approach

SNCA was the first gene associated with PD when in 1997 linkage analysis studies found the A53T mutation present in PD families (Polymeropoulos, 1997). Since then, multiple other *SNCA* mutations were identified in families with PD: A30P (Krüger et al., 1998), E46K (Zarranz et al., 2004), G51D (Kiely et al., 2013; Lesage et al., 2013), H50Q and A53E (Pasanen et al., 2014), but A53T remains the most frequent among these. Despite high penetrance, SNCA mutations are still a rare dominant form of PD. In addition to point mutations, duplications and triplication of the *SNCA* gene were later found in PD families (Wirdefeldt et al., 2011), with increased gene dosage usually associated with earlier onset and increased severity of disease. The central role of *SNCA* in PD, although largely still unknown, was also highlighted by the finding that the α-synuclein protein is the major component of LBs, the hallmark of PD (Spillantini et al., 1997).

Linkage analyses also led to the identification of leucine-rich repeat kinase 2 (*LRRK2*) mutations in PD families, which represents the most common PD gene known, with a mutation frequency that ranges from 2% up to 40% across different populations (Klein and Westenberger, 2012). Multiple mutations in *LRRK2* have been reported, of which the G2019S mutation is the most frequent, with an age-dependent penetrance of 28 % at age 59, 51 % at age 69 and 74 % at age 79 (Healy et al., 2008).

First identified in 1998 in Japanese patients with juvenile Parkinsonism (Kitada et al., 1998), *Parkin* mutations represent the most common known cause of early onset Parkinson's disease (EOPD), being present in 67% of PD patients with onset before age 20 (Periquet et al., 2003). The second most common causes of EOPD are *PINK1* mutations (Valente et al., 2004) and *DJ-1* mutations (Bonifati et al., 2003), with the latter being a more rare cause of juvenile PD. Mutations in the *ATP13A2* gene also result in a familial form of PD with a juvenile onset of atypical parkinsonism (Ramirez et al., 2006). Further studies resulted in the identification of other genes associated with PD including *PLA2G6* (Paisan-Ruiz et al.,

2009), *FBX07* (Di Fonzo et al., 2009), *EIF4G1* (Chartier-Harlin et al., 2011) and *GIGYF2* (Lautier et al., 2008).

More recently, GWAS studies have dramatically increased our ability to identify more genetic variations that contribute to the risk of developing PD. The first large PD GWAS studies were published in 2009 (Satake et al., 2009; Simón-Sánchez et al., 2009) and confirmed *SNCA* as an important susceptibility locus for idiopathic PD, highlighting the central role of α-synuclein in PD. In addition, *LRRK2* was also among the highest association signals together with *MAPT*, a gene previously found associated with increased risk for PD (Zabetian et al., 2007). Out of the remaining targets reaching genome-wide significance, the most recent and complete GWAS meta-analysis highlights mutations in the *GBA* gene, with an odds ratio (OR) of 3.51 (Lill et al., 2012), being classified has a high-risk locus for PD (Hardy, 2010). Other relevant risk factors for PD resulting from multiple GWAS studies included *HLA-DRA* (Hamza et al., 2010), *GAK-DGKQ* (Pankratz et al., 2009), *RAB7L1* (Simón-Sánchez et al., 2009) and *BST1* (Satake et al., 2009). In addition, next-generation sequencing analysis have been offering further insights into the genetics of PD through the identification of *VPS35* (Vilariño-Güell et al., 2011; Zimprich et al., 2011), *DNAJC13* (Vilariño-Güell et al., 2014), *DNAJC6* (Edvardson et al., 2012), *SYNJ1* (Krebs et al., 2013) (Quadri et al., 2013). Using a candidate gene approach, others study have also highlighted the relevance of *HTRA2* (Strauss et al., 2005), *UCHL1* (Leroy et al., 1998), *NPC1*(Kluenemann et al., 2013), *SMPD1* (Gan-Or et al., 2013) with previous studies demonstrating the association of GBA with PD (Neudorfer et al., 1996; Aharon-Peretz et al., 2004).

1.2 *GBA*

The *GBA* gene was mapped to chromosome 1q21 (Ginns et al., 1985) and comprises 11 exons and 10 introns, to make the gene 7.6 kilobases (kb) in length (Hruska et al., 2008). The complete genomic sequence of *GBA* was first published in 1989 (Horowitz et al., 1989). A highly homologous pseudogene (*GBAP*) lies 16 kb downstream of *GBA* with a 96% sequence identity to *GBA* and a size of 5.7 kb. The difference in length is caused by large deletions within several introns (introns 2, 4, 6 and 7) of *Alu* sequences in *GBAP* (Hruska et al., 2008). The high degree of sequence identity and the presence of this pseudogene at the same locus as the active gene can lead to recombination events and has contributed to the origin of mutations in *GBA* (Eyal et al., 1990; Winfield et al., 1997). *GBAP* is present only in primates and is absent in other species (Martinez-Arias, 2001). Although the presence of the pseudogene can potentially complicate sequencing and mutation identification, the identification of a 55-bp deletion in exon 9 of *GBAP* (Horowitz et al., 1989) offers a useful distinction that can be used for molecular analysis. The 85 kb region surrounding *GBA* is highly gene rich, encompassing a total of seven genes and two pseudogenes (Sidransky et al., 2009) and recombination events in this region are relatively frequent (Tayebi et al., 2003a).

GBA encodes the protein β-glucocerebrosidase (GCase), a lysosomal enzyme which metabolises the glycolipid glucosylceramide (GlcCer) into glucose and ceramide. Ceramide is the main precursor for various sphingolipids (SLs), which are membrane lipids containing a ceramide backbone (Kitatani et al., 2009). SLs are ubiquitous components of cellular membranes and play important roles in membrane structure and signaling events crucial for cellular responses (Futerman and Riezman, 2005; Giussani et al., 2014). SLs are important for cell viability in mammalian cells (Hanada et al., 1992), while ceramide has been suggested to play important roles in the regulation of stress response pathways (Hannun,

1996). One of the main sources of ceramide comes from the degradation of complex glycosphingolipids in acidic compartments of the cell, such as the lysosome, via the formation of GlcCer (Kitatani et al., 2009). Therefore, the efficiency of GlcCer conversion by GCase is crucial for maintaining the balance of cellular ceramide levels that will determine the regulation of multiple signaling pathways. GlcCer, which is obtained through a reaction catalysed by GlcCer synthase (GCS), is essential for cell viability. GlcCer is the precursor of lactosylcermide (LacCer) and complex glycosphingolipids, and is a component of cell membranes and lipid rafts (Messner and Cabot, 2010). GlcCer has also been shown to regulate membrane trafficking along the endocytic pathway (Sillence et al., 2002). Altered levels of GlcCer have also been found in patients with diabetes, cardiovascular disease, skin disorders and cancer (Messner and Cabot, 2010). Furthermore, GlcCer has been found to accumulate in the lysosomes in multiple models of Gaucher's disease (GD), the most common lysosomal storage disorder where GCase activity is highly reduced (explored in detail in Chapter 5)

The first *GBA* mutations were identified in the late 1980s and correspond to the alleles c.1448T>C (L444P) (Tsuji et al., 1987) and c.1226A>G (N370S) (Tsuji et al., 1988) (Figure 1)**.** To date, around 300 different mutations have been identified across *GBA*, including point mutations, frameshift mutations, recombinant alleles and splice-site alterations (Lopez and Sidransky, 2012). However, L444P and N370S are still the most common mutations found in most populations (Hruska et al., 2008). For the L444P mutation, a single base change at residue 444 in exon 10 results in the substitution of a leucine with a proline, and creates a new cleavage site for the *NciI* endonuclease. This alteration was initially predicted to impair the alpha helical structure of the protein in this region, ultimately causing reduced enzymatic activity (Tsuji et al., 1987). For the N370S mutation, a single base mutation in exon 9 results

in the substitution of the amino acid asparagine for serine at position 370, which was also predicted to affect the structure of GCase (Tsuji et al., 1988).

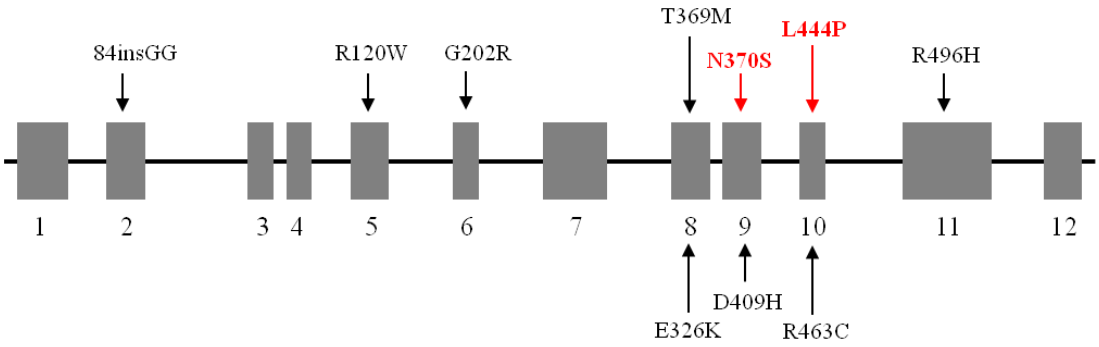

Figure 1 Schematic for *GBA* structure and distribution of most common mutations.

The X-ray structure of GCase was first reported in 2003 (Dvir et al., 2003) and showed to be composed of 3 domains (Figure 2). Domain I (residues 1–27 and 383–414) is composed of one three-stranded, anti-parallel β-sheet flanked by a perpendicular amino-terminal strand and a loop. Domain II (residues 30-75 and 431-497) consists of closely associated β-sheets forming an independent Ig-like domain. Domain III (residues 76-381 and 416-430) consists of a $(\beta/\alpha)_8$ TIM barrel and contains the catalytic site (Dvir et al., 2003). The N370 residue was confirmed to be located in the catalytic domain but far away from the active site (active-site residues E235 and E340), in the interface of domain II and III and was therefore proposed not to directly interfere with catalysis. It was later demonstrated that the N370S mutation results in a catalytically-deficient enzyme with unaffected stability but reduced flexibility (Wei et al., 2011). The exact mechanism by which it results in impaired activity is still unclear. Residue 444 was found located in the hydrophobic core of domain II which can disrupt the hydrophobic core, causing a conformational change and leading to altered folding in this domain. Domain II can have a crucial structural and regulatory function for GCase (Dvir et al., 2003). Other less common mutations were also identified with the

potential to either also affect the structure of the protein or even directly affect the catalytic activity when occurring near the active site. The establishment of the structure of GCase was crucial for the development of structure-based small molecules which target misfolded GCase and improve structural stabilisation, which ultimately increases enzyme activity.

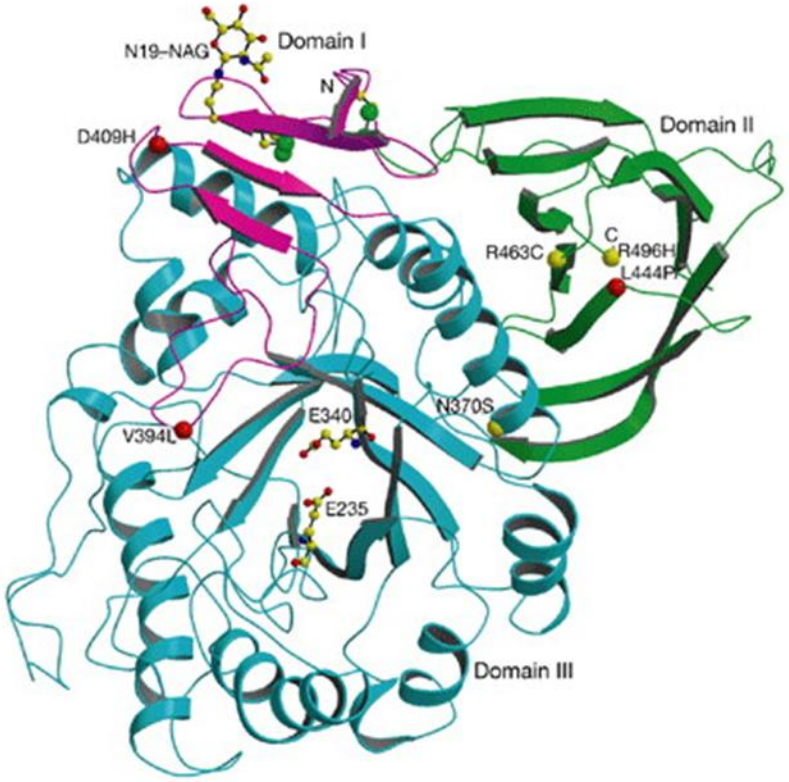

Figure 2 Simplified X-ray structure for GCase. Domain I is represented in magenta with the glycosylation site at N19 shown. The Ig-like domain II is shown in green. The catalytic domain III is shown in blue with representation of the active-site residues E235 and E340. Some of the most common mutations found in GCase are represented as balls. Adapted from (Dvir et al., 2003)

As with all lysosomal enzymes, GCase is synthesised on endoplasmic reticulum-(ER) bound polyribosomes (Erickson et al., 1985). After entering the ER, the enzyme undergoes N-linked glycosylation on four asparagine residues, namely N19, N59, N146 and N270 (Hruska et al., 2008) (Figure 3A). While in the ER the enzyme is subjected to ER quality control (ERQC) and if folded correctly the enzyme is shuttled to the Golgi apparatus where it undergoes further modifications before being trafficked to the lysosome (Bendikov-Bar et al., 2013) (Figure 3B). Misfolded proteins result in the activation of an ERQC stress response known as the unfolded protein response (UPR), which might be relevant for the pathogenesis of *GBA* mutations (Ron and Horowitz, 2005).

A

ARPCIPKSFGYSSVVCVC**N**ATYCDSFDPPTFPALGTFSRYESTRSGRRMELSMGPI
QA**N**HTGTGLLLTLQPEQKFQKVKGFGGAMTDAAALNILALSPPAQNLLLKSYFSEE
GIGYNIIRVPMASCDFSIRTYTYADTPDDFQLH**N**FSLPEEDTKLKIPLIHRALQLAQRP
VSLLASPWTSPTWLKTNGAVNGKGSLKGQPGDIYHQTWARYFVKFLDAYAEHKLQ
FWAVTAENEPSAGLLSGYPFQCLGFTPEHQRDFIARDLGPTLA**N**STHHNVRLLMLD
DQRLLLPHWAKVVLTDPEAAKYVHGIAVHWYLDFLAPAKATLGETHRLFPNTMLFAS
EACVGSKFWEQSVRLGSWDRGMQYSHSIITNLLYHVVGWTDWNLALNPEGGPNW
VRNFVDSPIIVDITKDTFYKQPMFYHLGHFSKFIPEGSQRVGLVASQKNDLDAVALM
HPDGSAVVVVLNRSSKDVPLTIKDPAVGFLETISPGYSIHTYLWRRQ

B

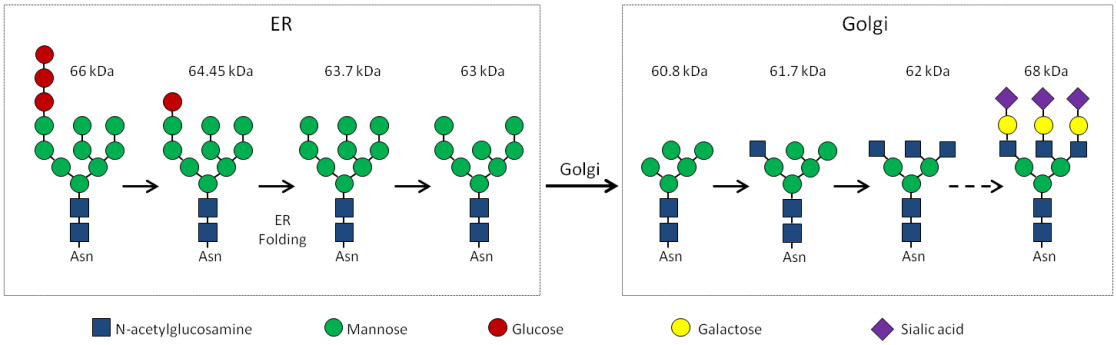

Figure 3 N-linked glycosylation of GCase. A) Sequence of the 497 residues of mature GCase with N-linked glycosylation sites show in red. B) Schematic representation of GCase processing within the ER and Golgi before targeting to the lysosomes. Predicted molecular mass of the different GCase forms are shown. Adapted from (Bendikov-Bar et al., 2013)

1.2.1 *GBA* and GD

Gaucher's Disease (GD) is the most common lysosomal storage disorder worldwide and is caused by either homozygous or compound heterozygous mutations in *GBA* (Swan and Saunders-Pullman, 2013). GD is an autosomal recessive disorder primarily affecting macrophages, and results in the enlargement of the lysosomal compartment owing to lipid accumulation (Sidransky and Lopez, 2012). The cellular specificity towards macrophages is yet unknown. Patients with GD usually manifest with anaemia, hepatosplenomegaly, bone disease, thrombocytopenia and, in some cases, neurological involvement (Sidransky et al., 2009). Homozygous *GBA* mutations are the most common mutation found in GD, usually, although variably, resulting in dramatic reductions of GCase protein levels and enzyme activity, ultimately causing accumulation of lipid substrates, particularly GlcCer. GD has been divided in three types based on clinical presentations, with the existence of both non-neuronopathic (type 1) and neuronopathic (type 2 and 3) forms of the disease (Hruska et al., 2008). An updated list of the main characteristics of each type of GD can be found in Table 2.

Table 2 Main characteristics of different types of GD (adapted from (Lopez and Sidransky, 2012)**).**

Type 1	Non-neuronopathic Pan-ethnic disorder (more common in Ashkenazi Jews) Clinically heterogeneous, with wide-ranging severity May present from childhood to adulthood, remain asymptomatic or go undiagnosed Bone disease is a common cause of morbidity Treated with enzyme replacement therapy MIM# 230800
Type 2	Acute neuronopathic Rare, pan-ethnic disorder Can present prenatally, at birth, or in the first year of life Rapidly progressive neurological deterioration Enzyme replacement therapy does not reverse or stop neurological progression Fatal within days to years MIM# 230900
Type 3	Chronic neuronopathic Multiple different phenotypes with variable longevity Typically manifests during childhood or early adulthood Patients usually develop horizontal saccadic eye movements Some patients develop myoclonic epilepsy Associated with learning disabilities in some patients MIM# 231000

1.2.2 *GBA* and PD

Initial clinical genetic studies of patients with GD led to the unexpected identification of heterozygous *GBA* mutations as a common genetic risk factor for PD. Almost two decades ago, GD patients were found to develop progressive Parkinsonian motor features and dementia (Neudorfer et al., 1996), which was later confirmed in several other reports (Machaczka et al., 1999; Tayebi et al., 2001; Bembi et al., 2003). In addition, post-mortem brain samples from GD patients were confirmed to have advanced LB pathology, the pathological hallmark of PD, which in some cases was predominantly found in the midbrain (Goker-Alpan et al., 2010). Furthermore, relatives of GD patients were found to have an increased incidence of PD and to carry *GBA* mutations (Tayebi et al., 2003b; Goker-Alpan et al., 2004; Halperin et al., 2006). These observations paved the way for an increased interest in understanding the basis of the association between *GBA*, PD and GD. Since then, several studies (described in detail in Chapter 4) have confirmed a high frequency of heterozygous *GBA* mutation in PD patients, which can be found in up to 31% of individuals in some populations (Sidransky et al., 2009).

Over time, this unexpected association resulted in the classification of *GBA* mutations as the most common known genetic risk factor for PD to date (Neumann et al., 2009). Many of these studies also confirmed that these patients are usually associated with an earlier onset of PD when compared to those without *GBA* mutations. Clinical features were also evaluated in PD patients carrying *GBA* mutations and were found predominantly in men. These patients develop more frequent hallucinations, together with symptoms of cognitive dysfunction or dementia (Neumann et al., 2009; Brockmann et al., 2011; Setó-Salvia et al., 2012), and with a higher frequency of olfactory dysfunction also being reported (Goker-Alpan et al., 2008). At a pathological level, PD patients carrying heterozygous *GBA* mutations have been show to present typical α-synuclein-immunoreactive LBs (Neumann et al., 2009), with GCase being

detected in 33–90% of LBs compared to 10% in patients without *GBA* mutations (Goker-Alpan et al., 2010). The reason why or how the presence of GCase in LBs contributes to pathogenesis is still unknown (Sidransky and Lopez, 2012).

1.2.3 *GBA* and related Lewy Body disorders

The finding of increased frequencies of heterozygous *GBA* mutations in PD led to similar studies in other related LB disorders. The first study completed in cases of dementia with Lewy bodies (DLB) confirmed the presence of heterozygous *GBA* mutations in 23% of patients (Goker-Alpan et al., 2006). A subsequent study, limited to the screening of N370S and L444P mutations, found positive heterozygous *GBA* mutations in 3.5% of DLB patients compared to a frequency of 0.4% in controls (Mata et al., 2008), while a later study identified *GBA* mutations in 6% of DLB cases (Farrer et al., 2009). A study by (Clark et al., 2009) further confirmed this observation by reporting heterozygous *GBA* mutations in 28% of 95 DLB patients, and further extending these results into AD, where 10% of cases were also found positive for *GBA* heterozygous mutations. Another study identified *GBA* mutations in 7.6% of DLB cases (Tsuang et al., 2012), while more recently a large multicentre analysis was completed on 721 DLB patients from 11 centres around the globe, confirming a significant association between *GBA* mutation carrier status and DLB with an odds ratio (OR) of 8.28 (Nalls et al., 2013), which is higher than reported for PD (OR of 5.43) (Sidransky et al., 2009). On the other hand, the association of *GBA* mutations with multiple systems atrophy (MSA), another PD related LB disorder, was not confirmed in multiple studies completed to date (Goker-Alpan et al., 2006; Segarane et al., 2009; Jamrozik et al., 2010). In PD and DLB, α-synuclein accumulates in neurons, while in MSA, α-synuclein deposits mostly in oligodendroglia as glial cytoplasmic inclusions rather than LB. This distinct

association with *GBA* mutations has been proposed to be relevant for disease pathogenesis (Halliday et al., 2011).

1.3. Autophagic lysosomal dysfunction in PD

Increasing evidence suggest that dysfunction of the autophagic-lysosomal pathway (ALP) might be an important mechanism in the pathogenesis of PD (Tofaris, 2012). Lysosomes are dynamic organelles central in the degradation of multiple intracellular components across different pathways, including endocytosis, autophagy, and other cellular trafficking pathways (Lübke et al., 2009). Through autophagic degradation, lysosomes are capable of metabolizing intracellular proteins, especially aggregated proteins such as α-synuclein, and to clear old or damaged cellular organelles such as mitochondria (via mitophagy) (Tofaris, 2012). The autophagic pathway is highly relevant in the pathology of PD since the two most studied pathways suggested to be pathogenic for PD are related to mitochondrial dysfunction and α-synuclein aggregation (Dehay et al., 2013). Evidence for the former come from studies involving PD genes associated with an earlier onset of disease (*PARKIN*, *PINK1* and *DJ-1*) and PD-related mitochondrial toxins (MPTP). Evidence for the latter come from studies on *SNCA* and *LRRK2* mutations and the broad confirmation of α-synuclein aggregation leading to the formation of LBs and Lewy neurites in PD, suggesting a defective protein handling pathway in the pathogenesis of PD.

1.3.1 Evidence from idiopathic cases and toxin models

Neurons are sensitive to altered protein degradation pathways, likely due to their long lived post-mitotic nature. Therefore, constitutive autophagy is central to neuronal survival (Dehay et al., 2013). Post-mortem analysis of brain tissue from idiopathic PD patients

supports a role for ALP dysregulation in the disease process. Ultrastructural analysis of dopaminergic neurons in the SNpc of PD patients revealed autophagic impairments including increased number of autophagic vacuoles (Anglade et al., 1997), with further evidence of autophagic dysfunction found in midbrain tissue from PD patients (Zhu et al., 2003). Another study showed reduced immunoreactivity for multiple lysosomal markers in PD nigral neurons, which was greater in neurons containing α-synuclein inclusions (Chu et al., 2009). Reduced levels of lysosomal-associated membrane protein (LAMP-2A) and heat shock chaprone-70 (HSC70) were also found in the SNpc of PD patients, which was shown to reflect a decreased cellular lysosomal fraction, together with elevated microtubule-associated protein 1A/1B-light chain 3B (LC3B-II) levels, suggesting increased autophagy (Alvarez-Erviti et al., 2010). Reduced LAMP1 levels and increased LC3B-II were also found in post-mortem SNpc PD samples by Western blot and immunohistochemistry, suggesting cellular lysosomal depletion and autophagosome accumulation in the brain of PD patients (Dehay et al., 2010).

Autophagic dysregulation has also been observed in toxin models of PD. In a MPTP mouse model of PD, autophagosomes were found to accumulate in neurons in response to decreased number of lysosomes in dopaminergic neurons, which was replicated in a dopaminergic cell line (BE(2)-M17 neuroblastoma cells) intoxicated with MPP+, the active metabolite of MPTP. Restoring lysosomal levels (by inducing autophagy or enhancing lysosomal biogenesis) in these models resulted in increased autophagosome (AP) clearance and attenuated cell death (Dehay et al., 2010). Increased levels of autophagosomes were also observed in other cellular models intoxicated with Parkinson-related neurotoxins, including rotenone (Chen et al., 2007) 6-OHDA (Dagda et al., 2008) and MPP+ (Zhu et al., 2007). On the other hand, in a chronic MPTP-treated rhesus monkey, cathepsin D, a major lysosomal enzyme involved in α-synuclein degradation (Sevlever et al., 2008), was found upregulated in

the caudate nucleus and was associated with increased number of lysosomes (Yelamanchili et al., 2011).

1.3.2 Evidence from traditional PD-associated genes

PD genetic evidences also support a primary role for lysosomal-autophagic impairments in the pathological process of PD. In fact, the commonly associated PD genes *LRRK2*, *SNCA*, *PINK1*, *Parkin* and *DJ1* all encode proteins involved in lysosome-related pathways, most notably via autophagy and mitophagy (Gan-Or et al., 2013). Mutations in *PINK1*, *Parkin* and *DJ-1* all lead to loss-of-function of proteins that are involved in the degradation of damaged mitochondria via mitophagy (Geisler et al., 2010; Thomas et al., 2011). Parkin is a ubiquitin ligase that is part of the ubiquitin proteasome system (UPS) and catalyses the addition of ubiquitin molecules to lysine residues on damaged proteins targeted for degradation (Abou-Sleiman et al., 2006b). *Parkin* mutations are believed to result in the loss of ubiquitin-ligase activity resulting in impaired substrate clearance and consequent aggregation of damaged and misfolded proteins (Shimura et al., 2000). Parkin was also shown to be recruited to damaged mitochondria and to mediate their elimination via mitophagy (Narendra et al., 2008), therefore regulating mitochondrial homeostasis. PINK1 is a serine/threonine kinase that localises to mitochondria (Qi et al., 2011) and the cytosol, and has been found in LBs from idiopathic and *PINK1*-mutant PD patients (Gandhi et al., 2006). PINK1 is recruited from the cytosol to damaged mitochondria triggering their degradation via autophagy (Narendra et al., 2010), and interacts with Parkin to regulate mitochondrial function (Clark et al., 2006; Park et al., 2006). PINK1 was shown to control mitochondrial translocation of Parkin to mitochondria (Kim et al., 2008; Vives-Bauza et al., 2010), therefore being an essential upstream initiator of Parkin-mediated mitophagy (Geisler et al., 2010).

PINK1 silencing was also shown to induce autophagy in multiple cellular models (Qi et al., 2011). *DJ-1* codes for a protein of uncertain function that has been shown to be translocated to mitochondria under conditions of oxidative stress (Canet-Avilés et al., 2004). DJ-1-deficient BE(2)-M17 dopaminergic cells were shown to acquire multiple mitochondrial abnormalities suggesting that DJ-1 may also play a role in maintaining mitochondria function together with Parkin and PINK1 (Thomas et al., 2011).

LRRK2 is a large, multi-domain protein with serine/threonine kinase activity whose function is yet unclear. Loss of *LRRK2* was shown to impair the ALP and result in α-synuclein accumulation in *LRRK2* KO mice (Tong et al., 2010). The *LRRK2*-G2019S mutation, commonly found associated with PD, has increased kinase activity and was shown to result in abnormal accumulation of swollen lysosomes in primary rat neuronal cultures (MacLeod et al., 2006) and increased number of autophagic vacuoles suggestive of autophagic activation in dopaminergic-like cells (Plowey et al., 2008). LRRK2 was shown to localise to endosomal-autophagic organelles in cultured HEK293 human cells with the R1441C mutation, resulting in impaired autophagy characterised by the accumulation of autophagic vesicles containing undegraded cargo (Alegre-Abarrategui et al., 2009). In the human brain, LRRK2 was also found localised to the endosomal-lysosomal compartment which was enlarged in patients with LB pathology (Higashi et al., 2009). Furthemore, iPSC-derived dopaminergic neurons obtained from PD patients carrying the G2019S *LRRK2* mutation were found to accumulate autophagic vacuoles indicating an autophagic deficit that was proposed to occur at the level of autophagosome clearance (Sánchez-Danés et al., 2012). Pharmacological inhibition of LRRK2 kinase activity was also shown to stimulate autophagy (Manzoni et al., 2013), while *LRRK2* overexpression in differentiated HEK293 cells resulted in a kinase activity dependent increase in autophagy induction (Gómez-Suaga et al., 2012).

Recently it was also shown that wild type (WT) LRRK2 can be degraded in the lysosomes via chaperone-mediated autophagy (CMA) while this degradation was compromised in *LRRK2* mutant G2019S neuroblastoma cells (Orenstein et al., 2013). Finally endogenous LRRK2 was found to be associated with autophagosome membranes and proposed to have a functional role in regulating autophagy in a mouse cell line (Schapansky et al., 2014).

Mutations in *SNCA* associated with PD (A53T, A30P and E46K) are thought to be pathogenic by a toxic gain-of-function mechanism likely resulting from misfolding and aggregation of the α-synuclein protein into oligomers or fibrils (Tofaris, 2012). The lysosome is a major site for α-synuclein degradation via macroautophagy (Webb et al., 2003) and CMA (Cuervo et al., 2004). Deficiencies in these cellular degradation pathways can lead to α-synuclein aggregation and result in LB formation, the pathological hallmark of PD. In both mice and *C. elegans* models, deficiency of the lysosomal enzyme Cathepsin D resulted in extensive α-synuclein accumulation which was reverted by Cathepsin D overexpression. This was also shown to be neuroprotective against α-synuclein induced cell (Qiao et al., 2008; Cullen et al., 2009). The reciprocal connection has also been shown by the observation that α-synuclein overexpression impairs autophagy in mammalian cell lines and in transgenic mice, with *post-mortem* brain samples from patients with dementia with LBs also reported to have altered levels of autophagic markers (Xilouri et al., 2009; Yu et al., 2009b; Crews et al., 2010; Winslow et al., 2010). Further work has also suggested that α-synuclein interferes with endosomal trafficking (Soper et al., 2011) and inhibits mitochondrial membrane fusion, leading to mitochondrial fragmentation (Kamp et al., 2010). Pathogenic α-synuclein mutants and post-translation α-synuclein modifications have also been shown to block lysosomal degradation and result in accumulation of α-synuclein and other substrates (Cuervo et al.,

2004; Martinez-Vicente et al., 2008). Overall, a new central role for the autophagic/lysosomal pathway in the pathogenesis of PD is clearly emerging (Tofaris, 2012).

1.3.3 Evidence from other PD-related genes

The AL degradation pathway may be central to multiple pathological processes determined by several PD-related mutations (Corti et al., 2011). In fact, multiple other PD-related genes have been mechanistically linked to ALP, the best examples coming from the genes encoding the lysosomal enzymes, *GBA* and *ATP13A2*.

Homozygous *GBA* mutations (leading to GD) result in a massive reduction of GCase lysosomal activity, which has been shown in mouse primary cortical neurons and in GD-induced pluripotent stem cell (iPSC)-derived neurons. In these models, decreased lysosomal degradation resulted in α-synuclein accumulation and toxicity by aggregation-dependent mechanisms (Mazzulli et al., 2011). Analyses of multiple GD mouse models also confirmed the accumulation of α-synuclein and ubiquitin aggregates in several brain regions (Xu et al., 2011). Further studies showed that overexpression of mutant GCase in a rodent midbrain cell line resulted in α-synuclein accumulation (Cullen et al., 2011). In a GD mouse model (homozygous *GBA*-D409V), increased GCase levels (using recombinant viral vectors expressing human *GBA*) caused a reduction in α-synuclein protein levels (Sardi et al., 2011). Finally, a feedback mechanism by which α-synuclein could inhibit GCase trafficking and result in reduced GCase lysosomal activity has also been demonstrated, highlighting the relevance of *GBA* in the pathology of PD (Mazzulli et al., 2011). Other studies have tried to replicate the enzymatic deficits caused by homozygous *GBA* mutations in cell and rodent models by inhibiting GCase activity using conduritol-β-epoxide (CBE). In one study, CBE was shown to result in increased protein levels of α-synuclein in SH-SY5Y neuroblastoma

cells, and within the SNpc of mice (Manning-Boğ et al., 2009). However, another study reports no alterations in the levels of α-synuclein in SH-SY5Y cells or rat primary neuronal cultures after CBE treatment, and therefore the relationship between α-synuclein and GCase is still unclear (Dermentzaki et al., 2013). A putative role for *GBA* in mitochondrial function and mitophagy was recently proposed in a study showing that GCase inhibiton by CBE could cause abnormalities in mitochondrial function and induce oxidative stress (Cleeter et al., 2013). However it is important to note that all these observations were made in the context of homozygous *GBA* mutations, while *GBA* mutations linked to PD are usually present only in the context of a single allelic mutation (Dehay et al., 2013).

How heterozygous *GBA* mutations could impair the ALP in the context of PD is still unknown, mostly due to the lack of appropriate models. Addressing this question was the main goal of the work developed in this thesis. No *in vitro* human model is yet available to investigate this question, and the only *GBA* heterozygous mutant models published are limited to human post-mortem studies and a mouse model with an uncommon mutation (D409V). Post-mortem brain analyses of heterozygous *GBA* mutants have shown that GCase is found in LBs (although variable) suggesting a possible contribution towards the process of α-synuclein aggregation (Goker-Alpan et al., 2010; Choi et al., 2011), reduced GCase enzymatic activity (Choi et al., 2011; Gegg et al., 2012), α-synuclein aggregation and increased autophagy (Gegg et al., 2012). A mouse model carrying the D409V *GBA* mutation, which has not been reported in either PD or GD patients, also shows reduced GCase activity with evidence of α-synuclein aggregation (Sardi et al., 2011). For the broader context of PD, the relevance of *GBA* has also been highlighted by a few studies in idiopathic patients. A first study reported a ~50% reduction in GCase activity and ~40% reduction of GCase protein levels in idiopathic PD brains (Mazzulli et al., 2011), with a later study reporting a 33% reduction of activity and ~35% reduced GCase protein levels in the SNpc of idiopathic PD

brains (Gegg et al., 2012). Furthermore, analysis of cerebrospinal fluid (CSF) from idiopathic PD patients revealed a 35% reduction in GCase activity compared to controls, with reductions in activity also observed for other lysosomal hydrolases (Balducci et al., 2007). Altogether, these results once again highlight the relevance of *GBA* in the pathology of PD, via the ALP, which can possibly be expanded further into the common idiopathic PD cases.

GBA is part of a recently identified and expanding group of lysosomal enzymes in which mutations have been associated with PD, including *SMPD1* (Foo et al., 2013; Gan-Or et al., 2013), *ATP13A2* (Ramirez et al., 2006) and *NPC1* (Kluenemann et al., 2013) as described earlier. *SMPD1* codes for a lysosomal acid sphingomyelinase that converts sphingomyelin to ceramide and mutations in this gene lead to Niemann-Pick disease type A. This disease results in a massive reduction of lysosomal enzyme activity, leading to substrate accumulation (Gan-Or et al., 2013). *NPC1* mutations result in Niemann-Pick disease type C and are believed to affect the correct folding of the protein leading to degradation via the proteasome and consequent loss-of-function of the NPC1 enzyme that is found in the lysosomes/late endosomes (Zampieri et al., 2012). This enzyme mediates intracellular lipid trafficking, and loss-of-function results in the accumulation of cholesterol and other lipids in the lysosomal compartment (Ordonez et al., 2012). *NPC1* knockdown in hESC-derived neurons was show to result in activation of autophagy and also in blockage of autophagy progression, which ultimately resulted in defective mitochondria clearance. Notably, this was also shown to be dependent, at least partly, on cholesterol trafficking and to affect neurons preferentially (Ordonez et al., 2012). In addition to the links with mitophagy, human neuropathological cases of NPC1 were reported to have α-synuclein-positive LB aggregations, which in some cases could be found in the SNpc (Saito et al., 2004; Chiba et al., 2014).

The *ATP13A2* gene codes for a neuronal-specific P-type lysosomal ATPase involved in lysosomal acidification and mutations in this gene underlie an autosomal recessive form of early-onset Parkinsonism (Ramirez et al., 2006). These mutations likely result in ER retention of truncated mutant proteins that become degraded by the proteasome, resulting in reduced targeting to the lysosome leading to loss-of-function (Ugolino et al., 2011). *ATP13A2* mutations have been shown to induce several lysosomal disturbances in fibroblasts, including impaired lysosomal acidification, decreased proteolytic processing of lysosomal enzymes, reduced degradation of lysosomal substrates and reduced clearance of autophagosomes (Dehay et al., 2012; Tresse et al., 2012). Similar results were obtained when *ATP13A2* was knocked down in BE(2)-M17 dopaminergic cells and mouse primary cortical neurons (Tresse et al., 2012), was associated with cell death, and could be reversed when *ATP13A2* levels were restored by overexpressing WT *ATP13A2* (Dehay, 2012). Importantly, levels of *ATP13A2* were also found to be reduced in dopaminergic neurons from the SNpc of idiopathic PD patients (Dehay et al., 2012). The identification of LBs with α-synuclein pathology in PD patients with *ATP13A2* mutations has not yet been reported, likely due to the lack of histopathological information (Dehay et al., 2013). However, immunohistochemical analyses have shown that over 90% of LBs found in the SNpc of idiopathic patients contain the ATP13A2 protein (Dehay et al., 2012). Furthermore, knockdown of the *ATP13A2* ortholog in *Caenorhabditis elegans* (*C. elegans*) was shown to enhance α-synuclein misfolding, while expression of *ATP13A2* was shown to rescue α-synuclein-induced dopaminergic degeneration in both *C. elegans* and rat primary midbrain neuronal models (Gitler et al., 2009). Impaired lysosomal proteolysis in *ATP13A2* mutant human PD fibroblasts or *ATP13A2*-defective human dopaminergic BE(2)-M17 neuroblastoma cells and mouse primary cortical neurons also resulted in α-synuclein accumulation (Dehay et al., 2012; Tresse et al., 2012). Conversely, α-synuclein silencing attenuates cell toxicity in

ATP13A2-depleted mouse primary cortical neurons (Tresse et al., 2012). It has been suggested that *ATP13A2* induced toxicity may be, at least in part, a result of impaired lysosomal degradation of α-synuclein (Tresse et al., 2012). *ATP13A2* loss-of-function has also been shown to impair mitochondrial function in *ATP13A2*-mutated human fibroblasts (Grünewald et al., 2012) and *ATP13A2*-depleted cell models (Gusdon et al., 2012) which was proposed to be associated with impaired mitophagy (Gusdon et al., 2012). Altogether, these observations suggest a pathogenic role for *ATP13A2* deficiency in lysosomal function and overall cell viability (Dehay et al., 2013). Furthermore, VPS35 and RAB7L1 code for proteins involved in endosomal-lysosomal trafficking (Zimprich et al., 2011; MacLeod et al., 2013), with *DNAJC6* and *SYNJ1* encoding proteins with roles in synaptic vesicles recycling (Bonifati, 2014), which have been together proposed to possible interfere with the lysosomal pathway (Trinh and Farrer, 2013).

1.4 Heterozygous mutations in PD

Autosomal recessive disorders are usually characterised by the absence of a pathological phenotype in heterozygous carriers, and only manifests in the presence of homozygous or compound heterozygous alleles. However, there are multiple lines of evidence in the literature that challenges this limited perspective, as discussed below, indicating that recessive alleles can also confer a risk for disease in the heterozygous state.

In the case of PD, one of the first pieces of evidence came from a large screen for *Parkin* mutations (autosomal recessive in PD) in PD patients, which reported that more than half of PD patients carrying *Parkin* mutations had only one mutated *Parkin* allele (Lücking et al., 2000). Since then many other PD patients carrying only heterozygous *Parkin* mutations have been identified (Hedrich et al., 2002; West et al., 2002). Similar observations were also made for PD patients carrying *PINK1* heterozygous mutations, also a putative recessive PD

gene (Bonifati et al., 2005; Klein et al., 2005; Abou-Sleiman et al., 2006a). Altogether, the relevance of these heterozygous mutations was highlighted by the confirmation that in fact more PD patients carry heterozygous *PARKIN* or *PINK1* mutations than homozygous or compounded heterozygous mutations (Klein et al., 2007). Furthermore, mutations in *DJ-1*, another recessive PD mutation have also been identified in the heterozygous state in multiple PD patients (Abou-Sleiman et al., 2003; Hedrich et al., 2004; Sadhukhan et al., 2012), with similar observations made also for *ATP13A2*, another recessive gene associated with PD, in Italian (Di Fonzo et al., 2007) and Asian (Lin et al., 2008) patients.

While in the previous cases the heterozygous mutation state seems to increase the risk of developing the same pathology induced by the homozygous mutation, in other cases the heterozygous state is associated with a different pathology. The best example for PD comes from genes usually associated with multiple lysosomal storage diseases. As described previously, homozygous (or compound heterozygous) mutations in *GBA* result in GD, an autosomal recessive lysosomal storage disorder. Once in the heterozygous state, *GBA* mutations become an important risk factor for PD, and are not usually found in GD. Of note, E326K mutations in *GBA* could represent an interesting exception since they were found present in a homozygous or heterozygous context in PD patients but not reported as a causative mutation for GD (Duran et al., 2013). Niemann-Pick disease type C is also an autosomal recessive lysosomal storage disorder, where cholesterol transport is impaired and can present in the clinic with neurological involvement. It is mostly caused by homozygous or compound heterozygous mutations in *NPC1* gene (Schulze and Sandhoff, 2011). Niemann-Pick disease type A is a closely related recessive disorder caused by homozygous or compound heterozygous mutations in the sphingomyelin phosphodiesterase-1 gene (*SMPD1*) (Rodríguez-Pascau et al., 2009). Two recent reports have identified PD patients carrying heterozygous mutations for both *NPC1* (Kluenemann et al., 2013) and *SMPD1*

(Gan-Or et al., 2013) suggesting that these mutations in the heterozygous state may be a relevant risk factor for PD. This further highlights the interest and relevance of possible converging mechanisms across PD and lysosomal storage diseases.

It is important to notice that although heterozygous mutations in recessive genes associated with PD can also be found in healthy individuals (Abou-Sleiman et al., 2006a; Klein et al., 2007; Nuytemans et al., 2010), they are less frequent. Heterozygous mutations are also more commonly found in patients than what would be mathematically expected (Klein et al., 2007), with a later age of onset compared to homozygous cases (Hedrich et al., 2002; Sun et al., 2006), although a worse disease progression has been confirmed (Marongiu et al., 2008). Neuroimaging studies have also identified preclinical alterations in multiple heterozygous mutation carriers. All these arguments combined support a role for heterozygous mutations as potential susceptibility factors in disease, and may have important implications for development of PD (Klein et al., 2007).

As an additional layer of complexity, some individuals carrying mutations in *LRRK2*, a dominantly transmitted gene, never develop PD, resulting in incomplete penetrance (Goldwurm et al., 2007). Klein and colleagues (Klein et al., 2007) first commented on these genetic challenges in PD when reviewing the literature for PD patients carrying *LRRK2*, *PINK1* and *PARKIN* mutations. They proposed that the increased risk of PD associated with heterozygous recessive mutations and reduced penetrance of dominant mutations are not simply a result of independent inheritance, but represent different complex manifestations making up a continuum of penetrance. They proposed penetrance can range from 100% for homozygous or compound heterozygous mutations, to 30–80% for heterozygous dominant mutations, and 1–25% for heterozygous recessive mutations. This model supports the idea that PD is a complex disorder in which cumulative genetic and environmental factors determine the age of onset and disease phenotype, a hypothesis previously proposed for

multiple human diseases (Badano and Katsanis, 2002). The identification of more recent heterozygous recessive alleles as risk factors for PD further supports this hypothesis, and further genetic analysis across different pathologies might bring further insights into the aetiology of multiple diseases.

1.5 The need for new models for study

Although much interest has arisen in recent years to understand how *GBA* mutations are involved in PD, the major limitation has been the lack of appropriate cell and animals models of study (Westbroek et al., 2011). Thus far, the models employed have been limited. Firstly, most studies have focused on cellular over-expression models of *GBA* genetic mutants (Cullen et al., 2011; Kong et al., 2013), *GBA* gene knockdown approaches (Osellame et al., 2013), or on homozygous mutant models based on our understanding of Gaucher's disease (Mazzulli et al., 2011)(Sardi et al., 2011). These systems clearly do not represent the heterozygous variants commonly associated with PD, and their conclusions, although informative on the cellular role of *GBA*, should be addressed with caution in the context of PD. Finally, recent post-mortem analysis of heterozygous mutant *GBA*-PD patients (Gegg et al., 2012) has provided interesting data on *GBA* in PD but gives a limited insight at the endpoint of disease. Overall, to date, no human functional dopaminergic neuronal model was yet available to investigate the impact of heterozygous *GBA* mutations in PD, which was one of the main goals of this thesis.

1.5.1 Induced pluripotent stem cells

In 1962, while at Oxford University, John Gurdon published a seminal report showing that differentiated/somatic cells could be reprogrammed to become pluripotent (Gurdon, 1962). This was the beginning of what was later named nuclear reprogramming and that resulted in

the famous cloning of "Dolly the sheep", the first animal cloned from a somatic cell (Wilmut et al., 1997). More recently, Shinya Yamanaka was able to identify the main genetic factors necessary for the conversion of a differentiated cell into a pluripotent stem cell state. The resulting cells were named induced pluripotent stem cells (iPSCs). This groundbreaking work was first reported in mouse cells in 2006 (Takahashi and Yamanaka, 2006) and later confirmed in human cells in 2007 (Takahashi et al., 2007) using the same four transcription factors – Oct3/4, Sox2, c-Myc and Klf4. In that same year, another group showed that a similar combination of transcription factors was also efficient in reprogramming human somatic cells (Yu et al., 2007). Since then, multiple groups have been focused on the optimization of reprogramming efficiencies and in the use of different reprogramming systems.

1.5.1.1 Reprogramming strategies

Initial hiPSC reprogramming methods used retrovirus to deliver the required transcription factors. The use of oncogenes in this process raised some concerns in the field, mostly if hiPSCs were to become a source of stem cells for transplantation. The use of retroviral vectors results in multiple random insertions in the genome. In addition, although transcription factors used have been shown to be silenced during reprogramming, there are still concerns over later reactivation of these factors, mainly for *c-Myc* and *Klf4* as they have been linked to oncogenesis (Hartfield et al., 2012). However, at the time this project started, the use of retrovirus was still the main technology available for cell reprogramming, and was therefore applied for the generation for all hiPSCs lines used in this thesis. Other improved gene delivery strategies using viral vectors were later introduced to reduce the integration

period of virus during reprogramming, including lentiviral vectors with a Cre-loxP system (Soldner et al., 2009) and a *piggyback* transposon system (Yusa et al., 2009).

Further progress resulted in the development of multiple non-integration systems for stem cell reprogramming. This included some non-viral methods like the delivery of episomal DNA vectors (Yu et al., 2009a) and transgene-free delivery methods by RNA transfection (Yakubov et al., 2010) or protein delivery (Cho et al., 2010). However some of these methods have shown poor efficiencies especially when used for hiPSCs or require multiple transfections resulting in elevated costs. Other integration-free viral methods have also been proposed including the use of adenoviral vectors (Stadtfeld et al., 2008) and Sendai viral (SeV) vectors (Fusaki et al., 2009; Nishimura et al., 2011). While the efficiency of adenoviral vectors has been quite challenging particularly in human cells, the use of SeV has become a very popular tool due to its high efficiency in introducing foreign genes with controllable expression. Due to great advantages offered by these recent technological developments, current lines being reprogrammed within the OPDC are using SeV.

In addition to iPSC-derived reprogramming strategies, adult cells have also been shown to be directly converted from one cell type into another. This direct reprogramming approach was first shown capable of generating neurons from mouse fibroblasts (Vierbuchen et al., 2010) and specific dopaminergic neurons from human fibroblasts (Caiazzo et al., 2011). Although direct reprogramming strategies could reduce the need for the generation of intermediate iPSC cells, the efficiency of this process is still low when compared to available viral methods.

Finally, multiple sources of somatic cells can be used for reprogramming strategies. In this study all hiPSC lines were generated from fibroblasts collected from multiple individuals, as fibroblast represent an easily accessible source of tissue requiring minimal

medical intervention. Within the OPDC colleagues have been able to successfully generate hiPSCs from blood samples, and multiple reports have shown that several other tissues can also be used including liver cells and adipose tissue (Lai et al., 2011).

1.5.1.2 hiPSC models of disease

hiPSC technology offers two main advantages to the field of disease modeling. Firstly, it allows the generation of populations of renewable cell populations from patients that can then be differentiated into multiple different cell types to model various human disorders that in many cases (mostly neurological) would be otherwise inaccessible. This is the case for PD where studying dopaminergic neurons from patients has previously been limited to post-mortem studies. This has been one of the biggest barriers for accessing physiologically relevant neurons for early stage disease research. Secondly, these patient-derived specific cells carry disease-associated alleles on the genetic background of the donor and will also likely include disease-permissive genetic modifiers that will offer a further advantage to better model cellular mechanisms of PD.

In recent years, hiPSCs have been generated from somatic cells and differentiated into multiple cell types to model various human diseases. Initial reports demonstrated the possibility of generating motor neurons from an amyotrophic lateral sclerosis (ALS) patient (Dimos et al., 2008) and from an SMA patient (Ebert et al., 2009), and peripheral neurons from patients with familial dysautonomia (FD) (Lee et al., 2009). hiPSCs from idiopathic PD patients were first differentiated into dopaminergic neurons in 2009 (Soldner et al., 2009), and later neurons were also differentiated from hiPSCs derived from AD patients (Yagi et al., 2011).

Overall, for the study of neurodegeneration in PD, differentiation of patient-derived hiPSCs into functional midbrain dopaminergic neurons provides a powerful tool to study the genetic contribution to Parkinson's in a highly physiological model of a previously inaccessible cell type. For the specific study of *GBA* mutations in PD development, this model will be essential for the analysis of the contribution of the specific heterozygous *GBA*

mutations commonly found in PD patients, overcoming many of the limitations imposed by current models of study available.

1.6 Aims of this thesis

- To develop an efficient protocol for the differentiation of dopaminergic neurons from hiPSCs (Chapter 3).
- To identify and derive dopaminergic neurons from PD patients carrying heterozygous *GBA* mutations, idiopathic PD patients and control individuals (Chapter 4).
- To investigate and elucidate the role of heterozygous *GBA* mutations in the context of PD related phenotypes in iPSC-derived dopaminergic neurons (Chapter 5)

Optimization of protocols used for the differentiation of hiPSC lines and some of the characterization analysis performed was a collaborative effort with colleagues in the lab. In some cases, as described throughout this thesis, gene and protein expression analysis on hiPSC lines differentiated by Hugo Fernandes (HF) was performed in collaboration with Elizabeth Hartfield (EH) and Jennifer Badger (JB).

Chapter 2

Material and Methods

2.1 Cell culture

All cell culture work described in this thesis was carried out in a Class II laminar flow cabinet under aseptic conditions, and cultures were maintained in saturated humidity incubators at 37°C with 5% CO_2.

2.1.1 Dopaminergic differentiation of mouse ES cells

Differentiation of E14Tg2A mouse ES cells (obtained from David Adams and Allen Bradlley, Wellcome Trust Sanger Institute) was performed using the "Human/Mouse Dopaminergic Neuron Differentiation Kit" (R&D Systems, SC001B), following manufacturers protocol as described briefly with some modifications.

Stage I: Expansion of undifferentiated ES cells. Undifferentiated E14Tg2A cells were expanded on gelatin-coated (0.1%, Sigma-Aldrich G1393) tissue culture plates, for 3-4 days,

with daily medium replacement. Cell culture medium consisted of Knockout Dulbecco's Minimal Essential Medium (KO-DMEM, Life Technologies, 10829018) supplemented with 15% Fetal Bovine Serum (FBS, Life Technologies), 100 μM Non-Essential Amino Acids Solution (Life Technologies), 55 μM β-mercaptoethanol, Leukemia Inhibitory Factor (recombinant mouse LIF, Merck Milipore, ESG1106), 100U/mL Penicillin, 100μg/mL Streptomycin and 2mMM L-Glutamine (Life Technologies, 10378-016).

Stage II: Embryoid Bodies (EB) formation. Embryoid body (EB) formation was induced by dissociation of cells into a single cell suspension with 0.05% Trypsin/EDTA (Sigma-Aldrich). Cells (2×10^6) were seeded on non-adherent 10 cm culture dishes in same media as described above but without LIF, and cultured for 4 days, with media changed on second day.

Stage III: Selection of Nestin-positive cells. EBs were transferred to an adhesive 10 cm tissue culture dish and left for 24hours in fresh medium to allow EBs attachment. Induction of nestin-positive cells was initiated by changing to medium consisted of DMEM/F-12 (Life Technologies, 11320-033) supplemented with Glucose (Sigma-Aldrich), 2mM L-Glutamine (Sigma-Aldrich), 1X Insulin/Transferrin/Selenium (ITS) supplement (as supplied by the kit), 1X bovine Fibronectin (as supplied by the kit) and 1X Penicillin-Streptomycin (P/S, Sigma-Aldrich). Cells kept for 6 days with medium changed every two days

Stage IV: Expansion of Nestin-positive cells. Cells were then dissociated with 0.05% Trypsin/EDTA and seeded onto glass coverslips (pre-coated with poly-D-Lysine and laminin, see below) in 12 well tissue culture dishes at a density of 3×10^5 cells/well. Medium

consisted of DMEM/F-12 (Life Technologies, 11320-033) supplemented with 1X Penicillin-Streptomycin (P/S, Sigma-Aldrich), 2mM L-Glutamine (Sigma-Aldrich), 1X N-2 Plus Supplement (as supplied by the kit), 1X Human FGF basic (as supplied by the kit), 1X Mouse FGF-8b (as supplied by the kit), 1X Mouse Shh-N (as supplied by the kit) and 0.2 mM Ascorbic Acid (Sigma-Aldrich). Cells kept for 4-6 days with medium changed every day.

Coating plates and coverslips with poly-D-Lysine and laminin. Whenever used, coverslips were first rinsed in 100% ethanol and allowed to dry before coating. 1X Poly-D-Lysine (Sigma-Aldrich, P6407) was added to the well/coverslip (enough to cover the surface) and incubated for 1-2 hours at room temperature or overnight at 4°C. Poly-D-Lysine was removed and wells washed 3 x 5 minutes with H_20, and allowed to air-dry. Laminin (mouse, 10μg/mL, Life Technologies, 23017-015) was spoted on the center of the well/coverslip and plates were incubated for 1 hour at 37 °C. Laminin was then removed and differentiation medium added.

Stage V: Differentiation of Dopaminergic neurons. Final dopaminergic differentiation was induced by changing the medium to medium composed of DMEM/F-12 (Life Technologies, 11320-033) supplemented with 1X Penicillin-Streptomycin (P/S, Sigma-Aldrich), 2mM L-Glutamine (Sigma-Aldrich), 1X N-2 Plus Supplement (as supplied by the kit) and 0.2 mM Ascorbic Acid (Sigma-Aldrich). Cells kept for 10-15 days with medium changed every two days.

2.1.2 Dopaminergic differentiation of human ES cells

Undifferentiated HUES2 cells (provided by Sally Cowley, Sir William Dunn School of Pathology, University of Oxford) were maintained by the Oxford Stem Cell Institute (OSCI), University of Oxford. EBs were made by Sally Cowley and Jane Vowles (OSCI) and were seeded on Geltrex coated plates (Life Technologies, 11320-033) in defined medium consisting of DMEM/F12 (Life Technologies), with 1X Penicillin-Streptomycin (P/S, Sigma-Aldrich), 1.5mM L-Glutamine (Sigma-Aldrich) and 1% N-2 Plus Media Supplement (R&D Systems). Induction of neural progenitor cell rosettes formation was induced by supplementing defined medium with 5μg/mL human plasma fibronectin (Millipore) and 200ng/mL of recombinant human noggin (Life Technologies) for four days, with media change in second day. Rosettes were then expanded in defined medium supplemented with 20ng/mL of recombinant human FGF basic (R&D Systems) with medium change every two days. For final dopaminergic differentiation, after seven days cells were dissociated with 0.05% Trypsin/EDTA and seeded onto glass coverslips (pre-coated with poly-D-Lysine and laminin) in 12 well tissue culture dishes at a density of 1.5 x 10^5 cells/cm^2. Cells were maintained for 7 to 21 days in defined medium supplemented with 1mM N^6,2′-O-dibutyryladenosine 3′,5′-cyclic monophosphate sodium salt (dbcAMP; Sigma-Aldrich). ROCK inhibitor (ROCKi) (10 μM, Tocris) was added in all medium during differentiation. Experiments were performed in collaboration with Dr Elizabeth Hartfield.

2.1.3 Dopaminergic differentiation of human iPS cells

Prior to differentiation, iPSC lines were adapted to feeder-free conditions using Matrigel (BD). Briefly, mTeSR™1 (StemCell Technologies) was supplemented with 10μM Y27632 (ROCKi, Calbiochem) on the day of passage. EBs were formed by dissociation of iPSCs with TryplE (Life Technologies) and seeded into Aggrewell plates (10,000 cells per EB; Stem Cell

Technologies) in mTeSRTM-1 medium (Stem Cell Technologies) supplemented with 10 µM Y27632 (Calbiochem), with a 75% daily medium change. After 4 days, EBs were harvested and neural induction was initiated (James Martin Stem Cell Facility, University of Oxford).

All materials for further differentiation were obtained from Life Technologies unless otherwise stated. EBs were plated onto Geltrex-coated plates in Neural Induction medium 1 (DMEM/F12 supplemented with 2 mM L-glutamine, N2 supplement, 1 mg/mL bovine serum albumin (BSA, Sigma-Aldrich), 10 µM Y27632 (Tocris), 10 µM SB431542 (Tocris), 200 ng/mL recombinant human Noggin, 500 ng/mL sonic hedgehog (SHH-C24II, R&D Systems], 0.7 µM CHIR99021 (Stemgent) and 1 % antibiotic/ antimycotic (Sigma-Aldrich). 50% medium change was done every two days. After 12 days, medium was changed to Neural Induction medium 2 (DMEM/F12 supplemented with 2 mM L-glutamine, N2 supplement, 1 mg/mL BSA (Sigma-Aldrich), 10 µM Y27632 (Tocris), 20 ng/mL sonic hedgehog (SHH-C24II, R&D Systems], 1 % antibiotic/ antimycotic (Sigma-Aldrich), 100 ng/mL FGF8a (R&D Systems), 5 µg/mL heparin (Sigma-Aldrich), 20 ng/mL Human Brain-Derived Neurotrophic Factor (BDNF) and 200 µM ascorbic acid (Sigma-Aldrich) and incubated for 8 days, until the appearance of dense neural rosette structures. 50% medium change was done every two days. Neural progenitor structures were manually dissected and replated as clumps onto Geltrex-coated plates in final differentiation medium (DMEM/F12 supplemented with 2 mM L-glutamine, N2 supplement, 1 mg/mL BSA (Sigma-Aldrich), 10 µM Y27632 (Tocris), 1 % antibiotic/ antimycotic (Sigma-Aldrich), 20 ng/mL BDNF, 20 ng/mL Human Glial-Derived Neurotrophic Factor (GDNF), 200 µM ascorbic acid (Sigma-Aldrich) and 0.5 mM dbcAMP (Sigma-Aldrich). Neurons were matured for two weeks in this medium before experimental procedures were carried out. Medium was changed every two days throughout the protocol.

2.2 DNA manipulation

2.2.1 DNA extraction

DNA was extracted from individual blood samples by Sam Evetts (OPDC) using the AutoPure LS® Kit (Qiagen). For confirmation, DNA was also extracted from iPSCs by me as follows:

Reagent	Components
Genomic DNA extract Cell lysis buffer	0.6 % SDS 100 mM NaCl 50 mM Tris-HCl (pH 8) 20 mM EDTA

Cells were lysed with genomic DNA extract lysis buffer as described above containing 50 µg/mL RNAse A with shaking at room temperature for 20 minutes for complete cell lysis. Cell lysate was scraped and incubated with 100 µg/mL of proteinase K at 37 °C overnight. Lysate was then extracted twice with 500 µL of chloroform with 1.5 mL Phase Lock Gel tubes (Eppendorf) and mixed by inversion before centrifugation at 16200 xg for 1 minute. DNA was then precipitated by addition of 30 µL of 5 M NaCl and 1.3 mL of absolute ethanol. Precipitate was chilled on ice for 5 minutes and pelleted by centrifugation at 16200 xg for 30 minutes at 4°C. DNA pellet was washed with 70% ethanol and centrifuged at 16200 xg for 30 minutes at 4°C. Supernatant was discarded and pellet allowed to air-dry before being resuspended in 100 µL of TE overnight at 4°C. DNA was later quantified using a NanoDrop system (Thermo Scientific).

2.2.1 Polimerase Chain Reaction (PCR)

Amplification of DNA for sequencing and identification of GBA mutations was done by PCR reaction. PCR reactions were carried out using AmpliTaq Gold DNA polymerase (Applied Biosystems) in 96-well plates (Starlab), on a PCR PeltierThermocycler (PTC-225, MJ Research). Conditions used as described below.

Reagent	**Amount**
DNA template	10 ng
10x Buffer	1.5 µL
$MgCl_2$ 25mM	1.5 µL
dNTPs 8mM	0.75 µL
Forward primer 1µM	0.75 µL
Reverse primer 1µM	0.75 µL
Taq Gold	0.2 µL
Mili-Q H_20	up to 15 µL

Temperature	Time	
95°C	10 minutes	
95°C	20 seconds	X 30 cycles
58-65°C	45 seconds	
72°C	60 seconds	
72°C	15 minutes	

Note: Annealing temperature was adjusted according to each reaction to provide optimal specificity.

2.2.2 DNA restriction digest

Genomic DNA regions of interest amplified by PCR were digested with restriction endonucleases for the identification of cleaved products resulting from the presence of heterozygous GBA mutations. For the identification of *GBA*-N370S and *GBA*-L444P mutations the endonucleases *XhoI* and *NciI* (both from New England Biolabs) were used respectively. Restriction digest reaction was performed as described:

Reagent	Volume
DNA	7 μL
10x Restriction buffer	1.5 μL
20x BSA	0.75 μL
Restriction enzyme	0.5 μL
Mili-Q H_20	up to 15 μL

Samples were incubated at required enzyme temperature (53° for *XhoI* or 58° for *NciI*) for 3 hours, and the results analysed by agarose gel electrophoresis.

2.2.3 Agarose gel electrophoresis

Agarose gels for DNA fragment analysis were prepared in 1x Tris-Borate EDTA buffer (TBE) (Sigma-Aldrich). For *NciI* digestion agarose (Sigma-Aldrich) at a concentration of 1.5% (w/v) was used. For *XhoI* digestion MacroSieve Low Melt Agarose (Flowgene) was used at a concentration of 2.5%-3% (w/v). Solution was heated in a microwave until agarose was dissolved and ethidium bromide added to a final concentration of 0.5mg/mL before pouring for gel formation. Electrophoresis was performed in 1x TBE buffer using a Sub-Cell GT gel electrophoresis system (BIO-RAD). Loading buffer 6x (1.5g Ficoll 400, Orange G dye and MiliQ H_20 up to 10 mL) was added to each sample before loading in the gel and 1kb-Plus DNA ladder (Invitrogen) was used for fragments size determination. Gel was imaged using a GelDoc XR transilluminatior system (BIO-RAD).

2.2.4 DNA sequencing

The regions to be sequenced were amplified via PCR using the same conditions as described above.

a. ExoSAP reaction

An ExoSAP reaction was carried out to remove PCR buffers, salts and dNTPs using exonuclease I (New England Biolabs) and shrimp alkaline phosphatase (SAP) (Promega). Each ExoSap reaction consisted of the following:

Reagent	**Volume**
PCR product	25 μL
10x SAP buffer	1 μL
SAP (500 U/ μL)	1 μL
Exonuclease I (20U/ μL)	0.1 μL
Mili-Q H_20	0.9 μL

Samples were incubated at 37°C for 1 hour and then 80°C for 20 minutes.

b. Sequencing reaction

Sequencing reactions were performed according to BigDye Terminator v3.1 Cycle Sequencing protocol (Applied Biosystems). The reaction mix consisted of the following:

Reagent	Volume
DNA template	5 µL
Primer (10 µM)	1 µL
5x Sequencing buffer	1.75 µL
BigDye	0.5 µL
Mili-Q H_20	1.75 µL

Temperature	Time	
96°C	60 seconds	
96°C	10 seconds	X 30 cycles
50°C	5 seconds	
60°C	60 seconds	

c. DNA precipitation

The product was then precipitated by adding 4 μL of EDTA/NaAc to each well followed by 50 μL of 100% ethanol. Mixture was vortexed before centrifugation at 3000 x *g* at 4°C for 30 minutes. The supernatant was removed and 70 μL of 70% ethanol added to each well to wash the DNA. After centrifugation at 1650 x *g* at 4°C for 15 minutes, the supernatant was discarded and the wells allowed to air dry for 10 minutes. Sequencing reactions were performed by the Sequencing Facility – Department of Zoology, University of Oxford. Results were viewed with ContigExpress software (VectorNTI, Life Technologies).

2.3 Analysis of mRNA expression

2.3.1 RNA extraction

Total RNA was extracted from cells in culture using TRIzol (Life Technologies) and purified using the RNeasy kit (QIAGEN). Cells were washed once with PBS before being incubated with 1mL of TRizol for homogenization. After 15 minutes at room temperature, sample was centrifuged at 9600 xg for 10 minutes at 4°C to get rid of debris. Supernatant was transferred to a fresh tube and 150 μL of choloroform was added for phase separation. Sample was mixed by shaking vigorously for 15 seconds and incubated at room temperature for two minutes. After centrifugation at 9600 xg for 10 minutes at 4°C, the upper aqueous phase was transferred to a new tube and an equal volume of ethanol (EtOH) was slowly added. The resulting solution was then loaded onto a RNase Easy Column (RNeasy kit, QIAGEN) and centrifuged at 9600 xg for 30 seconds. Flow through was discarded and 350 μL of RW1 buffer was added onto the column, before centrifugation at 9600 xg for 15 seconds. 80 μL of a solution containing RDD buffer and DNase I was added to the column membrane and

incubated at room temperature for 15 minutes. Column was then washed with 350 µL of RW1 buffer and centrifuged at 9600 xg for 30 seconds. Two further washing steps were performed by addition of 500 µL of RPE buffer and centrifuged at 9600 xg for two minutes, followed by another centrifugation step (no buffer added) to dry the membrane. Column was transferred to a new collection tube and 30 µL of RNase free water was added to elute RNA with centrifugation at 9600 xg for one minute. RNA was stored at -80°C.

2.3.2 cDNA synthesis

RNA was transcribed into complementary DNA (cDNA) with a SuperScript III Reverse Transcriptase Kit (Life Technologies) according to manufacturer's instructions. For each reaction, the following components were added:

Reagent	Volume
RNA	5 µg
Random Primers	150 ng
dNTP mix (10nM)	1 µL
RNase free water	Up to 13 µL

The mixture was then heated to 65°C for five minutes and incubated on ice for one minute. After Brief centrifugation to collect tube contents the following components were added:

Reagent	Volume
First Strand Buffer (5x)	4 μL
DTT (0.1M)	1 μL
RNase OUT Recombinant RNase inhibitor	1 μL
SuperScript III Reverse Transcriptase	1 μL

The mixture was mixed by pipetting gently up and down before being incubated at room temperature for 5 minutes. The sample was then incubated at 55°C for 60 minutes and inactivated by heating at 70°C for 15 minutes. The cDNA was stored at -20°C and could then be used for PCR amplification.

2.3.3 RT-PCR

Polymerase chain reactions (PCR) were set up with 20 ng of cDNA using GoTaq DNA Polymerase products (Promega). Primer sequences used as follows:

Table 3 Primer sequences used for RT-PCR

Primer	Sequence 5'-3'
FOXA2_F	GACAAGTGAGAGAGCAAGTG
FOXA2_R	ACAGTAGTGGAAACCGGAG
LMX1A_F	AACGACAGCTTCTGGCATGA
LMX1A_R	TCAAGATGGTTCTCGGACGT
EN1_F	GCTATCCTACTTATGGGCTCA
EN1_R	GGAGTGGTTGTACAGTCCCT
NURR1_F	CGACATTTCTGCCTTCTCC
NURR1_R	GGTAAAGTGTCCAGGAAAAG
OCT4_F	AAAGCTCTGCAGAAAGAACTCG
OCT4_R	CTCACTCGGTTCTCGATACTGG
GAPDH_F	CAGGGCTGCTTTTAACTCTGG
GAPDH_R	AAGTTGTCATGGATGACCTTGG

2.4 Analysis of protein expression

2.4.1 Western Blot/immunoblotting

a. Protein Extraction

Western blotting was carried out on whole cell lysates extracted using Radio-Immunoprecipitation Assay (RIPA) buffer as described:

Reagent	Components
RIPA buffer	Tris-Hcl pH 8.0 (50mM) NaCl (150mM) Sodium Deoxycholate (0.5% w/v) SDS (0.1% w/v) NP-40 (1% w/v) Protease inhibitor cocktail (1x) (Roche)

Cells in culture were washed once with cold PBS and scraped into 1 mL of cold PBS. Cells were centrifuged at 1500 xg for two minutes at 4°C and supernatant was discarded. Cell pellet was lysed in RIPA buffer with sonication for 5 seconds. After incubation on ice for 30 minutes, the lysate was centrifuged at 1200 xg for 10 minutes at 4°C to pellet nuclear fraction. Supernatant was collected, and protein content determined by BCA assay, before storage at -80°C.

b. Gel Preparation

SDS Polyacrylamide gel electrophoresis (SDS-PAGE) was performed using either Criterion Tris-HCl 4-15% precast polyacrylamide gel (BIO-RAD) run on a Criterion Cell electrophoresis system (BIO-RAD) or using home-made 15% polyacrylamide gels run on a Mini-PROTEAN Tetra Cell electrophoresis system (BIO-RAD). For the latter, resolving gels were prepared as follows:

Reagent	**Source**
Mili-Q H_20	
30% acrylamide mix	BIO-RAD
1.5M Tris-HCl pH 8.8	
10 % SDS	BIO-RAD
10% ammonium persulfate	Sigma-Aldrich
TEMED	Sigma-Aldrich

Gel mixture was applied to the casting apparatus (BIO-RAD) and left to solidify for 45 minutes at room temperature.

b. Immunoblot

Reagents used as described:

Reagent	Components
Laemmli buffer 5x (100 mL)	30 mL Tris-HCl pH6.8 10 g SDS 50 mL glycerol 20 mL β-mercaptoethanol 250 mg bromophenol blue
Running buffer 1x (1 L)	3.03 g Tris base 14.4g glycine 1 g SDS Mili-Q H_20 up to 1 L
Transfer buffer 1x (1 L)	5.82 g Tris base 2.93 g Glycine 200 mL MetOH Mili-Q H_20 up to 1L
TBS-Tween 1x (1 L)	20 mL Tris 1mM pH 7.5 8 g NaCl Mili-Q H_20 up to 1L 1 mL Tween20

Before loading, protein samples were denatured for 10 minutes at 95 °C in 1x Laemmli buffer. Between 3-10 μg of total protein were loaded per lane in described polyacrylamide gels and run at 200 V in Running buffer. Two molecular weight markers were also run in each gel to allow protein size determination, namely Spectra Multicolor Broad Range Protein Ladder (Thermo Scientific) and MagicMark XP Western Protein Standard (Life Technologies). Time of electrophoresis depended on size of proteins of interest to be analysed. Transfer of proteins to a PVDF membrane was done either using: a) Trans-Blot Turbo Transfer System (BIO-RAD) using Trans-Blot Turbo Midi PVDF transfer Packs, following manufacturer's instructions; or b) PVDF membrane (Merck-Milipore) in Transfer buffer at 100 V for 70 minutes on a Criterion Blotter (BIO-RAD). After transfer, PVDF membranes were washed twice in TBS-Tween (10 minutes, with shaking) and then blocked in 5% non-fat milk (Sigma-Aldrich) diluted in TBS-Tween for 1 hour at room temperature. Membranes were then incubated with corresponding primary antibodies diluted in 1% non-fat milk overnight at 4°C with shaking. Antibodies used for Western blot are described in Table 4.

Table 4 Antibodies used for immunoblotting

Antibody	Host	Type	Source	Catalog No.	Dilution
Tuj1	rabbit	monoclonal	Covance	MMS-435P	1:500
TH	rabbit	polyclonal	Milipore	AB5622	1:500
DAT	rabbit	polyclonal	Alpha-diagnostic	DAT13-A	1:1000
β-Actin	rabbit	polyclonal	Abcam	AB8227	1:5000
GBA	mouse	monoclonal	Abcam	AB55080	1:200
LIMP2	rabbit	polyclonal	ProSci	4621	1:1000
Bip	rabbit	polyclonal	Abcam	AB21685	1:1000
Calreticulin	rabbit	polyclonal	Thermo Scientific	PA3-900	1:5000
IRE1-α	rabbit	monoclonal	Cell Signalling	3294	1:1000
PDI	rabbit	monoclonal	Cell Signalling	3501	1:1000
Calnexin	mouse	monoclonal	Cell Signalling	2679	1:1000
LC3-II	mouse	monoclonal	Nanotools	5F10	1:200
Beclin1	rabbit	monoclonal	Abcam	AB51031	1:1000
p62	mouse	monoclonal	Abcam	AB56416	1:500
TFEB	rabbit	polyclonal	Proteintech	13372-1-AP	1:200
LAMP1	mouse	monoclonal	Santa Cruz	SC-20011	1:100
LAMP2a	rabbit	polyclonal	Abcam	AB18528	1:1000
Cathepsin D	mouse	monoclonal	Abcam	AB6313	1:1000
α-synuclein	mouse	monoclonal	Covance	SIG-39730	1:1000
PERK	rabbit	monoclonal	Cell Signalling	5683	1:1000

After primary antibody incubation, membranes were washed twice in TBS-Tween (for 10 minutes, with shaking), and incubated with corresponding horseradish peroxidase-conjugated secondary antibodies (BIO-RAD) at 1:5000 dilution in 1% non-fat milk at room temperature for 1 hour with shaking. Membranes were then washed three times in TBS-Tween (10 minutes, with shaking). Chemiluminescence signal was detected using a chemiluminescent HRP substrate Immobilon Western (Merck Milipore) and imaging was performed on a GelDoc XR system (BIO-RAD). Quantification was performed using Image J software.

2.4.2 Immunofluorescence

Reagents used:

Reagent	Components
IF block solution	0.1 % Triton X-100 10% normal goat/donkey serum TBS solution
IF wash solution	0.1 % Triton X-100 TBS solution

After differentiation in culture wells containing coated-coverlips, cells were washed in PBS and then fixed in 4% paraformaldehyde (PFA) for 15 minutes at room temperature. Wells were then washed twice with PBS and cells blocked with IF block solution for 30 minutes. Wells were washed twice with DPBS and corresponding primaries antibodies were diluted in IF block solution and added to the wells for overnight incubation at 4°C with shaking. Antibodies used for immunofluorescence are described in Table 5:

Table 5 Antibodies used for immunofluorescence

Antibody	Host	Type	Source	Catalog No.	Dilution
Tuj1	mouse	monoclonal	Covance	MMS-435P	1:500
MAP2	rabbit	polyclonal	Merck Milipore	AB5622	1:1000
TH	rabbit	polyclonal	Merck Milipore	AB152	1:500
AADC	rabbit	polyclonal	Merck Milipore	AB1569	1:500
LAMP1	mouse	monoclonal	Santa Cruz	SC-20011	1:200
LAMP1	rat	monoclonal	Santa Cruz	SC-19992	1:200
GBA	mouse	monoclonal	Abcam	AB55080	1:100
LC3-II	Rabbit	polyclonal	Sigma-Aldrich	L7543	1:200
LC3-II	mouse	monoclonal	Nanotools	5F10	1:200

After primary antibody incubation, wells were washed twice with IF wash buffer. Corresponding secondary antibodies (Alexa Fluor IgG Antibodies, Life Technologies) were diluted in IF block solution and added to the wells for incubation for 60 minutes while protected from light. Wells were then washed three times (10 minutes each) with IF wash buffer. On second washing step, DAPI was added to IF washing buffer fluorescent staining of cell nuclei. Coverslips were then mounted using Vectashield mounting medium (Vector Laboratories) and imaged by fluorescent microscopy using a Nikon Eclipse TE-2000 microscope (Nikon Instruments) or a Leica SP5 confocal microscope (Leica Microsystems).

2.5 Dopaminergic functional assays

2.5.1 High Performance Liquid Chromatography (HPLC)

a. Cellular preparation for intracellular dopamine content analysis

Dopaminergic neurons differentiated in 6-well plates were washed twice in Hank's balanced salt solution (HBSS) with calcium and magnesium (Life Technologies). After lysis in 0.1 M perchloric acid ($HClO_4$) (PCA, Sigma) (500µL/well) for 5 minutes, cells were scraped and collected into opaque 1.5 mL tubes and snap-frozen in dry ice. Samples were stored at -80°C until HPLC analysis. For cells treated with L-3,4-dihydroxyphenylalanine (L-DOPA), 100 µM L-DOPA was added to the medium 6 hours prior to collection. Cells were washed, lysed, collected and stored as described before.

b. Sample analysis

Samples were analysed for dopamine (DA), 3,4-dihydroxyphenylacetic acid (DOPAC), L-DOPA, noradrenaline (NA) and homovanilic acid (HVA) using HPLC with electrochemical detection using a system previously established by Dr Lara Lourenco Venda. Samples were homogenised with a needle and filtered by centrifugation at 1500 xg for 5 minutes at 4°C using Ultrafree centrifugal 0.22 μm filters (Millipore) to remove cell debris. 150μL of solution were then transferred to autosampler vials (Fisher Scientific). Samples (50 μl) were injected onto the HPLC column (250-mm Microsorb C18 reverse-phase column) using an autosampler (Jasco) and detected using an LC-4B electrochemical detector (Decade, Antec). Mobile phase consisted of 13% methanol, 0.12 M NaH_2PO_4, 0.8 mM EDTA and 3.2mM octanesulphonic acid (OSA) at pH 3.43. Flow rate was 1 mL/min. Results were normalised to total protein levels of samples analysed determined by bicinchoninic acid (BCA) assay. Peaks were identified by comparison with the pattern obtained for a standard solution prepared with each of the monoamines of interest to be detected. Experiments were performed in collaboration with Dr Elizabeth Hartfield and Dr Brent Ryan

2.5.2 Dopamine Transporter (DAT) uptake assay

Functional DAT activity was quantified by incubating differentiated cultures with ^{3}H-Dopamine (DA) (10 nM, GE Healthcare) as previously described (Fountaine and Wade-Martins, 2007). Briefly, neuronal cultures were washed twice with PBS prior to addition of ^{3}H-DA either in the presence or absence of mazindol (10 μM, Sigma) at several time points (0-30 minutes). Uptake was stopped by the addition of ice-cold PBS followed by lysis in sodium hydroxide (1 M). A small sample was collected for protein analysis and the remainder was added to 5mL scintillation fluid (OptiPhase SuperMix, Perkin-Elmer) and

scintillation quantified using a scintillation counter (Beckman Coulter). Results were normalized to protein content determined by BCA assay. Experiments were performed in collaboration with Dr Elizabeth Hartfield.

2.6 GCase activity

a. Reagents

Solution	Components
Citrate-Phosphate Buffer pH 5.4 (100 mL)	22.2 mL 0.1 M Citric Acid 27.8 mL 0.2 M Dibasic sodium phosphate MiliQ H_20 up to 100mL
GCase Lysis Buffer	Citrate-Phosphate Buffer pH 5.4 0.25% v/v Triton X100 (Sigma-Aldrich) 0.25% w/v Taurocholic acid (Sigma-Aldrich)
Glycine-Sodium Hydroxide buffer pH 10.4 (200 mL)	50 mL 0.1M Glycine 38.6mL 0.1M Sodium hydroxide MiliQ H_20 up to 200mL

b. Protocol

Differentiated dopaminergic cultures were lysed and sonicated in GCase Lysis Buffer. Following incubation on ice for 30 minutes, samples were centrifuged at 1200 xg for 10 minutes at 4 °C. The supernatant was collected and protein levels determined by BCA assay. Working solutions were prepared for each sample to get equal protein concentration solutions for all samples. For each experimental sample 4μg of protein were used. For each condition one sample was pre-incubated with 2.5 mM conduritol-B-epoxide (CBE, BML-S104, Enzo) for 30min at room temperature. These samples were used as a negative control and to provide background values for GCase activity. All samples (4μg) were incubated with 5 mM 4-methylumbelliferyl β-D-glucopyranosidase (4-MUGlc, M3633, Sigma-Aldrich) and incubated at 37 °C for 1 hour. The reaction was stopped by adding excess Glycine buffer and fluorescence detected on a Synergy HT plate reader (BioTek) at excitation 360 nm and emission 440 nm. Final GCase activity values were calculated as the difference between CBE un-treated and CBE treated samples. All samples were done in triplicate.

2.7 Immunogold electron microscopy

Cells grown on polyester filters were fixed in 3% paraformaldehyde/0.05% glutaraldehyde and prepared for immunogold EM by standard methods (Morris et al., 2006). Briefly, filters were stained with uranyl acetate (2 % w/v in distilled water), dehydrated through increasing concentrations of methanol (70-100 %) and embedded in LR Gold resin (Agar, Reading UK). Ultra-thin sections (50-80 nm) were prepared by use of a Reichert Ultracut S ultratome (Leica, Milton Keynes, UK), mounted on 200-mesh nickel grids, incubated at room temperature with either anti-profilin antibody (dilution 1:200, 2 hour) or anti-TH antibody (1:200, 2 hour) followed by Protein A-15 nm gold complex for 1 hour (1:60). All antisera

were diluted in 0.1M phosphate buffer containing 0.1 % egg albumin. As a negative control, the primary antibody was replaced by non-immune sera and immunogold labelling was not observed. After immunolabelling sections were lightly counterstained with lead citrate and uranyl acetate and examined with a JEOL transmission electron microscope (JEM-1010, JEOL, Peabody, MA, USA) and representative micrographs were prepared. The area of the cells was analysed using Axiovison (version 4.5) image analysis software and the number of lysosomes counted for 8 cells per group. Methods supplied by Dr Helen Christian, DPAG, Oxford

2.8 α-synuclein ELISA

An in-house ELISA for the accurate quantification of α-Syn concentration was developed by using two commercially available α-Syn-specific antibodies: the monoclonal Syn-1 (BD Transductions) as the capture antibody and the polyclonal C-20 (Santa Cruz) as the detection antibody, which was used after its covalent conjugation with HRP (Emmanouilidou et al., 2011). Briefly, each ELISA plate (Corning Costar) was coated for 24 hrs at room temperature with 0.5 μg/ml of Syn-1 antibody (50 μl per well) in 100 mM NaHCO3, pH 9.3. The plates were washed three times in wash buffer (50 mM Tris-HCl, 150 mM NaCl and 0.04 % Tween-20) and 50 μl of sample was added. Recombinant human α-Syn (Chemicon) (as standard) was diluted in 50 % TBST/BSA (10 mM Tris-Cl, pH 7.6, 100 mM NaCl, 0.1% Tween-20 and 1% BSA) and 50% cell culture medium. Samples of conditioned medium were 2-fold diluted in TBST/BSA prior to addition to the wells. To allow antigen binding, plates were incubated at 37 ^{o}C for 2.5 hrs. After washing three times with wash buffer, 50 μl of HRP-conjugated C-

20 antibody (1:4000 diluted in TBST/BSA) was added to each well and further incubated for 1 hr at room temperature. The wells were washed and 50 µl of chemiluminogenic HRP substrate (UptiLight HS ELISA HRP substrate, Interchim) was added to each well. Following incubation for 10 minutes at room temperature, chemiluminescence was integrated for 1s. Standards and conditioned medium samples were measured at least in duplicate. Methods supplied by Dr Kostas Vekrellis, University of Athens, Greece.

2.9 Clinical cohort

Participants were recruited to this study having given signed informed consent, which included mutation screening and derivation of hiPSC lines from skin biopsies (Ethics committee: National Health Service, Health Research Authority, NRES Committee South Central – Berkshire, UK, who specifically approved this part of the study - REC 10/H0505/71).

Chapter 3

Differentiation and characterisation of dopaminergic neuronal cultures from embryonic stem cells and induced pluripotent stem cells.

3.1 Introduction

Developmental studies over the last decades have contributed vastly to the current understanding of neuronal developmental. The knowledge has been extended to *in vitro* neurogenesis modelling, starting from mouse and more recently applied in human stem cells models. This has led to significant improvements in the capacity to generate ventral midbrain dopaminergic neurons, amongst other types of cells.

Specification of regional identity within the central nervous system (CNS) occurs during early stages of development, and midbrain dopaminergic neurons develop during a narrow window of early CNS development (Studer, 2012). Recapitulation *in vitro* of this differentiation *timing* is of crucial importance since precursor cells within the CNS rapidly become region-specific, limiting their differentiation potential.

Almost 75% of all dopaminergic neurons found in the adult CNS are located in the ventral midbrain (VM) (Hegarty et al., 2013). In the embryo, the development of the VM is regulated by signals secreted from two main signalling centres: the floor plate and the isthmus (Hegarty et al., 2013). The floor plate secretes the sonic hedgehog (Shh) signalling protein and the floor plate region of the mesencephalon gives rise to midbrain dopaminergic neurons (Ono et al., 2007). The isthmus is found in the midbrain-hindbrain boundary and secretes Wnt1 and fibroblast growth factor 8 (FGF8), which are important signals for midbrain differentiation (Chung et al., 2009). However, intricate/cooperative interactions between these molecules which are essential for midbrain dopaminergic development are still not fully understood and are difficult to replicate *in vitro*. The midbrain region matures into different types of ventral midbrain dopaminergic neurons, establishing three different regions namely A8, A9 and A10. These will give rise to the retrorubral (RRF), substantia nigra pars compacta (SNpc) and ventral tegmental area (VTA), respectively. Dopaminergic neurons from the A9 region project to the dorsal striatum via the nigrostriatal pathway (Hegarty et al., 2013) and represent the population mostly affected in PD, being responsible for most of the associated motor dysfunction (Studer, 2012).

Tyrosine hydroxylase (TH) is the rate-limiting enzyme for dopamine synthesis (Figure 4) and is the most common used marker to identify midbrain dopaminergic neurons.

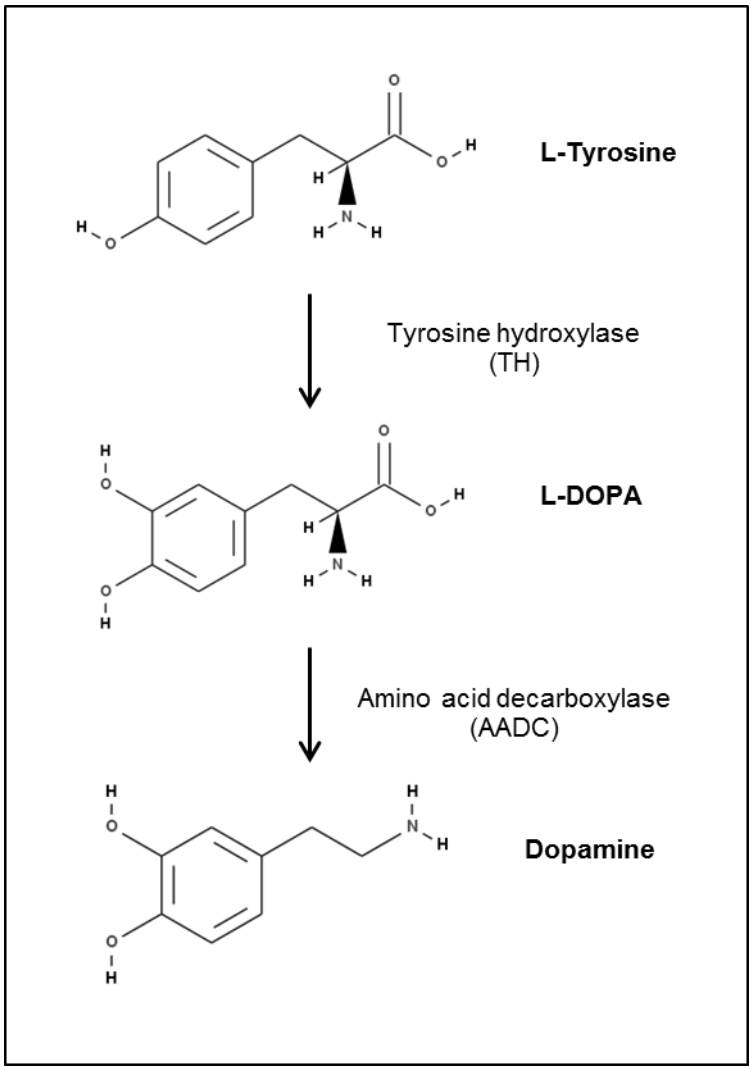

Figure 4 Pathway for the biosynthesis of dopamine. Tyrosine is hydroxylated to form L-DOPA by tyrosine hydroxylase. L-DOPA is then decarboxylated by AADC to form dopamine

However, TH expression is not specific for the midbrain and is also found in other catecholaminergic neurons (Studer, 2012) and several efforts have been made in recent years to identify specific markers for this cell population. Developmental studies have shown that ventral midbrain neuronal precursors express the floor plate markers LMX1A (Andersson et al., 2006) and FOXA2 (Kittappa et al., 2007), and further maturation into dopaminergic neurons results in the expression of EN1 (Davis and Joyner, 1988; Simon et al., 2001), Nurr1 (Zetterström, 1997) and the post-mitotic marker Pitx3 (Smidt et al., 1997). Of particular relevance for Parkinson's studies is the expression of the GIRK2 protein which has been suggested as an A9 neuronal marker, although its expression has also been reported in the VTA (Reyes et al., 2012). Altogether, these markers represent a reliable panel for the classification of DA neurons aiming at developing functional DA neuronal populations.

Since the advent of human induced pluripotent stem cells (hiPSCs), although efforts have been made to apply the developmental principles to the generation of dopaminergic neurons from these human pluripotent cells, efficient protocols were clearly required at the time this project started. Although some initial reports demonstrated the expression of TH-positive neurons derived from hiPSCs, some had no quantification of differentiation efficiency (Chambers et al., 2009) or very limited characterization of neuronal function (Cai et al., 2010). In addition, both reports used hiPSCs of embryonic origin (human fetal lung fibroblasts), which our lab has observed and others have shown (Theka et al., 2013) to have increased differentiation potential compared with hiPSCs of adult origin. A third report had shown a very low rate of differentiation efficiency, with only 3% of total cells expressing TH (Soldner et al., 2009). Later in 2010, two reports became available for hiPSCs dopaminergic differentiation (Cooper et al., 2010; Hargus et al., 2010), but both reported very low efficiencies of differentiation (up to 5% TH cells) and again without functional characterization of those neurons. The clear need for an efficient protocol led us to develop a

method that would allow the differentiation of functional DA neurons, which we could then utilise for further detailed studies on PD-related mechanisms. Due to the initial lack of human patient-derived hiPSC lines at the time the project started, conditions for efficient dopaminergic differentiation from mouse and human embryonic stem cells were initially optimised. All hiPSC lines used in this study were reprogrammed from adult fibroblast cells collected from a clinical cohort established within the Oxford Parkinson's Disease Centre (OPDC) and subsequently maintained at the James Martin Stem Cell Facility at the University of Oxford as described previously (Hartfield et al., 2014).

3.2 Dopaminergic differentiation of mouse ES cells

In order to better understand the principles regarding midbrain cell fate differentiation E14Tg2A mouse embryonic stem cells (mESCs) (Peruzzi et al., 2009) were cultured and differentiated into dopaminergic neurons. Using the commercially available Human/Mouse Dopaminergic Neuron Differentiation Kit (R&D Systems; SC001B), dopaminergic neurons were obtained after 3 weeks in culture. Cell differentiation was monitored throughout the protocol by bright field imaging (Figure 5) starting with the formation of EBs from undifferentiated cells, expansion of induced Nestin-positive cells, and finally, the formation of extensive neurite branching and neuronal networks. These networks were confirmed to be composed mostly of neurons as they expressed both the early neuronal marker Tuj1/β-3 Tubulin (hereafter referred to as Tuj1; Figure 6) and the mature neuronal marker MAP2 (Figure 7). Furthermore, these cultures were confirmed to contain high numbers of dopaminergic neurons, as confirmed by expression of TH (Figure 8). In addition, the expression of neuronal and dopaminergic markers was further confirmed by Western blot analysis of the proteins TH, neurofilament heavy chain (NFH) and Tuj1 (Figure 9).

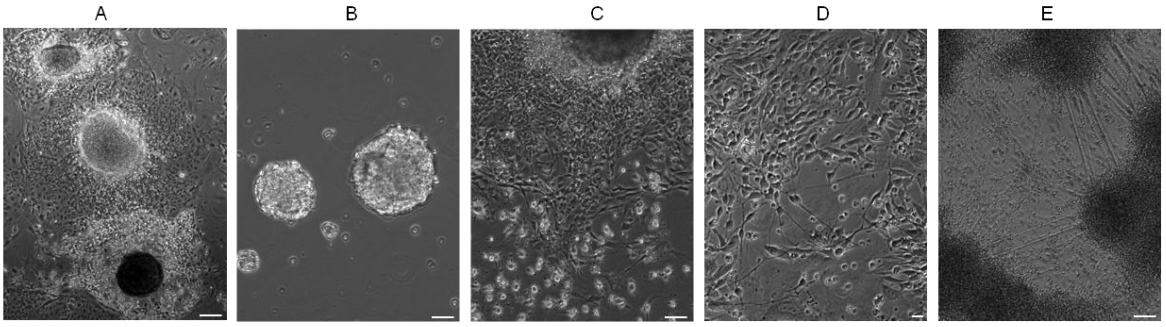

Figure 5 Bright field imaging of the sequencial steps involved in the dopaminergic differentiation of mESCs. A) Expansion of undifferentiated cells. B) Embryoid bodies formation. C) Selection of Nestin positive cells. D) Expansion of selected cells. E) Final dopaminergic neuron differentiation. Scale bar 70 μm.

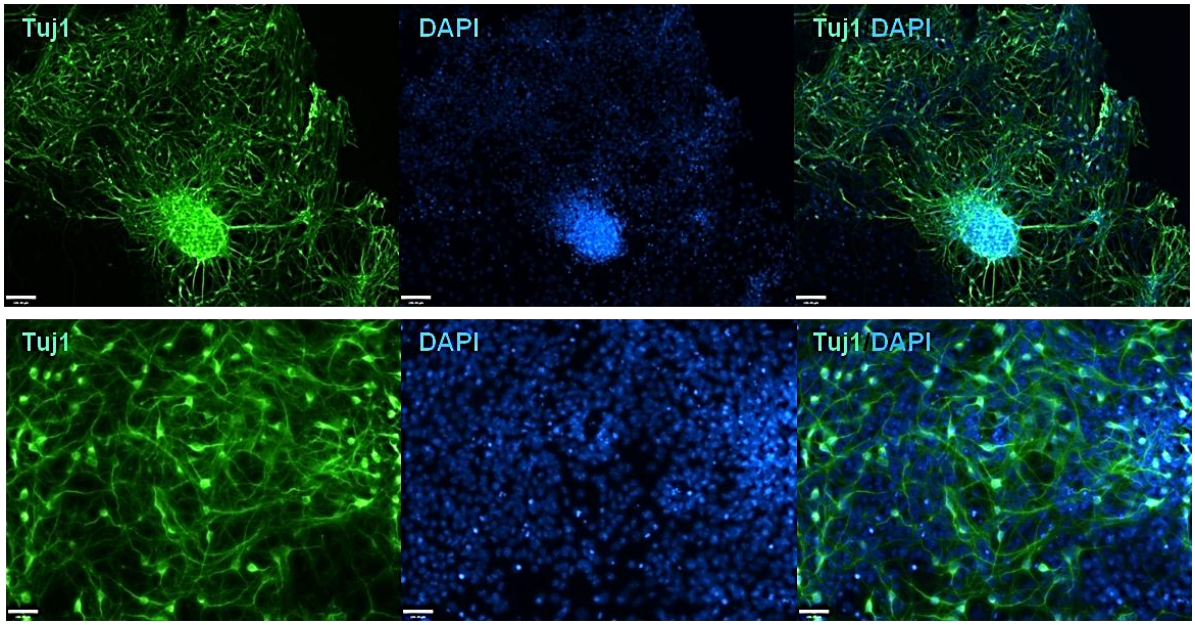

Figure 6 Efficient neuronal differentiation of mESCs. Immunocytochemistry analysis of differentiated neuronal cultures at day 31 showing high expression of the neuronal marker Tuj1 (green) and DAPI (blue). Scale bar: Top panel 70 µm, bottom panel 35 µm.

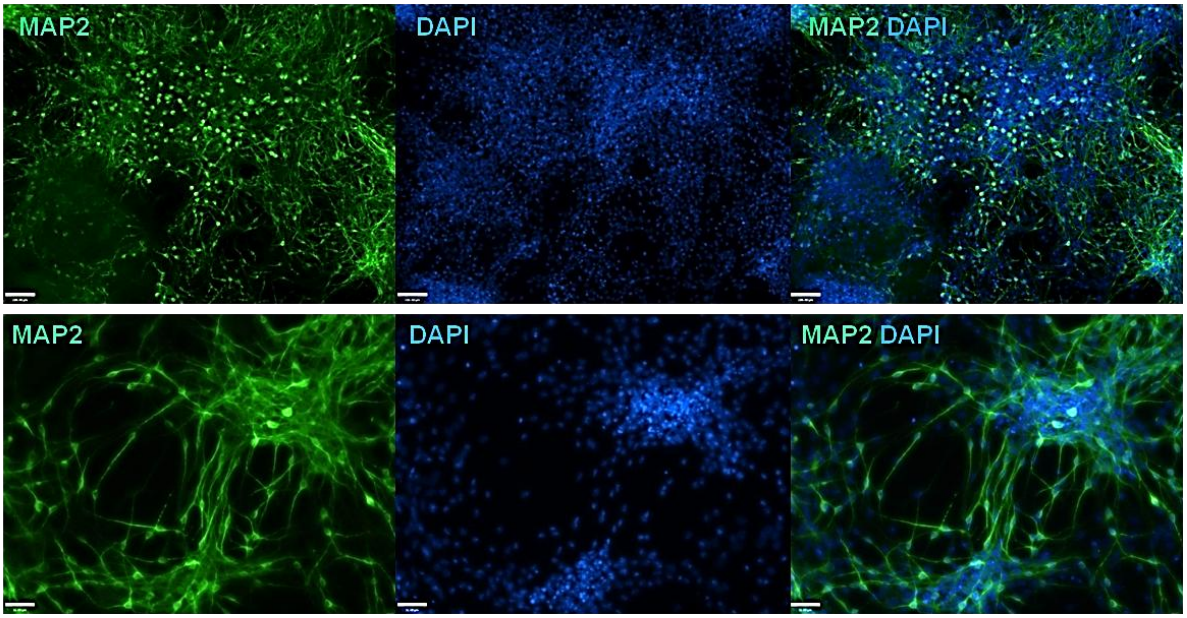

Figure 7 Differentiation of mature neurons from mESCs. Immunocytochemistry analysis of differentiated neuronal cultures at day 31 showing high expression of the mature neuronal marker MAP2 (green) and DAPI (blue). Scale bar: Top panel 70 µm, bottom panel 35 µm.

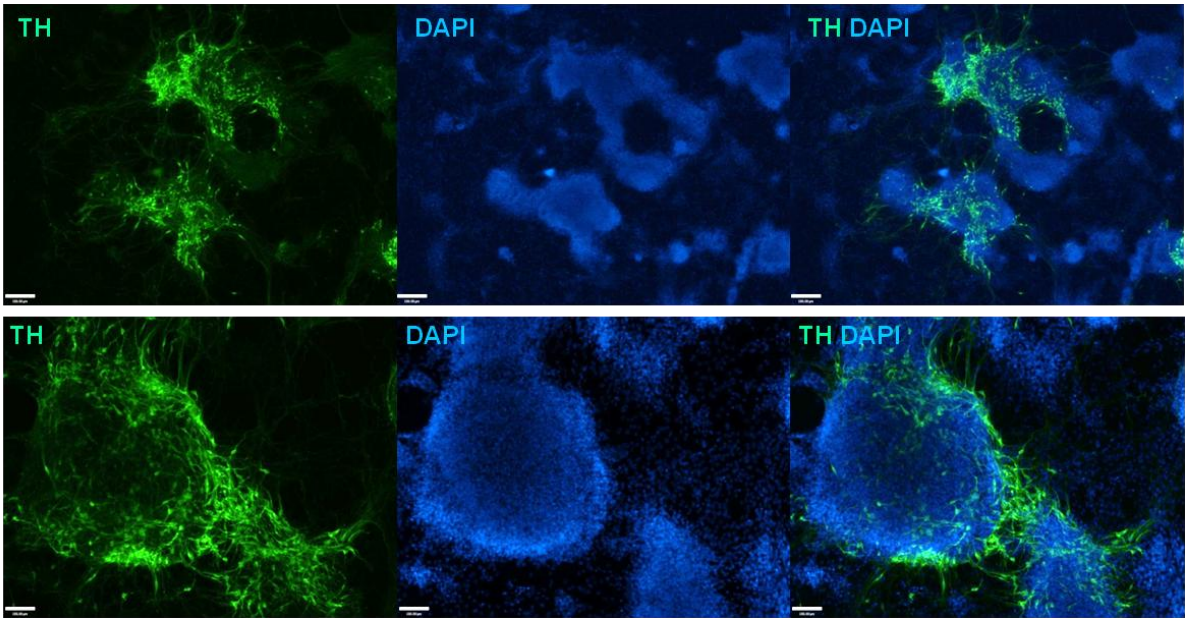

Figure 8 Dopaminergic neuronal differentiation from mESCs. Immunocytochemistry analysis of differentiated neuronal cultures at day 31 showing a high number of cells expressing the dopaminergic marker TH (green) and DAPI (blue). Scale bar: Top panel 70 µm, bottom panel 35 µm.

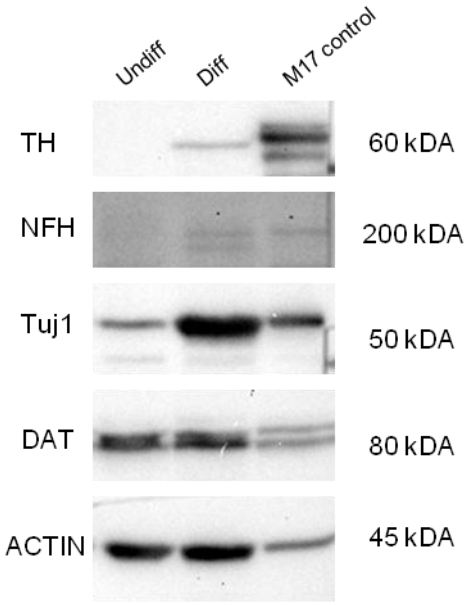

Figure 9 Dopaminergic neuronal protein expression in differentiated mESCs. Western blot analysis of undifferentiated (Undiff) and differentiated (Diff) mESCs. BE-(2)-M17 cells were used as control. Shown is the increase in expression of neuronal markers (NFH and Tuj1) and dopaminergic markers (TH and DAT) in dopaminergic differentiated cultures compared to undifferentiated cells. B-actin was used as a loading control. Lower intensity band for Actin on "M17 control" samples corresponds to lower amount of total protein loaded compared to "Undiff" or "Diff" samples.

3.3 Dopaminergic differentiation of human ES cells

Initial experiments in the human embryonic stem cell (hESC) line (HUES2) (Cowan et al., 2004) with the same Human/Mouse Dopaminergic Neuron Differentiation Kit (R&D Systems) used for mESCs were unsuccessful. Therefore, a new protocol described by Iacovitti L. et al 2007 (Iacovitti et al., 2007) was adapted with some modifications. Briefly, EBs were seeded onto Geltrex-coated plates in media supplemented with N-2 Supplement, Fibronectin and Noggin to induce the formation of neural rosettes. Four days later, bFGF was added to the media to allow expansion of rosettes. One week later cells were replated in media supplemented with dbcAMP to induce final differentiation of dopaminergic neurons. Using this protocol, HUES2 cells were differentiated into cells expressing Tuj1 and TH (Figure 10). However, most samples didn't survive this protocol (most cells died during the last step) and differentiation efficiency was low. High-performance liquid chromatography (HPLC) analysis of HUES2 dopaminergic cultures showed traces of 3,4-Dihydroxyphenylacetic acid (DOPAC), most likely as a result from the metabolization of dopamine by monoamine oxidase (MAO) (Table 6), while dopamine was not detected. To prevent degradation of dopamine in further experiments, the MAO inhibitor pargyline was added to the culture medium for 24 hours before harvesting cells for analysis.

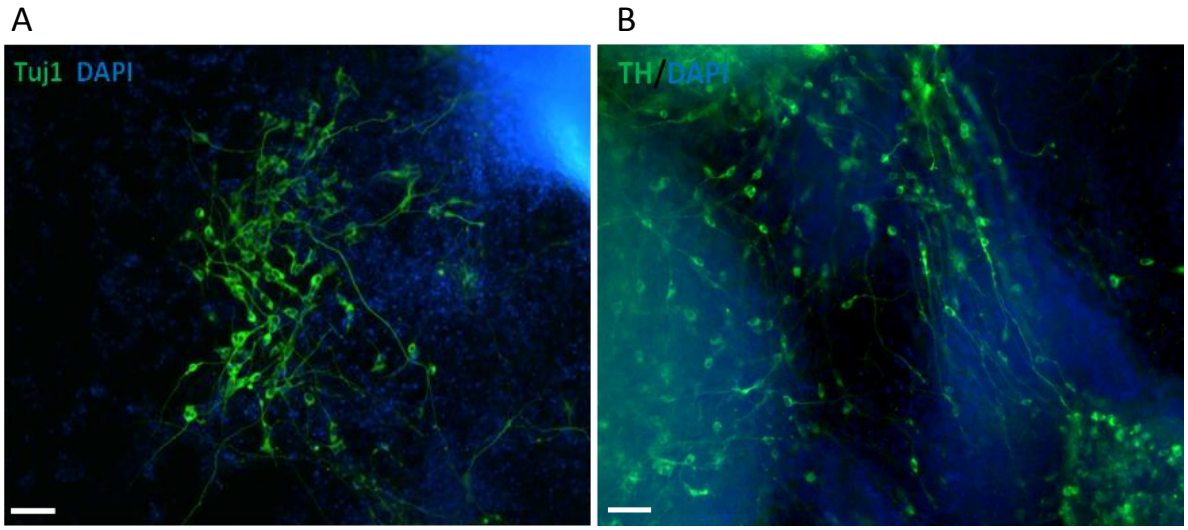

Figure 10 Differentiation of dopaminergic neurons from HUES2 cells. Immunocytochemistry analysis of differentiated neuronal cultures (HUES2) at day 21 showing expression of the neuronal marker Tuj1 (A) and the dopaminergic marker (TH) (B), and DAPI (blue). Scale bar: 70 µm. Obs: Only cells not replated for final step of differentiation survived.

Table 6 Synthesis of DOPAC by differentiated HUES2 cells. HPLC analysis of differentiated HUES cells after 21 days confirms the production of DOPAC

	Reten. Time [min]	Response	Amount [pM]	Amount [%]	Compound Name
HUES2 B18-Jun-2010	4.827	129.13	0.171	100	DOPAC
HUES2 A18-Jun-2010	4.823	51.701	0.183	100	DOPAC

Some optimizations were implemented to improve the reliability and efficiency of this protocol. These included the use of EBs made by forced aggregation in Aggrewell plates (Stem Cell Technologies) (Figure 11a). Aggrewell EBs of different cell densities (500, 1000, 2000 and 4000 cells/EB) were also tested in collaboration with our collaborators at James Martin Stem Cell Facility, with the highest density EBs being more robust and stable, compared to lower density EBs. Y-27632, a selective inhibitor of p160-Rho-associated coiled kinase (ROCK) was previously shown to increase survival of hES cells, by reducing apoptosis (Watanabe et al., 2007). The addition of ROCK inhibitor (ROCKi; Y27632) to the media in our cultures was shown to increase the size of neural progenitor cell colonies (Figure 11b). Since then, Y-27632 has been shown to increase survival and proliferation of hES-derived neural progenitor cells (Rungsiwiwut et al., 2013), to promote proliferation of cultures astrocytes (Yu et al., 2012) and to maintain proliferation of human mesenchymal stem cells (Nakamura et al., 2013). With the implemented optimizations the protocol became more robust and neurons expressing Tuj1 and TH more abundant (Figure 12).

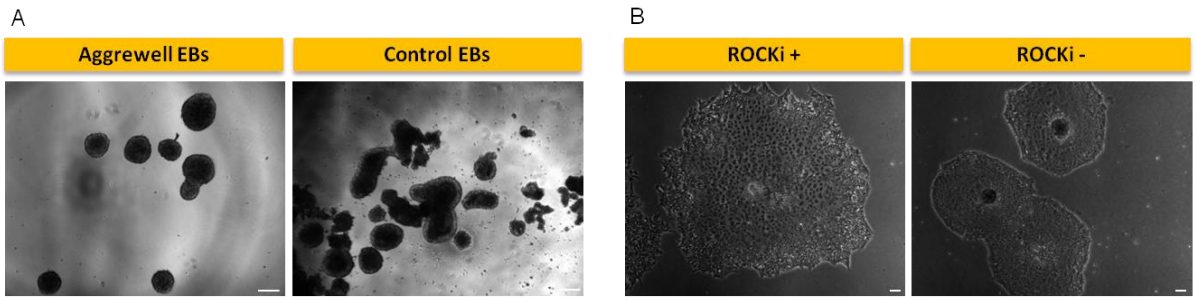

Figure 11 Optimisation of EB formation and survival. Further protocol adjustments to optimize differentiation efficiency of human stem cells. A) EBs obtained by forced aggregation in Aggrewell plates were more uniform forming less cystic structures. B) Cells grown in the presence of ROCKi show increase cell growth area after 4 days in culture. Scale bar 70 µm.

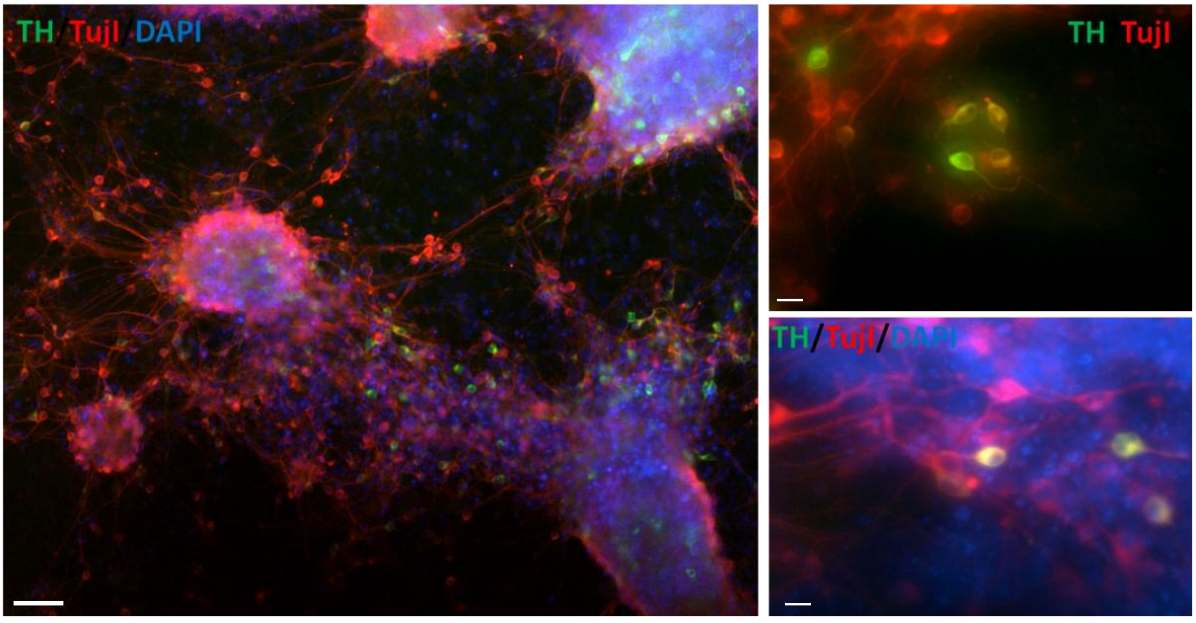

Figure 12 Optimisation of HUES2 differentiation into dopaminergic cultures. Immunocytochemistry analysis of differentiated neuronal cultures (HUES2) at day 21 showing expression of the neuronal marker Tuj1 (red), the dopaminergic marker (TH) (green), and DAPI (blue). Scale bar: Left panel 70 µm, right panels 18 µm.

3.4 Dopaminergic differentiation of human iPSCs

Upon availability of the first hiPSC lines generated from control healthy individuals, we applied the differentiation protocol previously developed for hESCs in the DF19.9 hiPSC line (see Table 7 below). Although cells differentiated into dopaminergic cultures containing neurons expressing Tuj1 and TH, the differentiation efficiency was not very high (Figure 13).

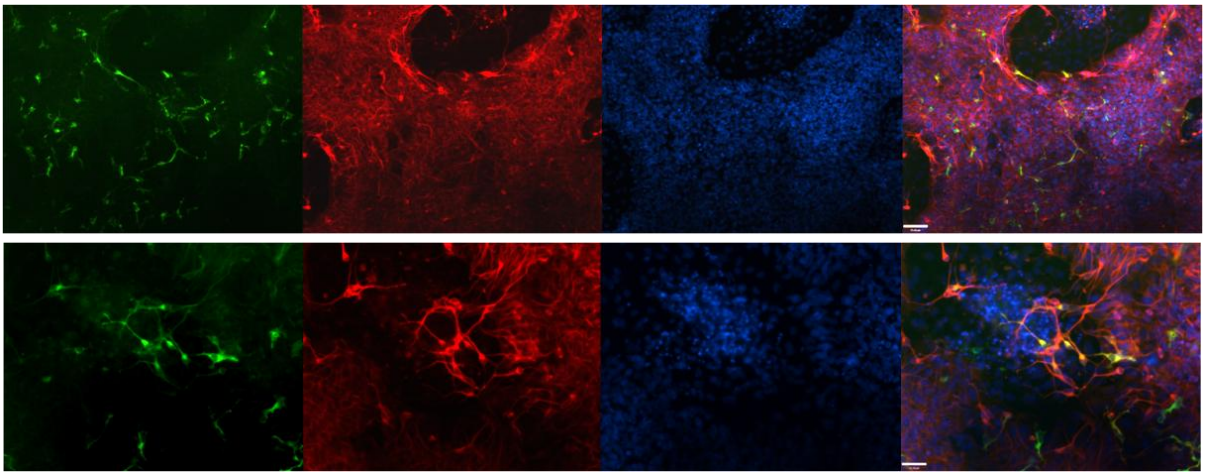

Figure 13 Differentiation of dopaminergic neurons from hiPSC DF19.9 cells. Immunocytochemistry analysis differentiated neuronal cultures (DF19.9) at day 21 showing expression of the dopaminergic marker (TH) (green), the neuronal marker Tuj1 (red) and DAPI (blue). Scale bar: Top panel 70 μm, bottom panel 35 μm.

Therefore, further alterations were introduced to the protocol, based upon a later report from *Cai J. et al 2010* (Cai et al., 2010) in which they described a protocol for dopaminergic neuron differentiation of hiPSCs. Alterations included the addition of B27 supplement, and expansion of the final step of differentiation with dcAMP from 1 to 3 weeks. However, these alterations did not improve dopaminergic differentiation efficiency which was also reflected by no dopamine being detected by HPLC.

In order to improve differentiation efficiency and maturation of dopaminergic cells, a new protocol was developed based on a report from (Chambers et al., 2009), with several alterations (Figure 14). Briefly, EBs prepared from hiPSCs were plated in the presence of SMAD signalling inhibitors (Noggin and SB431542) to initiate neuronal induction, together with CHIR99021 (potent WNT signalling activator), sonic hedgehog (SHH) and FGF8a for midbrain floor plate induction (Kriks et al., 2011; Xi et al., 2012). By day 20, visible neural rosette structures (Figure 15) were manually dissected and re-plated for differentiation into dopaminergic neurons with ascorbic acid, cAMP, BDNF and GDNF for fifteen days.

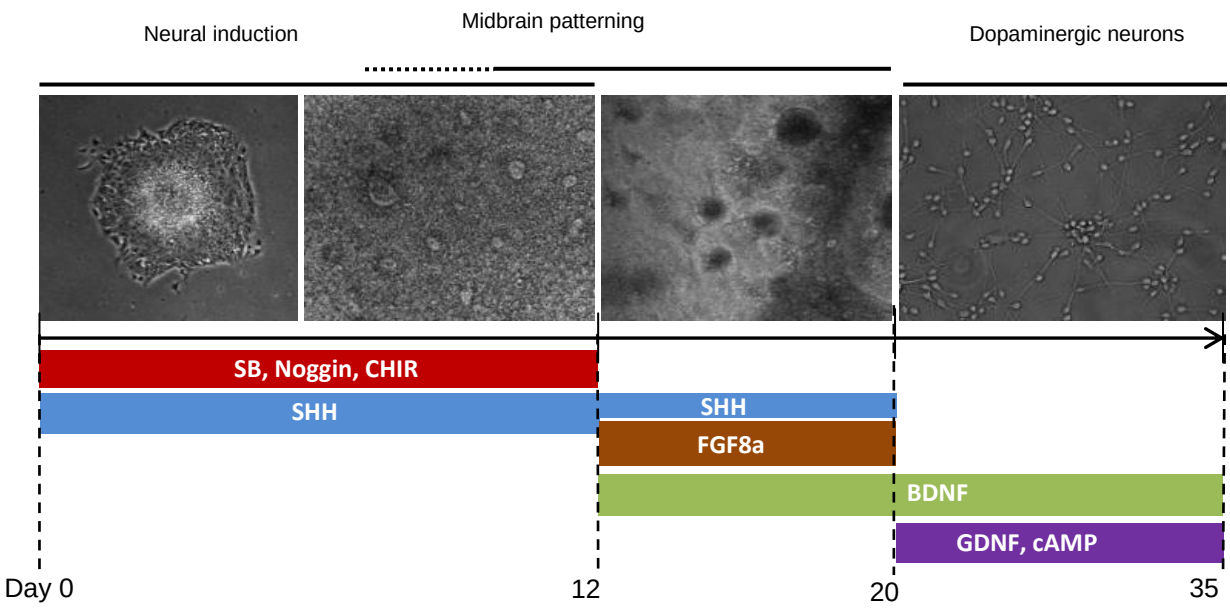

Figure 14 Dual SMAD inhibition differentiation protocol developed for differentiation of dopaminergic neuronal cultures from hiPSCs. Schematic overview of conditions used for differentiation of hiPSCs into dopaminergic neuronal cultures, with bright field representations of cells at several stages of differentiation. SB, SB431542; CHIR, CHIR99021.

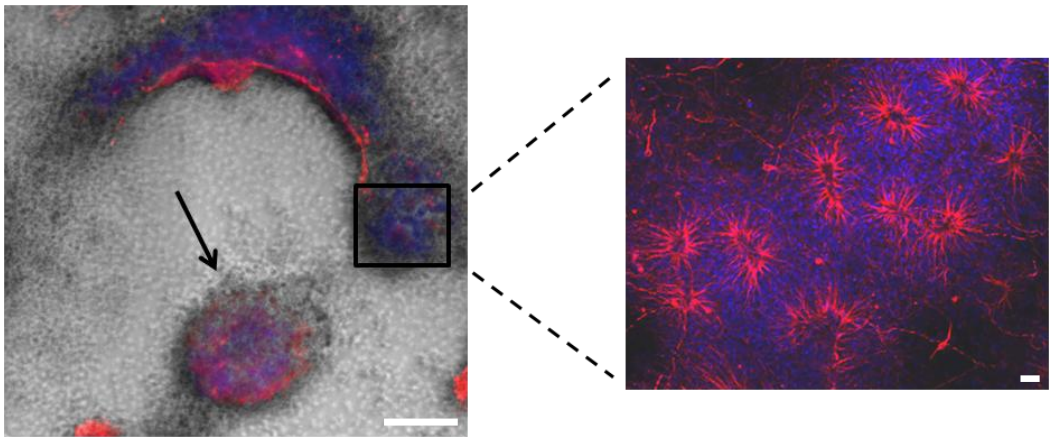

Figure 15 Neural rosettes and neural-like structures selected and replated for the final stage of dopaminergic differentiation. Left shows a merged image of bright field and immunolabelled cells for DAPI (blue) and the early neuronal marker Tuj1 (red). Right image shows with higher magnification an example of neural rosettes which were manually passaged for the final differentiation. Tuj1 (red) and DAPI (blue). Scale bar 70 μm.

This protocol was then applied to multiple control hiPSC lines made available at the time. IMR90-4 (Figure 16), Control 1#1 (Figure 17), Control 1#2 (Figure 18), Control 1#6 (Figure 19) and Control 2 hiPSC lines (Table 7) were all successfully differentiated into dopaminergic neurons following this protocol, as determined by expression of TH and Tuj1.

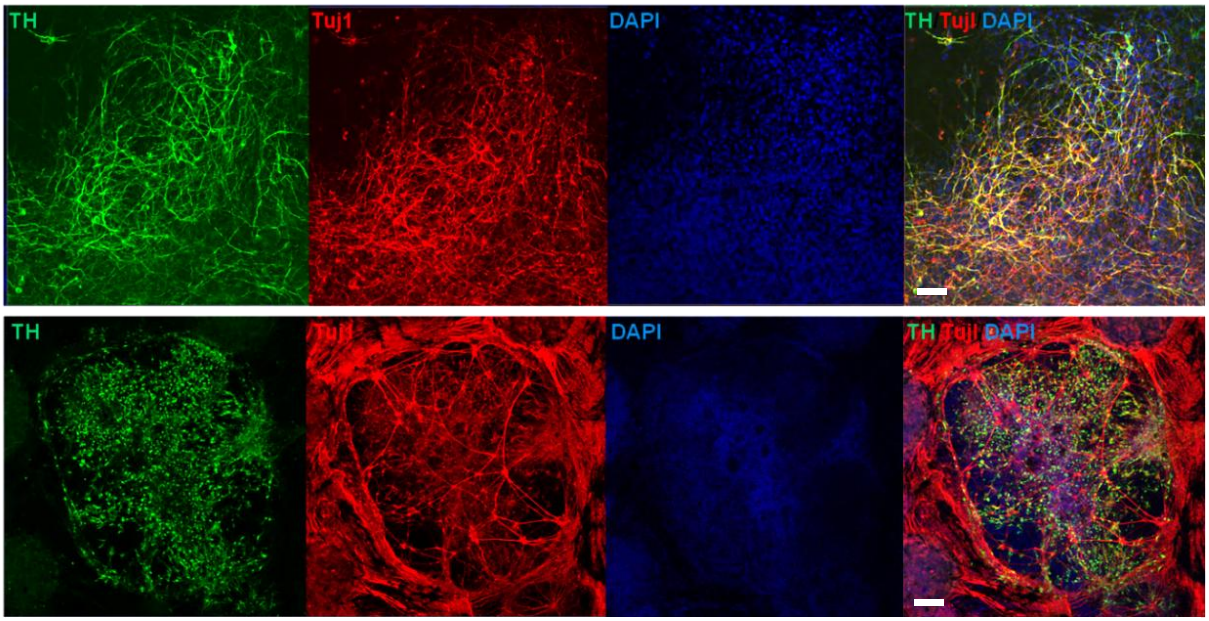

Figure 16 Differentiation of dopaminergic neurons from the IMR90-4 hiPSC line. Immunocytochemistry analysis of differentiated neuronal cultures (IMR90-4) at day 35 showing expression of the dopaminergic marker (TH) (green), the neuronal marker Tuj1 (red) and DAPI (blue). Scale bar: Top panel 35 µm, bottom panel 70 µm.

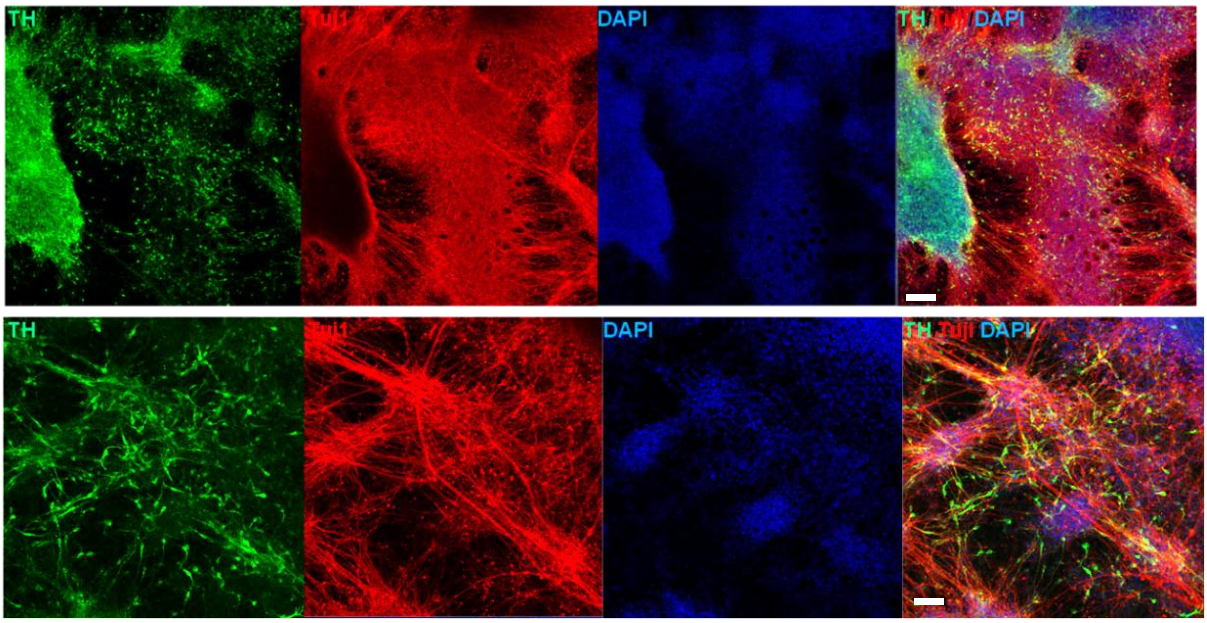

Figure 17 Differentiation of dopaminergic neurons from the Control 1#1 hiPSC line Immunocytochemistry analysis of differentiated neuronal cultures (Control 1#1) at day 35 showing expression of the dopaminergic marker (TH) (green), the neuronal marker Tuj1 (red) and DAPI (blue). Scale bar: Top panel 70 µm, bottom panel 35 µm.

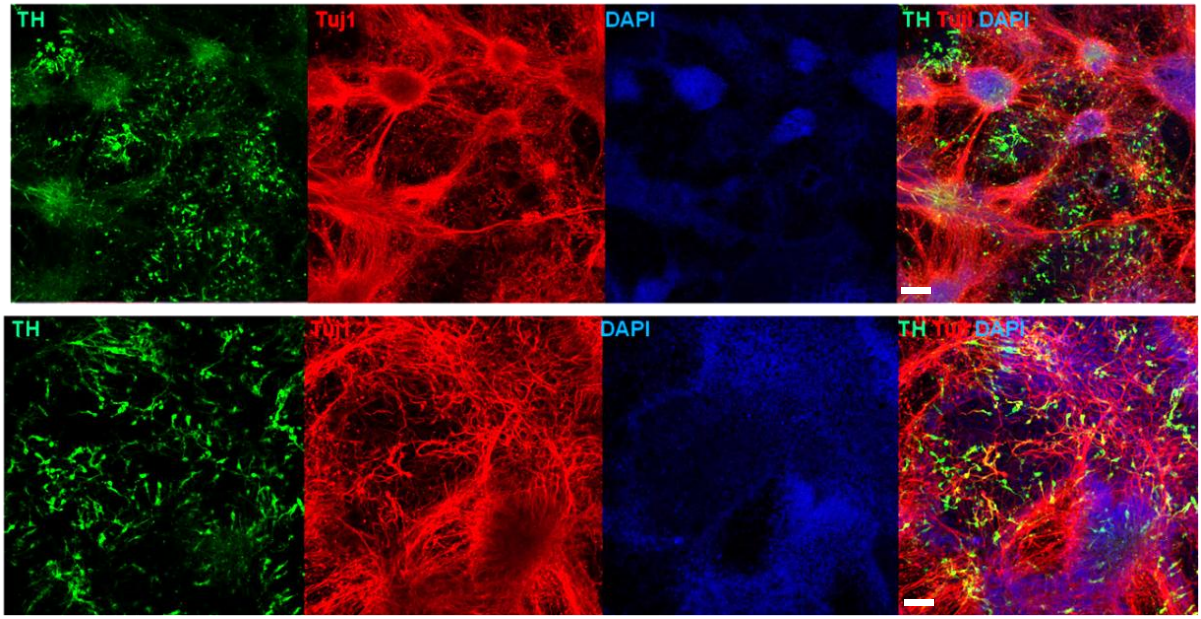

Figure 18 Differentiation of dopaminergic neurons from the Control 1#2 hiPSC line. Immunocytochemistry analysis of differentiated neuronal cultures (Control 1#2) at day 35 showing expression of the dopaminergic marker (TH) (green), the neuronal marker Tuj1 (red) and DAPI (blue). Scale bar: Top panel 70 µm, bottom panel 35 µm.

It is important to note that clonal line 6 from Control 1 (Control 1#6), although capable of efficient dopaminergic differentiation (Figure 19), was found to have a translocation and amplification of part of chromosome 2 (Hartfield et al., 2014). Therefore, this line was not included in further experiments.

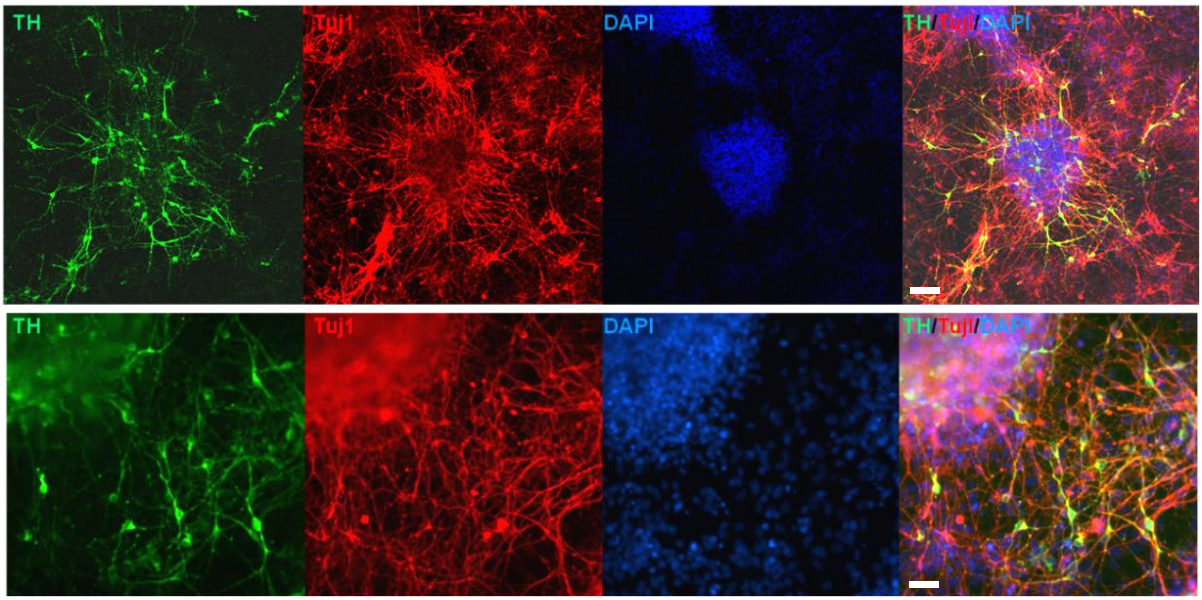

Figure 19 Differentiation of dopaminergic neurons from the Control 1#6 hiPSC line. Immunocytochemistry analysis of differentiated neuronal cultures (Control 1#6) at day 35 showing expression of the dopaminergic marker (TH) (green), the neuronal marker Tuj1 (red) and DAPI (blue). Scale bar: Top panel 35 μm, bottom panel 18 μm.

In collaboration with Dr Elizabeth Hartfield, differentiation efficiency was assessed by quantification of β-3tubulin and TH-expressing cells, across multiple rounds of differentiation. Both Control 1 and Control 2 cell lines differentiated with similar efficiency into neurons (around 40% of total cells) and into TH expressing neurons (around 35% of total neurons) (Figure 20). Only these 2 lines were considered for further studies as they were newly generated within the OPDC and could be later compared with PD derived lines using the same methodology.

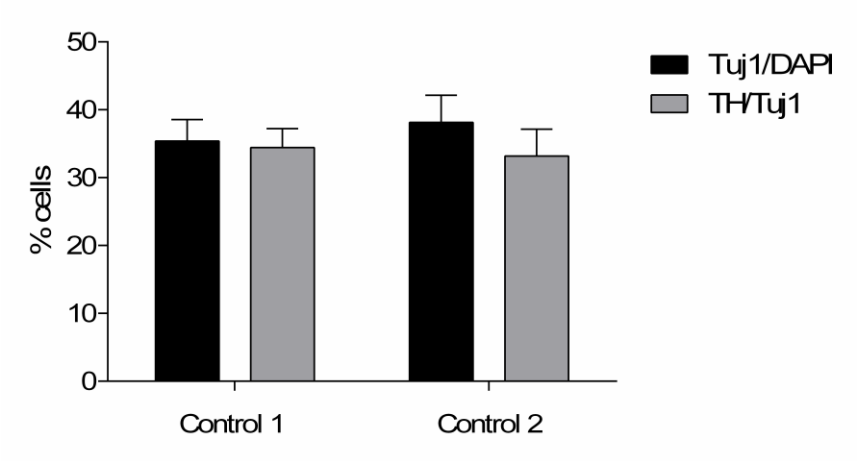

Figure 20 Efficiency of neuronal and dopaminergic differentiation for control hiPSCs. Neuronal and dopaminergic differentiation efficiency across control lines used, expressed as percentage of total cells. Control 1 includes data from two independent clonal lines (#1 and#2). Data represent mean ± SEM of at least 3 independent differentiations. Two-way ANOVA with Tukey post hoc analysis, not significant. Differentiation of hiPSCs was performed by HF. Quantification of cells expressing neuronal (TUJ1) and dopaminergic neurons (TH) markers was performed by EH.

Table 7. Detailed description of control hiPSC lines used for dopaminergic differentiation in this study.

hiPSC ID	Details	Reprogramming strategy	Tissue of origin	Source
Control 1#1 Control 1#2 Control 1#6	Clones derived within OPDC	Lentiviral transduction (Oct3/4, Sox2, c-Myc, Klf4 and NANOG)	Human adult dermal fibroblasts	LONZA
Control 2	Clones derived within OPDC	Lentiviral transduction (Oct3/4, Sox2, c-Myc, Klf4 and NANOG)	Human adult dermal fibroblasts	OPDC
DF19.9	Commercially available	Nucleofection with EBNA episomal vectors (OCT4, SOX2, NANOG, LIN28, c-Myc, KLF4, and SV40LT)	Human foreskin fibroblasts	WiCell
IMR90-4	Commercially available.	Lentiviral transduction (OCT4, SOX2, NANOG, and LIN28)	IMR-90 fetal lung fibroblasts	WiCell

To confirm that the derived DA neurons were of mature ventral midbrain origin, gene expression studies were performed in collaboration with Dr Jennifer Badger. RT-PCR analysis of differentiated dopaminergic cultures showed downregulation of the pluripotency gene *OCT4* and upregulation of the midbrain floor plate markers FOXA2 and LMX1A, in addition to the mature dopaminergic neuron markers EN1 and NURR1 (Figure 21). Further work carried out in our laboratory by Dr Elizabeth Hartfield confirmed that TH-expressing cells were also shown to co-express the floor plate marker FOXA2, the post-mitotic midbrain neuronal marker PITX3, and importantly also with GIRK2, a putative marker for the PD susceptible A9 DA neurons (Hartfield et al., 2014). Altogether, these results further suggest a mature midbrain identity of the differentiated dopaminergic cultures obtained using the developed protocol.

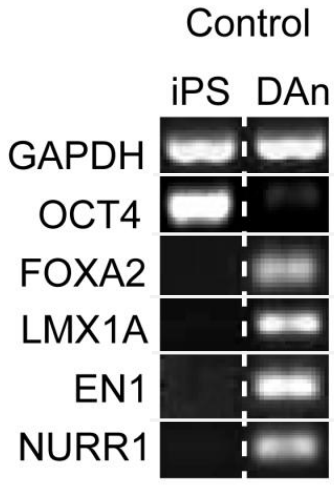

Figure 21 Differentiated dopaminergic cultures from control hiPSC lines express multiple markers with ventral midbrain characteristics. RT-PCR analysis shows reduced expression of the pluripotency marker OCT4 and increased expression of floor plate markers (FOXA2 and LMX1A) and mature dopaminergic markers (EN1 and NURR1) in differentiated cultures (DAn) vs undifferentiated cells (hiPSCs). Differentiation into dopaminergic cultures, RNA extraction and preparation and primers design performed by HF. RT-PCR reaction and gel imaging performed by JB.

Finally, the expression of proteins relevant for this study and possibly implicated in PD pathology like GBA, LAMP1 and α-synuclein were also confirmed in dopaminergic neurons derived from hiPSCs (Figure 22).

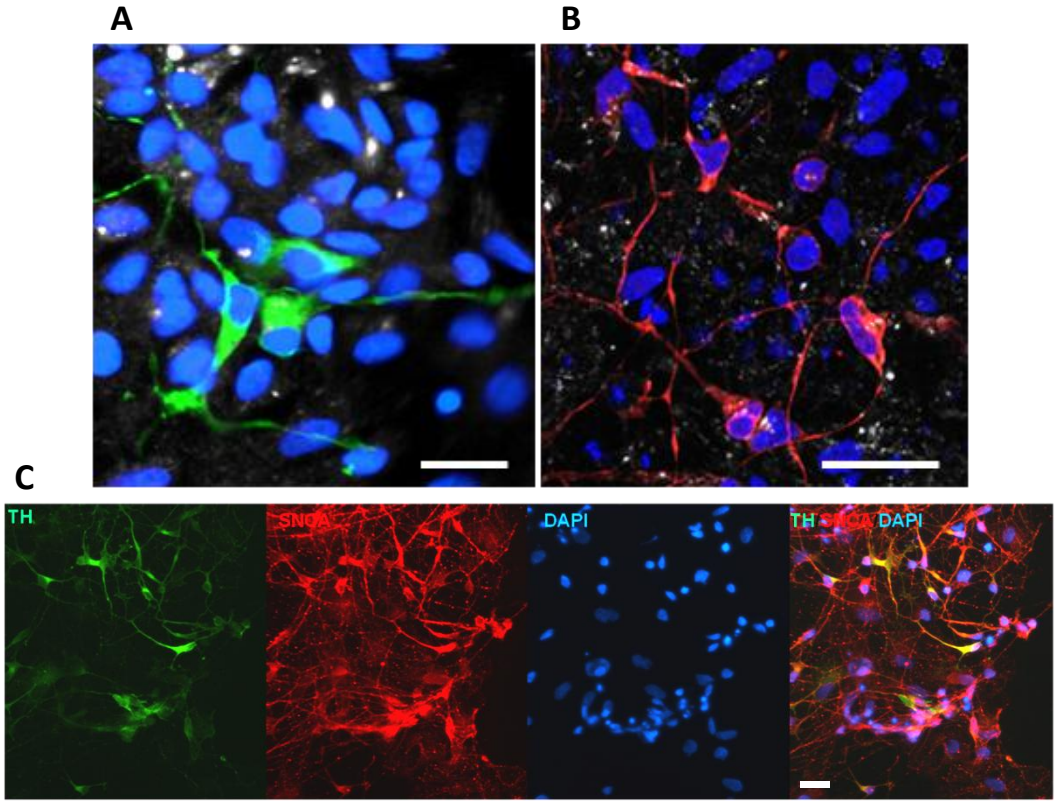

Figure 22 Expression of multiple proteins possible implicated in the pathogenesis of PD, in dopaminergic neurons derived from hiPSCs. Immunocytochemistry analysis of differentiated neuronal cultures. **A**) Expression of the dopaminergic marker (TH) (green), the lysosomal enzyme GBA (white) and DAPI (blue). **B**) Expression of the dopaminergic marker (TH) (red), the lysosomal marker LAMP1 (white) and DAPI (blue). **C**) Expression of the dopaminergic marker (TH) (green), α-synuclein red (white) and DAPI (blue). Scale bar: 18 μm.

3.5 Human iPSCs derived dopaminergic neurons are functional

To confirm that the differentiated neurons were also functionally active the dopaminergic function of these neurons was investigated. In addition to TH, the expression of amino acid decarboxylase (AADC), another enzyme involved in dopamine synthesis was also confirmed to be highly expressed in differentiated dopaminergic cultures (Figure 23A). Dopamine synthesis was also confirmed by HPLC analysis of differentiated dopaminergic cultures (Figure 23B). Dopamine is generated from the precursor L-3,4-dihydroxyphenylalanine (L-DOPA) by the AADC enzyme, which we confirmed earlier to be expressed in differentiated neurons. To determine if there was any limitation in terms of L-tyrosine availability in the media for production of dopamine or TH activity that could repress efficient dopamine production by differentiated dopaminergic neurons, cultures were supplemented with L-DOPA. This resulted in a great increase of dopamine levels, which indicates AADC activity (Figure 23B)

Detection of the dopamine transporter (DAT), a crucial element for dopamine homeostasis, was shown by Dr Elizabeth Hartfield in our laboratory (Hartfield et al., 2014). Functional DAT activity was also confirmed using ^{3}H-DA uptake which could be blocked by mazindol, a selective DAT inhibitor (Figure 23C).

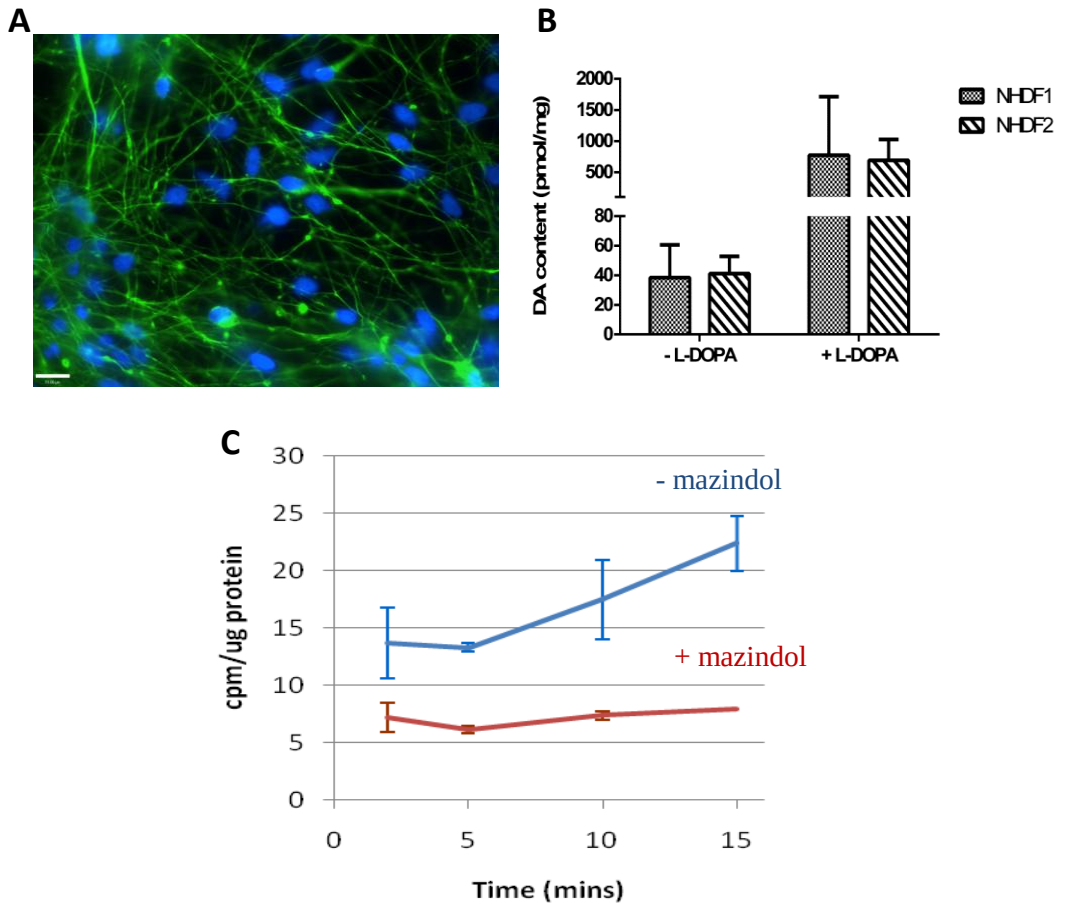

Figure 23 hiPSCs derived dopaminergic neurons are functional. **A**) Immunocytochemistry analyses confirmed high expression of ADDC (green) in differentiated dopaminergic cultures. **B**) Quantification of dopamine content in differentiated neurons by HPLC. Differentiated neurons produced dopamine (48.98 pmol/mg ± 0.389) and were responsive to L-DOPA (933.14 pmol/m g± 220.71. Data shown are from 4-6 wells each of 2 independent experiments and is expressed as mean ± SEM. **C**) Tritiated dopamine (3H-DA) uptake shows that dopaminergic neuronal cultures derived from hiPSCs have DAT-dependent uptake of dopamine that is blocked by the DAT inhibitor mazindol. Scale bar: 18 µm.

Furthermore, it was observed that differentiated dopaminergic cultures obtained from hiPSCs in culture established dense neuronal networks with extensive branching (Figure 24).

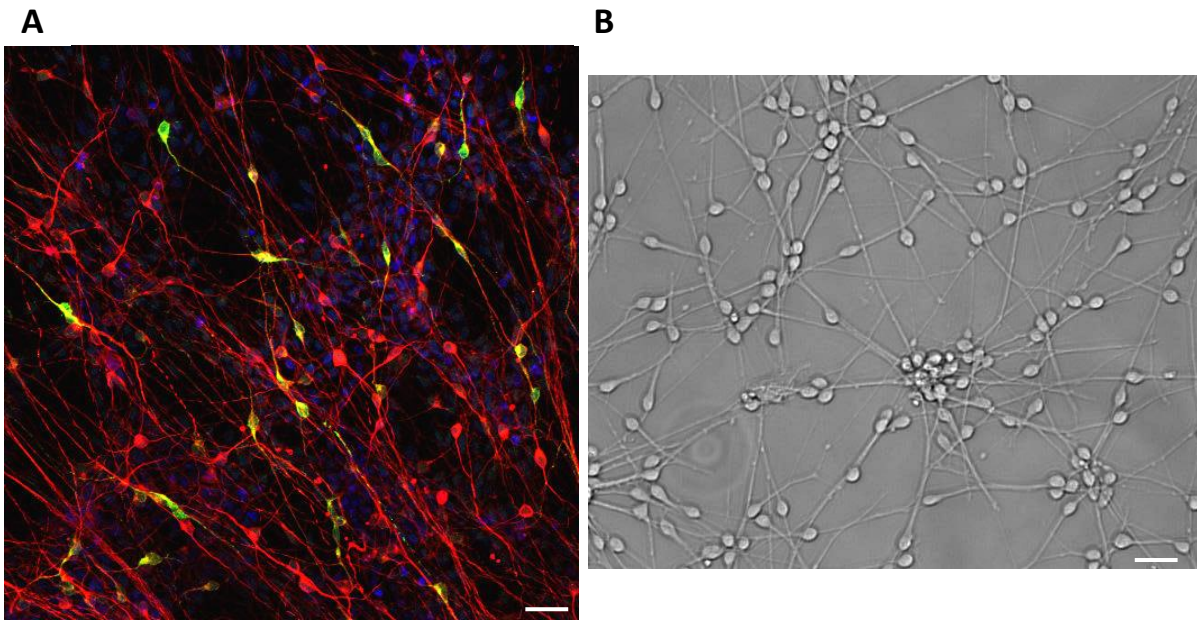

Figure 24 hiPSC-derived dopaminergic cultures developed into dense neuronal networks with extensive brancing. After 35 days of differentiation, dopaminergic neuronal cultures developed vast neuronal networks. **A**) Immunocytochemistry representation showing expression of the dopaminergic marker (TH) (green), the neuronal marker Tuj1 (red) and DAPI (blue). B) Bright field image of differentiated dopaminergic neuronal cultures. Scale bar 35 μm.

Neurons extended vast neurites from neuronal progenitor clusters, which ended up connecting with neurons from neighbouring clusters, reaching vast lengths (Figure 25). Importantly, long term in vitro culture of dopaminergic cultures was also attained, as cells survived up to at least 7 months in culture, developing extensive and further intricate neuronal networks (Figure 26)

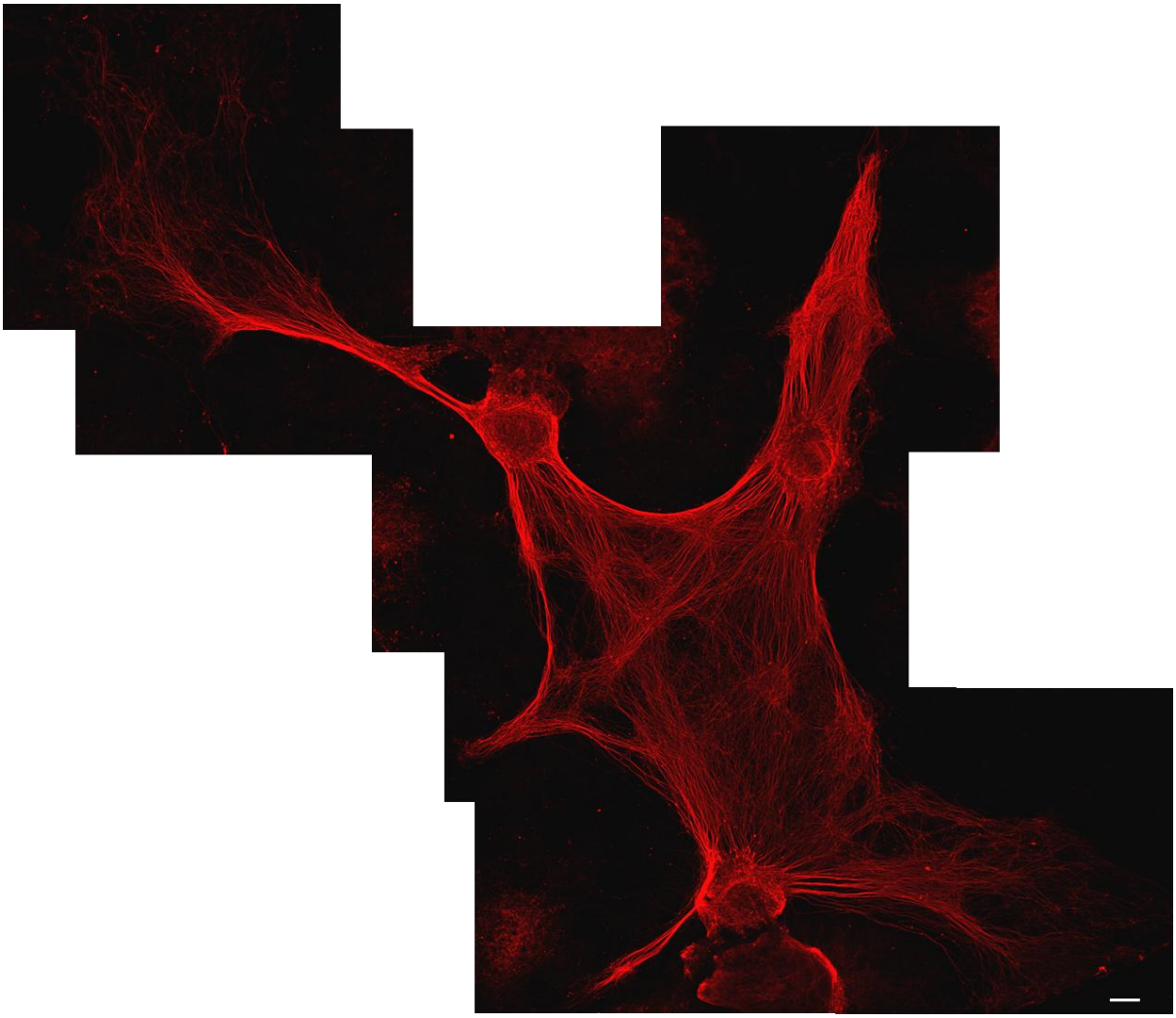

Figure 25 Differentiated hiPSCs established long neurites. Differentiated dopaminergic cultures developed dense neuronal structures with connections made between distant neuronal rosette structures, with axons reaching vast lengths. Immunocytochemistry representation showing expression of the neuronal marker Tuj1 in red. Scale bar 175 µm.

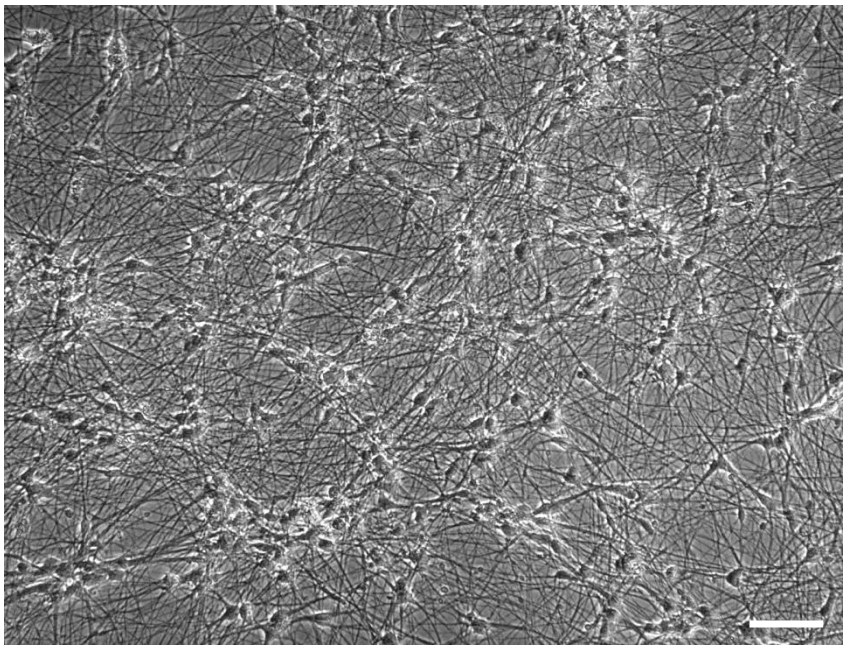

Figure 26 Differentiated hiPSCs were stable after long periods of time in culture. Bright field image of a 7 month old dopaminergic culture derived from a control hiPSC line showing extensive and intricate neuronal networks. Scale bar 70 μm.

3.6 Discussion

In this chapter the derivation of dopaminergic neurons from several types of stem cells was explored. Mouse ESCs were initially tested and successfully differentiated into TH-expressing neurons. While waiting for the availability of human iPSCs, either from commercial sources or reprogrammed by collaborators, a protocol for dopaminergic differentiation using hESCs was optimised. This approach aimed at developing an efficient protocol for the neuronal differentiation of hESCss that could later be applied to hiPSCs. However when the hESC protocol was applied to hiPSCs, the differentiation efficiency was limited.

We then developed a new protocol, based on a previously published report by (Chambers et al., 2009) using hiPSCs of embryonic origin, with multiple modifications based on several protocols published at the time. This protocol was the first to suggest a novel neural induction strategy based on an initial dual inhibition of SMAD signalling, by inhibiting BMP signalling using noggin, and inhibiting TGFβ signalling using the compound SB431542 (Chambers et al., 2009). The use of alternative BMP signalling inhibitors has since been reported, including dorsomorphin (Mak et al., 2012) and LDN-193189 for hESCs (Kriks et al., 2011) and for hiPSCs (Xi et al., 2012). The use of an early high dose of a more potent SHH recombinant protein (SHH-C24II) for floor plate induction was introduced based on an initial report in hESCs by (Fasano et al., 2010), and later supported by others (Kirkeby et al., 2012). Early activation of WNT signalling suggested by (Cooper et al., 2010) for midbrain patterning of neural progenitors was also incorporated in our protocol after the identification of a potent activator, CHIR99021 (CHIR) in DA differentiation of hESCs (Kriks et al., 2011). The concentration and time of exposure to this small molecule was then adjusted based on later reports (Kirkeby et al., 2012; Xi et al., 2012). Others have used the compound CT99021,

another GSK3β inhibitor as an alternative to WNT signalling activation (Kirkeby et al., 2012). Finally, the specific use of FGF8a to improve midbrain development, as suggested by (Cooper et al., 2010) was also integrated in the protocol.

This newly developed protocol, when applied to multiple hiPSCs derived from healthy control individuals, was found to be efficient for obtaining ventral midbrain dopaminergic neurons. Differentiation efficiency attained with our protocol (35% TH/Tuj1) was comparable to results from some labs that have published their results in the meantime (Devine et al., 2011; Mazzulli et al., 2011; Seibler et al., 2011; Cooper et al., 2012; Sánchez-Danés et al., 2012; Rakovic et al., 2013; Reinhardt et al., 2013), and better than reported by others (Soldner et al., 2009; Cai et al., 2010; Cooper et al., 2010; Nguyen et al., 2011). The short period of time needed to develop dopaminergic neurons using this protocol is also an advantage when compared to many of the protocols available (Cooper et al., 2010)(Cai et al., 2010)(Byers et al., 2011)(Jiang et al., 2012). Confirmation of expression of further midbrain mature markers other than just TH is of utmost importance, and I and colleagues in our laboratory have extensively characterized our iPSC-derived neurons to confirm their identity (Hartfield et al., 2014). In addition, and crucial for further dopaminergic specific analysis, differentiated dopaminergic cultures were shown to produced dopamine and be responsive to L-DOPA, indicating highly active ADDC, which expression was also confirmed by immunofluorescence. Functional DAT activity was also demonstrated, confirming that these mature differentiated cultures of dopaminergic neurons are able to synthesise and uptake dopamine. Expression of these markers suggests that dopaminergic neurons in culture acquired a neurotransmitter identity(Hegarty et al., 2013). Further functional studies of neurons differentiated using this protocol were performed by others in our lab, including demonstration of a physiological resting membrane potential of -70 mV. Spontaneous sub-threshold pace-making and regular calcium oscillations were also confirmed (Hartfield et al.,

2014) which are typical characteristics of the A9 dopaminergic neurons (Guzman et al., 2009) more susceptible in PD. This extensive battery of functional assays has been disregarded in some published reports, which might render the interpretation of results obtained using those protocol more difficult.

As cells differentiated for longer periods of time, neurons established dense neuronal elongations with extensive branching where axons/neurites were capable of reaching vast distances. This observation might be highly relevant as extensive axonal network characteristic of A9 neurons has been suggested to render these neurons more vulnerable to cell death in PD, due to a high energy demand associated with this arborisation (Pissadaki and Bolam, 2013). Long term stability of these cultures was also achieved, as cells were shown to be stable for up to 7 months in culture, developing even more complex morphological networks. Altogether, this could be potentially relevant for future studies on cell interaction, energy demand and cell maturation studies in the future.

All control hiPSCs used in this study were generated within the OPDC and were subjected to rigorous quality control tests and are fully characterized elsewhere (iPS-OX1-19 (Van Wilgenburg et al., 2013); Control 1#1 and Control 1#2 (Hartfield et al., 2014)). This included genome integrity assessment by Illumina CytoSNP-12-v2.0 array, silencing of retroviral transgenes used for reprogramming and pluripotency assessment by TRA-1-60 and SSEA-4 expression and by Pluritest (Müller et al., 2011) analysis. Cell lines that failed this vast battery of tests for pluripotency and genome integrity were discarded. The example of Control 1#6 is given where a translocation was detected, although dopaminergic differentiation didn't seem to be affected. We believe that for a detailed and comprehensive study of mechanisms involved in disease pathology it is of outmost importance to confirm the quality and stability of the lines used, and discard the ones that do not fit these pre-established requirements.

Chapter 4

Identification of PD patients carrying heterozygous *GBA* mutations and establishment of patient-derived dopaminergic cultures

4.1 Introduction

4.1.1 Screening for *GBA* mutation carriers

After the first clinical reports of increased frequency of PD in relatives of Gaucher's disease (GD) patients (Tayebi et al., 2003b; Goker-Alpan et al., 2004; Halperin et al., 2006), many PD centres worldwide assessed the frequency of glucocerebrosidase (*GBA*) mutations in their cohorts. In 2004, *Lwin et al* (Lwin et al., 2004) first reported *GBA* mutations in 21% of autopsy brain samples from 57 PD patients. These mutations were more frequent among younger subjects and the vast majority of those (83.3%) were due to heterozygous *GBA* mutations. In that same year, another study confirmed the high frequency of *GBA* mutations in a group of 99 PD patients of Ashkenazi Jewish ancestry, where 31.3% carried a *GBA* mutation (Aharon-Peretz et al., 2004). Since then, several other groups have observed similar results in several populations across the world, usually associated with an earlier onset of PD (Table 8)

Table 8 Published studies for frequency of *GBA* mutations found in PD populatons.

Reference	Population sample(n)		GBA mutation frequency (%)		Most common variant	Population
	PD	Control	PD	Control		
(Lwin et al., 2004)	57	44	21.0	0.0	N370S	Mixed
(Aharon-Peretz et al., 2004)	99	1543	31.3	6.2	N370S	Ashkenazi
(Clark et al., 2005)	160	92	10.7	4.3	N370S	Ashkenazi
(Sato et al., 2005)	88	122	5.7	0.8	Rec*Nci*1	Caucasian (Canadian origin)
(Toft et al., 2006)	311	474	2.3	1.7	N370S	Norwegian
(Eblan et al., 2006)	33	31	12.0	3.2	Rec*Nci*1, L444P	Mixed (non-Jewish)
(Wu et al., 2007)	518	339	3.1	1.2	Rec*Nci*1, L444P	Taiwanese
(Clark et al., 2007)	278	179	13.7	4.5	N370S, c.84dupG	(Mixed, 64% Jewish)
(Ziegler et al., 2007)	92	92	4.3	1.1	L444P	Chinese
(Tan et al., 2007)	331	347	2.4	0.0	L444P	Chinese
(Spitz et al., 2008)	65	267	3.0	0.0	L444P	Brazilian
(De Marco et al., 2008)	395	483	2.8	0.2	L444P	Italian
(Mata et al., 2008)	721	554	2.9	0.4	N370S, L444P	Mixed
(Gan-Or et al., 2008)	420	333	17.9	4.2	N370S	Ashkenazi
(Kalinderi et al., 2009)	172	132	4.7	0.8	H255Q, L444P	Greek
(Bras et al., 2009)	230	430	6.1	0.7	N370S, N396T	Portuguese
(Neumann et al., 2009)	790	257	4.2	1.2	N370S, L444P	British
(Nichols et al., 2009)	1325	359	12.6	5.3	N370S, L444P, E326K, T369M	Mixed (<10 Jewish)
(Mitsui et al., 2009)	534	544	9.4	<0.1	R120W, Rec*Nci*1	Japanese
(Saunders-Pullman et al., 2010)	250	-	12.8	-	N370S	Ashkenazi
(Mao et al., 2010)	616	411	3.2	0.2	only L444P screened	Chinese
(Sun et al., 2010)	402	413	2.7	0.0	L444P	Chinese

(Hu et al., 2010)	328	300	1.8	0.7	only N370S screened	Chinese
(Lesage et al., 2011a)	1130	391	6.7	1.0	N370S	European
(Lesage et al., 2011b)	194	177	4.6	0.5	N370S, L444P, Rec*Nci*1	North Africa
(Huang et al., 2011)	967	780	3.7	0.3	L444P	Chinese
(Noreau et al., 2011)	212	189	3.8	0.5	L444P, p.L236F, p.S378L, p.W417G	French-Canadian
(Ma et al., 2012)	277	291	3.2	0.0	L444P, N188S, P201H, R257Q, S271G	Korean
(Wang et al., 2012)	208	298	3.4	0.3	L444P	Chinese
(Zhang et al., 2012)	195	443	3.1	0.0	L444P	Chinese
(Emelyanov et al., 2012)	330	240	2.7	0.4	N370S	Russian
(Setó-Salvia et al., 2012)	225	186	9.8	0.5	N370S, L444P	Spanish
(Kumar et al., 2013)	360	348	5.8	1.4	N370S	Serbian
(Li et al., 2014)	144	100	21.5	1.0	L444P, R120W	Japanese
(González-Del Rincón et al., 2013)	28	252	5.5	0.0	L444P	Mexican
(Winder-Rhodes et al., 2013)	259	-	3.5	-	N370S, L444P	British

Taken together, these studies confirmed a high frequency of heterozygous GBA mutations in Ashkenazi Jewish PD patients which ranged from 10.7% up to 31.3% (Aharon-Peretz et al., 2004; Clark et al., 2005; Saunders-Pullman et al., 2010). In European populations, 2.3-9.8% of patients with PD were found to carry *GBA* mutations, while in Asia the frequency ranged from 1.8-4.3%. This lower frequency in the Asian population could be explained, at least in part, by continuous reports of the absence of N370S *GBA* mutations in these populations, which is one of the most frequent *GBA* mutations associated with PD elsewhere. Further studies around the world, including PD populations of mixed origin, reported mutation frequencies that ranged from 2.9% to 21%. Interestingly, studies of familial PD in the USA

(Nichols et al., 2009) and Japan (Mitsui et al., 2009; Li et al., 2014) have found very high frequencies of *GBA* mutations which range from 9.4-21.9% of PD cases, suggesting that *GBA* mutations also plays an important role in familial PD.

Besides differences in ethnic origin, the variation observed in the frequency of *GBA* mutations across the different reports could be due to differences in sample sizes, and the strategies used for screening. While some groups screened the entire coding region of the gene for a more complete analysis, others focused only on the most common mutations associated with PD, of which N370S and L444P were the primary targets. In order to overcome these limitations, a multi-centre international collaborative study was published in 2009 (Sidransky et al., 2009), incorporating 5691 PD patients and 4898 controls from 16 centres from 12 countries spanning four continents. All patients were screened for the two most common mutations, N370S and L444P, which together were found in 15% of Ashkenazi Jewish PD patients and in 3% of patients from other ethnic ancestries. Where GBA was fully sequenced (1883 non- Ashkenazi Jewish patients) GBA mutations were found in 7% of PD patients, which supports the need to sequence all exons for accurate determination of GBA mutation frequency among different populations. This study also confirmed that patients who carried a GBA mutation had an earlier onset of PD (4 years earlier), were more likely to have a family history of the disease, and more likely to have atypical clinical manifestations (Sidransky et al., 2009). Furthermore, this study also showed that the odds ratio for a patient with PD to carry a *GBA* mutation is 5.43, which means that patients with PD are five times more likely to harbour a *GBA* mutation when compared to healthy controls. Overall, this multi-centre study confirms a strong association between PD and mutations in GBA. Lastly, it is important to note that initial GWAS studies did not identify *GBA* as a PD-associated gene which was suggested to be a consequence of the existence of several rare variants with incomplete penetrance (Sidransky and Lopez, 2012), or

the presence of a neighbouring pseudogene (GBAP) that usually has Pro444 and Ser370 alleles, which could reduce the signal to noise ratio in GWAS (Trinh and Farrer, 2013). However in the most complete GWAS meta-analysis done to date and recently published, GBA mutations were found to be statistically significantly associated with PD (Lill et al., 2012).

Individuals screened for this study are part of a clinical cohort established by the Oxford Parkinson's Disease Centre. This cohort aims at recruiting 1200 PD patients, 300 at-risk individuals and 300 controls by 2015 to undertake a comprehensive multidisciplinary analysis with the goal of understanding the early pathological pathways involved in PD. The "at-risk" group consists of first-degree relatives from PD patients and individuals with idiopathic rapid eye movement (REM) sleep behaviour disorder, as some studies suggest that REM sleep disorder can be an early manifestation of PD, starting many years before significant neuronal degeneration. In fact, recent long term studies have confirmed that up to 80% of patients with REM sleep behaviour disorder developed neurodegenerative syndromes later in life, with PD development being one of the most common (Iranzo et al., 2013)(Schenck et al., 2013).

4.1.2 Establishment of PD hiPSC-derived dopaminergic cultures from PD patients

At the start of this project, only one study reported differentiation of dopaminergic neurons from PD patients (Soldner et al., 2009). To date, multiple reports (23 in total) on hiPSC derived neuronal models of PD have been published, but none has yet looked at lines derived from PD patients carrying heterozygous *GBA* mutations. Almost all reports (except from one) failed to fulfil three main criteria that we established as fundamental. First, most reports focused only on familial forms of PD caused by specific mutations, while sporadic forms of PD have been much mostly neglected. Only four studies have differentiated DA neurons from idiopathic PD patients (Park et al., 2008; Soldner et al., 2009; Hargus et al., 2010; Sánchez-Danés et al., 2012), out of which only one ventured into phenotypic analysis reporting reduced number of neurites and neurite arborisation together with autophagic impairments (Sánchez-Danés et al., 2012). This is crucial, as idiopathic cases represent the majority of PD patients (up to 90%), and should therefore be incorporated in these studies. Second, many of these studies used a very limited number of PD patients in their studies frequently leading to analysis using lines from one single patient (Byers et al., 2011; Devine et al., 2011; Nguyen et al., 2011; Seibler et al., 2011; Soldner et al., 2011; Aboud et al., 2012; Chung et al., 2013; Rakovic et al., 2013; Su and Qi, 2013), and in many studies only one single clonal line was derived from each individual in study. Variability across patient iPSC lines with similar genotypes and between different clonal lines (intra-patient variability) derived from the same individual have been frequently reported (Hu et al., 2010; Devine et al., 2011; Thatava et al., 2013) and should be taken in consideration in hiPS disease modelling studies. Third, comparison of differentiation efficiency across lines from which the results are obtained has not been done in several of these reports (Soldner et al., 2011; Imaizumi et al., 2012; Chung et al., 2013; Su and Qi, 2013), which becomes highly relevant when differentiation efficiencies reported are low. In addition, some reports rather than differentiating hiPSCs into

dopaminergic neurons, the most vulnerable cell type in PD, differentiate hiPSCs into early neural progenitor cells (NPCs) (Aboud et al., 2012), human neural stem cell (NSC) (Liu et al., 2012a) or glutamatergic neurons (Chung et al., 2013). Others lack sufficient characterization to confirm a ventral midbrain A9 dopaminergic population in their model (Devine et al., 2011).

The first aim of this chapter was to screen a clinical cohort established within the OPDC to identify PD patients carrying heterozygous *GBA* mutations - N370S and L444P. The second aim was to derive dopaminergic cultures from identified PD patients carrying heterozygous *GBA* N370S mutations together with idiopathic PD patients, following the protocol developed in Chapter 2 using control lines.

4.2 *GBA* mutation screen

To investigate the role of GBA mutations in the pathology of PD in a novel human *in vitro* system, PD patients carrying mutations of interest had first to be identified, from which hiPSC lines could be generated. For this purpose genomic DNA collected from a PD clinical cohort available within the OPDC was screened. The decision was made to focus on the two most common mutation identified so far in PD populations, namely N370S and L444P which represent over 50% of total mutations found associated with PD in patient cohorts (Sidransky et al., 2009). N370S and L444P positive cases were identified by PCR amplification of the genomic region containing the *GBA* gene, followed by restriction endonuclease digestion (Figure 27a, b) and confirmed by genome sequence analysis (Figure 27c, d). PCR primers, annealing temperatures and restriction enzymes used are listed in Table 9. Specific primers were designed in order to avoid the amplification of the non-functional GBA pseudogene. The L444P mutation creates a cleavage site for the *NciI* restriction enzyme. For the N370S mutation, a mismatch was introduced in the forward primer to create a restriction site for the *XhoI* restriction enzyme as previously described (Aharon-Peretz et al., 2004).

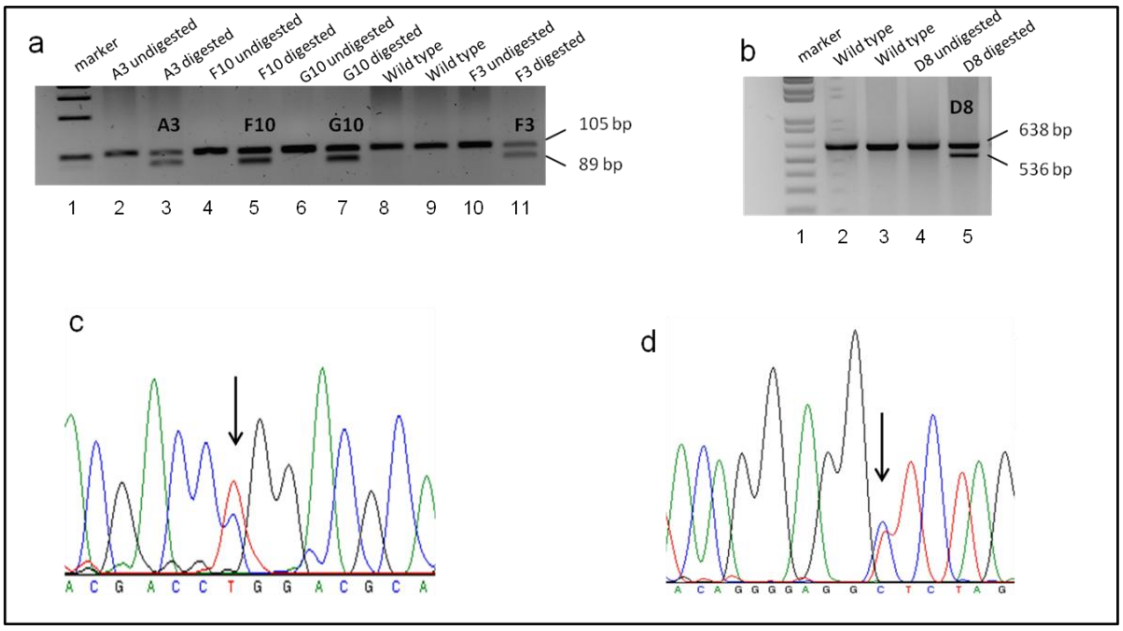

Figure 27 *GBA* mutation screening for N370S and L444P variants in patients with PD. a) PCR analysis of the N370S mutation. When the mutation is present (lanes 3, 5, 7 and 9), the enzyme XhoI digests a 105bp product, producing an additional fragment of 89 bp. b) PCR analysis of the L444P mutation. When the mutation is present (lane 5), the enzyme NciI digests a 638 bp product, producing an additional fragment of 536 bp. Detailed analysis by genomic sequencing of the previously identified cases, further confirmed the presence of L444P (c) and N370S (d) GBA heterozygous mutations.

Table 9 Primers and restriction enzymes used for identification of N370S and L444P variants of *GBA* gene. *A mismatch was introduced in the forward primer for N370S mutation detection to create a restriction site

Mutation	Primer Sequence (5'to 3')	Size of fragment(bp)		Anneal temp(°C)	Enzyme	Exon
		WT	Mutant			
N370S	F- GCCTTTGTCCTTACCCTC*G R- GACAAAGTTACGCACCCAA	105	89,16	53	XhoI	9
L444P	F-GGAGGACCCAATTGGGTGCGT R- ACGCTGTCTTCAGCCCACTTC	638	536,102	58	NciI	10

Within the OPDC cohort, multiple PD patients were identified as carrying heterozygous *GBA* mutations, with a total combined frequency of 2.83% PD patients carrying N370S and L444P heterozygous mutations. The detailed frequencies found in PD patients, at-risk individuals and control groups can be found in Table 10.

Table 10 Total number of individuals screened for heterozygous *GBA* mutations N370S and L444P. Number of positive cases identified is indicated together with the respective carrier frequency in the population screened

	N370S		L444P	
	No. tested	**No. carriers (%)**	**No. tested**	**No. carriers (%)**
PD Patients	606	10 (1.65)	635	8 (1.26)
At risk group	75	4 (5.3)	87	1 (1.15)
Controls	200	1 (0.5)	199	0 (0)

As previous studies reported that an early onset of PD may be associated with *GBA* mutations, the age of disease onset of the patients identified in the current study was analyzed. Age of diagnosis determined by clinicians was used as the most reliable criteria to evaluate age of onset. No differences were found for the average age of disease onset across the different groups of PD patients studied, with an average of 62.0 years for N370S PD patients, 59.8 years for *GBA* L444P and 61.5 for idiopathic patients (Figure 28).

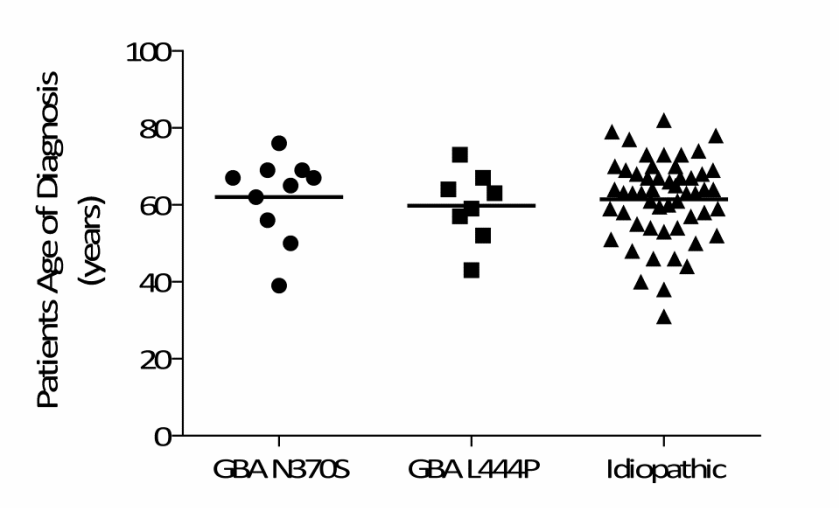

Figure 28 Age of PD diagnosis for patients identified with heterozygous N370S and L444P *GBA* mutations and idiopathic PD. Represented is the age of diagnosis determined by clinicians for PD patients identified in the clinical cohort screened. N370S n=10; L444P n=8; Idiopathic n=52.

4.3 Establishment of PD hiPSC derived dopaminergic neurons from PD patients

In Chapter 3 the development of a new protocol for differentiation of hiPSCs into dopaminergic neuronal cultures was described, and the efficiency in deriving midbrain dopaminergic neuronal cultures confirmed across multiple control lines. After the identification of PD patients of interest, multiple hiPSC lines were generated by our collaborators (OPDC, James Martin Stem Cell Facility, University of Oxford) from PD patients carrying *GBA* mutations together with idiopathic PD patients. Several hiPSC lines were selected from multiple individuals across the several groups of interest to proceed with analysis. Selection was based on the confirmation that all lines meet the quality criteria established and described in the previous chapter. This included confirmation of genome integrity, silencing of retroviral transgenes used for reprogramming and pluripotency assessment. This included lines from 2 control individuals (already described in Chapter 3), from 2 idiopathic PD patients and from 2 PD patients carrying heterozygous N370S mutations (Table 11). Also included were different clonal hiPSC lines derived from some individuals in order to account for clonal variability. Due to limitations in time and resources, we were unable to proceed further with analysis of the hiPSCs lines available from L444P *GBA* PD patients. It was decided to proceed with the differentiation of multiple lines only from N370S cases, as this is the most common *GBA* mutation associated with PD.

Table 11 Summary of PD patient-derived hiPSC lines used in this study.

	ID	OPDC ID	Gender	Age (biopsy)	Age (Onset)	Genotype	Lines used
Control	Control 1	NHDF	F	44	-	wt/wt	Control 1#1 Control 1#2
	Control 2	OX1	M	36	-	wt/wt	Control 2
N370S *GBA*	GBA-PD 1	MK071	F	81	77	N370S/wt	GBA-PD 1#1 GBA-PD 1#2
	GBA-PD 2	MK088	M	46	40	N370S/wt	GBA-PD 2
Idiopathic	IDI-PD 1	MK024	F	63	60	Idiopathic	IDI-PD 1
	IDI-PD 2	JR023	M	56	54	Idiopathic	IDI-PD 2

The protocol developed in Chapter 3 for differentiation of control hiPSC lines was applied to PD-derived hiPSCs. All lines successfully differentiated into dopaminergic neuronal cultures as determined by Tuj1 and TH immunocytochemistry (Figure 29).

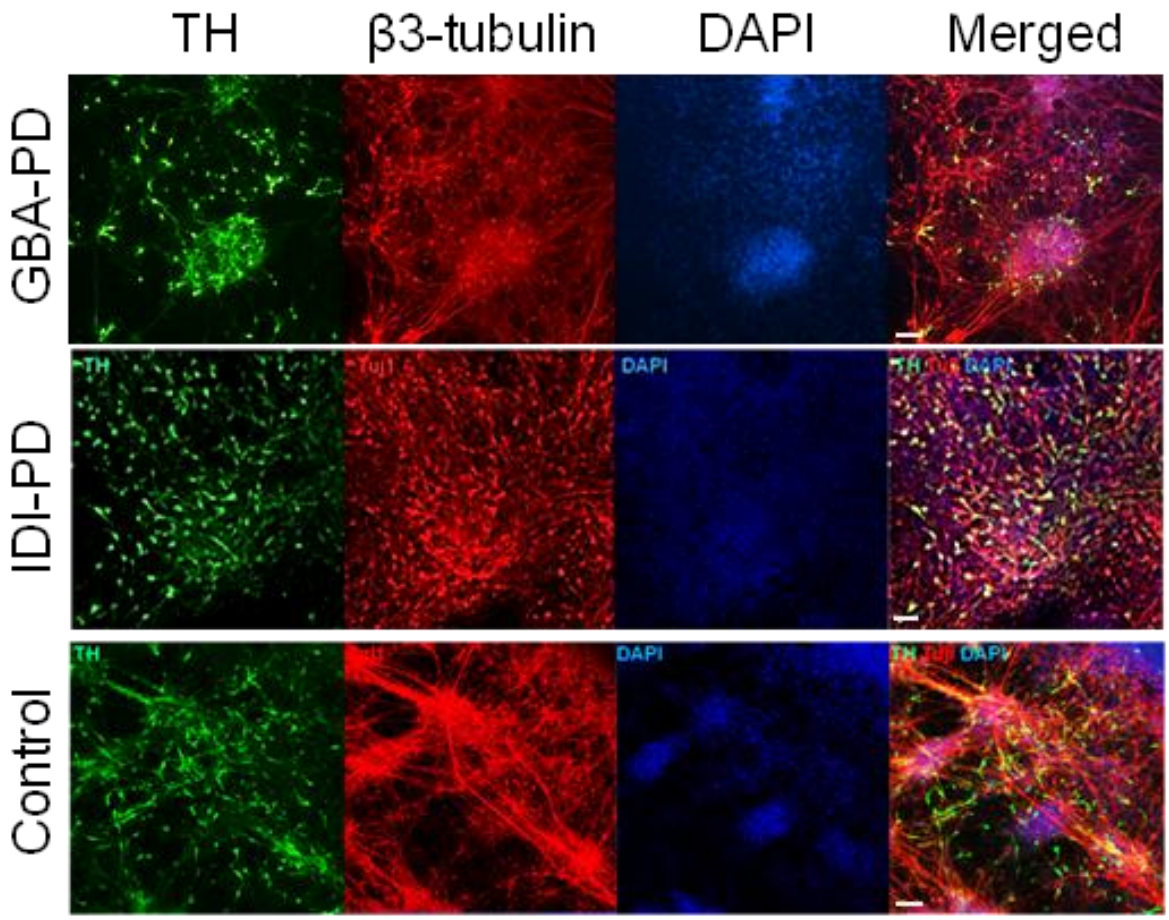

Figure 29 Differentiation of dopaminergic neuronal cultures from *GBA*-PD, idiopathic PD and control hiPSC lines. Immunocytochemistry analysis of differentiated dopaminergic neuronal cultures at day 35 showing high expression levels for the neuronal marker β-3 tubulin (red), the dopaminergic neuron marker TH (green) and DAPI (blue).

Differentiation efficiency was determined in collaboration with Dr Elizabeth Hartfield by counting cells expressing the neuronal marker Tuj1 and the dopaminergic marker TH (Figure 30). All cell lines differentiated with equivalent efficiencies across multiple rounds of independent differentiations, with approximately 35% of neurons expressing TH, similar to what was observed previously for control lines.

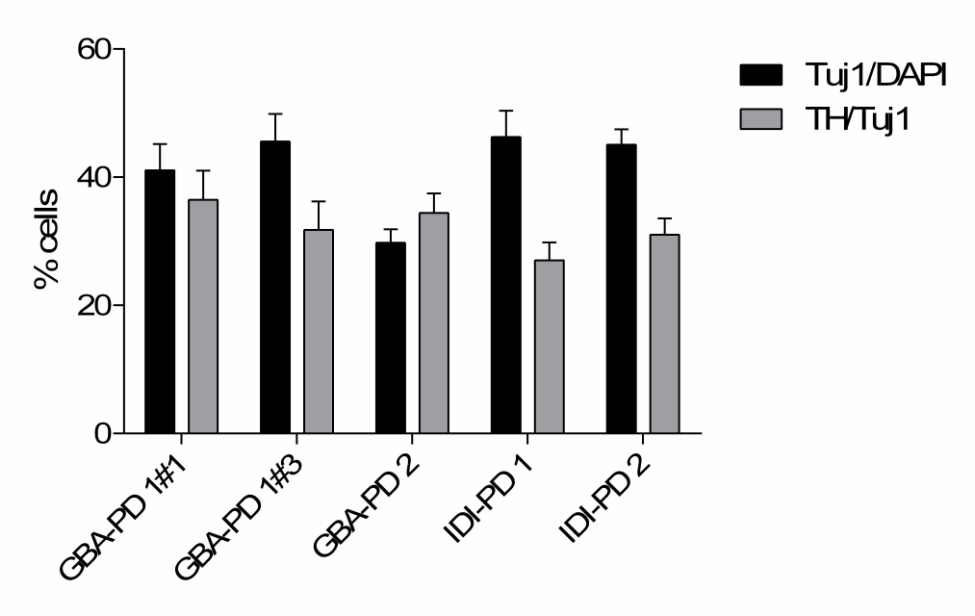

Figure 30 Efficiency of dopaminergic differentiation for PD hiPSCs. Analysis of neuronal and dopaminergic differentiation efficiency across all hiPSC lines used, including clonal lines from same individual for GBA-N370S mutant and idiopathic PD patients, expressed as percentage of total cells. Data represent mean ± SEM of at least 3 independent differentiations. Two-way ANOVA with Tukey post hoc analysis, not significant. Differentiation into dopaminergic cultures and immunofluorescence preparation (fixation and staining) performed by HF. Cell counting performed by EH.

Further midbrain characterization was also done for PD derived dopaminergic neuronal cultures, in collaboration with Dr Jennifer Badger. RT-PCR analysis demonstrated that, similar to what was observed with control lines, differentiated dopaminergic cultures expressed the floor plate markers *FOXA2* and *LMX1A*, in addition to the mature dopaminergic neuron markers *EN1* and *NURR1*, whilst the level of the pluripotency marker *OCT4* was much reduced after dopaminergic differentiation (Figure 31).

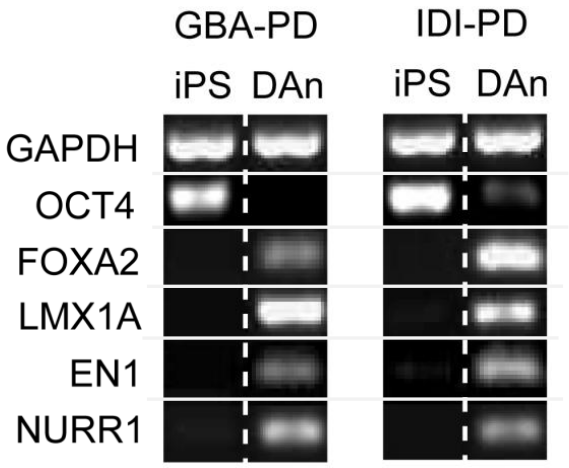

Figure 31 Differentiated dopaminergic cultures from PD-patients hiPSCs express multiple markers with ventral midbrain characteristics. RT-PCR analysis shows reduced expression of the pluripotency marker *OCT4* and increased expression of floor plate markers (*FOXA2* and *LMX1A*) and mature dopaminergic markers (*EN1* and *NURR1*) in differentiated cultures (DAn) and undifferentiated cells (iPS). Differentiation into dopaminergic cultures, RNA extraction and preparation and primers design performed by HF. RT-PCR reaction and gel imaging performed by JB.

4.4 Discussion

The aim in this chapter was to identify PD patients carrying heterozygous *GBA* mutations of interest (N370S and L444P) from which hiPSC lines could be derived. Those lines were then differentiated into dopaminergic neuronal cultures, together with hiPSC lines from idiopathic PD and control individuals.

4.4.1 *GBA* mutation screen

Hitherto, the most complete study exploring the frequency of GBA mutations in PD populations was published in 2009 by *Sidranksy et al* (Sidransky et al., 2009), which included data from multiple centres around the world. While in the subset of participants (non-Ashkenazi) where GBA was fully sequenced 7% of PD patient were found to carry *GBA* mutations, this value dropped to 3% when screened only for N370S and L444P, compared to less than 1% in control populations. Due to technical limitations, our study involved the screening of only these two mutations, which represent the most common mutations found associated with PD (Sidransky et al., 2009). Our results showed that 1.65% of PD patients in our cohort carried heterozygous N370S mutations (vs. 0.5% in control group), while heterozygous L444P mutations were found in 1.26 % of PD patients (vs. 0.0% in control group). Combined, these two mutations were found in 2.83% of PD patients in our cohort, which resembles the frequency determined (3%) in the multicentre study described above (Sidransky et al., 2009). Two other reports were published focusing on British populations of PD patients that were not included in the multicentre analysis. The first by *Neumann et al* (Neumann et al., 2009) used a clinical cohort of similar demographic characteristics dimensions to ours, and reports a total frequency of GBA mutations in 4.18 % of PD patients (vs. 1.17 % in controls). The slightly higher frequency reported in this study reflects the more in depth analysis done, as all *GBA* exons were sequenced looking for multiple different GBA

mutations. Once again, this supports the need to sequence all exons for determining with accuracy the total frequency of all *GBA* mutations present in the population, which was one of the limitations of our study. However, if one focus only on the positive cases identified for L444P and N370S in this study, a total frequency of 2.41% in PD patients is found, which is comparable to our results. A more recent study by *Winder-Rhodes et al* (Winder-Rhodes et al., 2013) reports a total GBA carrier frequency of 3.5% in another British cohort, after entire gene sequencing. Again, if one focus on only N370S and L444P cases, a lower combined frequency of 2.3% is found. Overall, the results obtained in our study are in accordance with, and very similar to, previously reported ones, either in British or in more global populations.

Another important aspect frequently associated with *GBA* mutations in PD patients relates to an earlier onset of disease. The multicentre analysis of thousands of individuals around the world reported that PD patients carrying heterozygous *GBA* mutations developed the disease on average 4 years earlier compared to those without mutations (54.9 years vs 58.8 years) (Sidransky et al., 2009). A similar observation was made by Neumann et al 2009 where, on average, PD developed 6 years earlier in *GBA* mutant carriers compared to idiopathic cases (52.7 years vs 58.7 years). However, after careful analysis of data in this last study, if only carriers of N370S and L444P heterozygous mutations are considered, the combined age of onset for GBA mutant carriers increased to 55.1 years old. Splitting the two groups even further, one can observe that the age of onset for N370S carriers is 62.6 years and for L444P carriers of 49.1 years old. This variability might also be a consequence of the low number of patients identified in each group, which makes interpretation difficult. Interestingly, in the second British cohort study published (Winder-Rhodes et al., 2013), if one considers only *GBA* mutant carriers, no difference in the age of onset is observed when compared to all PD patients involved in the study (67.1 years vs 67.4 years, respectively). This result comes in agreement with the observations made in our study where no differences

were observed in age of onset between idiopathic patients and carriers of heterozygous *GBA* mutations. PD patients carrying heterozygous N370S and L444P *GBA* mutations presented with a combined average age of onset of 61.0 years old compared to 61.5 years for idiopathic PD patients. It is important to highlight, that the low number of mutation carriers also identified in our study might render interpretation of these result difficult and conclusions should be cautious, especially when comparing to the multicentre study where a much higher number of carriers was involved, and conclusions are likely more representative of a global PD population.

4.4.2 Establishment of PD hiPSC derived dopaminergic neurons from PD patients

The lack of information regarding the impact of heterozygous *GBA* mutations in PD is mostly a result of the lack of an appropriate human model, and the uncertain extrapolations being made from different models of *GBA* modulation (e.g. GD models) were the main drivers behind our study. Therefore, we report here for the first time, the differentiation of hiPSCs derived from PD patients carrying a heterozygous *GBA* mutation, namely N370S, into dopaminergic neuronal cultures. To efficiently determine the contributions of heterozygous *GBA* mutations in PD pathology we decided that the inclusion in this study of hiPSC lines derived from idiopathic PD patients was important. This aspect has been overlooked in almost all reports (with one exception (Sánchez-Danés et al., 2012)) that have used hiPSCs to model PD, as they have focused exclusively in familial forms caused by specific mutations. These studies tend to report results using cell lines from 1 single PD individual (Byers et al., 2011; Devine et al., 2011; Nguyen et al., 2011; Seibler et al., 2011; Soldner et al., 2011; Aboud et al., 2012; Chung et al., 2013; Rakovic et al., 2013; Su and Qi, 2013), data from which can be difficult to interpret, as it does not represent the natural inter-patient variability

expected within each group. In our study, lines from 2 individual patients within each group (control, N370S mutant carriers and idiopathic PD) were included. Different clonal lines were also included for some individuals, which is also commonly absent in previous studies. Nevertheless, we recognize that an even higher number of lines from more individuals within each group would be the most efficient way to control for expected variability.

The protocol developed in Chapter 3 for control lines was confirmed to be effective in generating high numbers of neurons and dopaminergic neurons across all PD lines in this study, which is an improvement on previously lower efficiency protocols (Nguyen et al., 2011; Seibler et al., 2011; Rakovic et al., 2013) where TH positive cells could represent only up to 3% of total cells (Cooper et al., 2012). In several other reports, no quantification of differentiation efficiency was determined prior to the establishment of comparisons across different neuronal populations of cells obtained for different lines used (Imaizumi et al., 2012; Jiang et al., 2012; Chung et al., 2013; Orenstein et al., 2013; Su and Qi, 2013). Here, similar differentiation efficiencies were confirmed across all hiPSC lines used before any phenotypic analyses were attempted, which precludes any differentiation related event from interfering with later results. Finally, further ventral midbrain characterization of differentiated PD hiPSC confirmed a pattern of multiple markers expression similar to what was attained for control lines. The cell lines here described were confirmed to efficiently differentiate into DA neuronal cultures and could therefore be utilised for phenotypic analyses, as described in the following chapter.

Chapter 5

Phenotypical analysis of dopaminergic neuronal cultures from idiopathic and heterozygous *GBA* mutation carriers PD patients

5.1 Introduction

The relevance of *GBA* in the pathology of PD emerged from clinical observations that GD patients and heterozygous *GBA* mutation carriers had an increased risk of developing PD (Sidransky et al., 2009). Ever since this discovery, the mechanisms underlying the relationship between *GBA* and PD have been explored, but so far remain elusive, mostly due to the lack of relevant human models of study. Both loss-of-function and gain-of-function mechanisms have been proposed, but these are limited to homozygous mutant *GBA* models that result in GD, models with artificial modulation of protein expression or activity and human post-mortem studies.

5.1.1 Gain-of-function hypotheses

Support for gain-of-function hypotheses centre around mechanisms of GCase misfolding and ER retention, that can result in ER stress activation and ultimately burden the overall proteasomal and lysosomal protein degradation systems (Sidransky and Lopez, 2012).

GCase is synthesized on ER bound polyribosomes where it undergoes N-linked glycosylation, before being subjected to ER quality control events, which ensure proper folding and trafficking. If folded correctly, it is transported to the Golgi for further N-linked glycans processing before being trafficked to the lysosomes (Ron and Horowitz, 2005).

Initial studies on homozygous mutant *GBA* fibroblasts from GD patients revealed reduced levels of GCase protein, which was caused by rapid degradation of the protein (Ron and Horowitz, 2005). Decreased GCase levels were also detected in GD patient-derived hiPSC lines, a phenotype that was maintained after differentiation into neuronal cultures (Tiscornia et al., 2013), dopaminergic neurons (Mazzulli et al., 2011) and into macrophages (Panicker et al., 2012). In addition, brain samples from GD patients (Choi et al., 2011) and mouse models with homozygous *GBA* mutations (Sun et al., 2011) were also found to have reduced GCase protein levels. Further analysis in this studies confirmed that the reduced GCase levels could be explained by ER retention of misfolded GCase caused by homozygous mutations. Accumulation of misfolded GCase resulted in degradation of the protein by the ubiquitin-proteasome system (UPS), a process known as ER-associated degradation (ERAD) (Ron and Horowitz, 2005). As a consequence, a high proportion of GCase failed to reach the lysosome, and the total levels were reduced. Further reports confirmed trafficking deficits within the ER in GD fibroblasts (Schmitz et al., 2005; Wang et al., 2011), and have shown that these deficits could be partially restored by pharmacological chaperones like Diltiazem

and Lacidipine, which enhance the cellular protein folding (Rigat and Mahuran, 2009; Wang et al., 2011; Wang and Segatori, 2013).

Instead of being targeted to the lysosomes via the mannose-6-phosphate pathway like most lysosomal enzymes (Braulke and Bonifacino, 2009), GCase was found to be instead transported via a specific association with the lysosomal integral membrane protein type 2 (LIMP-2) (Reczek et al., 2007). LIMP-2 is a transmembrane protein that was also genetically associated with PD (Yap et al., 2011; Lopez and Sidransky, 2012) although this was not confirmed in a later study (Goker-Alpan et al., 2010). GCase was shown to associate with LIMP2 in the ER and became dissociated in the lysosome in a pH-dependent mechanism (Reczek et al., 2007), which was later confirmed by others (Zachos et al., 2012). In a LIMP2 KO mouse model lysosomal transportation of GCase was blocked and GCase was secreted instead. Importantly for the context of GBA mutant-gain-of-function hypothesis, LIMP-2 over-expression resulted in increased lysosomal transportation of ER-retained mutant GCase (Reczek et al., 2007). Only one report has explored the relevance of LIMP2 in the context of *GBA* mutations. In GD patients it was shown that the different disease severity in two siblings with GD could be, at least in part, explained by a heterozygous mutation in SCARB2, the gene that codes for LIMP-2. The most severely affected sibling had reduced LIMP2 protein expression, reduced GCase levels and reduced GCase trafficking to the lysosomal compartment, suggesting that modulation of LIMP2 could serve as a therapeutic strategy for GD (Velayati et al., 2011).

Accumulation of excessive misfolded proteins within the ER can result in the activation of an event known as ER stress/UPR activation (Høyer-Hansen and Jäättelä, 2007), which serves to eliminate misfolded proteins within the cell and can be neuroprotective (Beavan and Schapira, 2013). In the context of *GBA*, ER stress activation has been confirmed in homozygous *GBA* mutant fibroblasts (Wang et al., 2011)(Wei et al., 2008; Lee et al., 2011;

Maor et al., 2013), in fibroblasts from GD mutation carriers (Maor et al., 2013) and in *Drosophila* GD models (Maor et al., 2013). UPR impairment caused by excessive accumulation of misfolded proteins in the ER, can also result in the targeting of those proteins for degradation via the autophagic system, resulting in increased autophagic demand (Dawson and Dawson, 2011). This observation has been made in several studies of other pathologies, but has yet to be explored in the context of PD-related *GBA* mutations, and even in the context of *GBA* homozygous mutations only two studies have been reported. Of particular relevance, one study reports no alterations in the protein levels of two major modulators of autophagy, beclin-1 and LC3-II in fibroblasts from GD patients (Pacheco et al., 2007), while in an aggressive mouse model of GD (GBA KO), a down regulation of the autophagic pathway was observed, characterized by reduced LC3-II levels and reduced autophagic flux (Osellame et al., 2013). However, the relevance of this last report in the context of PD-related *GBA* heterozygous mutations is debatable, as these animals have a complete GBA knockout and die within 2 weeks of birth. Therefore their autophagic alterations could reflect a different pathway of cellular deterioration.

Overall, accumulation of misfolded GCase in the ER, resulting from homozygous *GBA* mutations, could potentially overwhelm the proteasomal and lysosomal systems, responsible for degradation of other proteins. In the context of PD pathology, this could be relevant for the degradation of α-synuclein**,** a protein that is found aggregated in PD (Sidransky and Lopez, 2012).

5.1.2 Loss-of-function hypotheses

Alternative to gain of function events, *GBA* mutations could result in the loss of function of GCase leading to lysosomal dysfunction that could disrupt α-synuclein degradation and to enzymatic substrate accumulation and consequent alterations in lipid metabolism.

In this context, fibroblasts from GD patients carrying homozygous GBA mutations show significantly reduced levels of GCase activity; ~90% when compared to controls with wild-type (WT) GBA (Ron and Horowitz, 2005; Rigat and Mahuran, 2009). At a neuronal level, reduced GCAse activity levels were also observed in brain samples from GD patients (Choi et al., 2011). hiPSC lines derived from these patients also had reduced GCase activity levels (Tiscornia et al., 2013), and a similar phenotype was observed when these hiPSC lines were differentiated into macrophages (Panicker et al., 2012), neuronal cultures (Panicker et al., 2012; Tiscornia et al., 2013) and into dopaminergic neuronal cultures (Mazzulli et al., 2011). Mouse models with homozygous GBA mutations were also found to have reduced GCase activity (Xu et al., 2003; Mazzulli et al., 2011; Sun et al., 2011).

The lysosome is a major cellular compartment for protein degradation crucial for maintaining cellular proteostasis (García-Arencibia et al., 2010). Both mutated *GBA* or decreased amounts of WT GCase could result in decreased GCase activity and therefore, reduced lysosomal function. Lysosomes are involved in the degradation of substrates through different autophagic pathways; chaperone mediated autophagy (CMA), macroautophagy and microautophagy (García-Arencibia et al., 2010). Reduced lysosomal activity can therefore impair the proper autophagic degradation of multiple proteins, including α-synuclein, which is mainly degraded through CMA, but can also go through the proteasomal pathway (Cuervo et al., 2004). This could ultimately result in reduced α-synuclein turnover, leading to cellular accumulation or aggregation of α-synuclein (Beavan and Schapira, 2013). Studies so far have

shown that GCase shRNA-mediated KD in mouse cortical neurons compromised lysosomal protein degradation that ultimately resulted in increased α-synuclein levels (Mazzulli et al., 2011). Similar results were observed in hiPSC derived dopaminergic cultures from a GD patient (Mazzulli et al., 2011). Another study also reported compromised lysosomal function in hiPSC-derived macrophages from further GD patients (Panicker et al., 2012). More detailed analysis confirmed a physical interaction between α-synuclein and GCase, which occurs only at the acidic pH found in the lysosomes (Yap et al., 2011), suggesting that GCase might have a beneficial role in α-synuclein processing, which is disturbed when *GBA* is mutated (Sidransky and Lopez, 2012). In post-mortem brain samples from GD patients (homozygous for GBA mutations), GCase was present in more than 80% of Lewy bodies (Goker-Alpan et al., 2010), supporting its interaction with α-synuclein. Furthermore, another report has shown that overexpression of GCase mutants in the rodent cell line MES23.5 of midbrain origin also resulted in accumulation of α-synuclein in a dose-dependent manner (Cullen et al., 2011), while another report showed that α-synuclein levels could be reduced in a mouse model of GD by increasing GCase activity (Sardi et al., 2011). However, one recent study reported no alterations in α-synuclein levels or lysosomal function after GCase inhibition, in differentiated neuronal cells or primary neuronal cultures (Dermentzaki et al., 2013). Finally, in mouse cortical neurons a novel mechanism has been proposed by which α-synuclein could impair the trafficking of GCase. α-synuclein overexpression inhibited the ER-Golgi trafficking of GCase, causing it to accumulate in the ER and resulting in impairments in lysosomal function (Mazzulli et al., 2011).

Another factor that can result from GBA loss-of-function and interfere with lysosomal function and α-synuclein accumulation relates to alterations in lipid metabolism. GCase breaks down the glycolipid glucosylceramide (GlcCer) into glucose and ceramide. GD patients present with accumulation of the substrate GlcCer in the lysosomes of macrophages

(Westbroek et al., 2011). Accumulation of GlcCer has also been observed in GD patient hiPSC-derived macrophages (Panicker et al., 2012), and neurons (Orvisky et al., 2002). Furthermore, GCase KD in mouse cortical neurons resulted in GlcCer accumulation (Mazzulli et al., 2011), and accumulation of this substrate has also been observed in GD mouse models (Xu et al., 2003; Mazzulli et al., 2011; Sun et al., 2011). It has also been suggested that GlcCer accumulation might further impair lipid metabolism in PD. It has been proposed that excess substrate can accumulate in lipid rafts, which are regulators of protein and lipid sorting and trafficking, resulting in changes in lipid homeostasis (Westbroek et al., 2011). Accumulation of a second potentially toxic substrate, glucosylsphingosine (ClcSph), the deacylated form of GlcCer, was also observed in the plasma (Dekker et al., 2011) and in spleen samples from GD patients (Orvisky et al., 2002), in GD patient hiPSC-derived macrophages (Orvisky et al., 2002), and in a GD mouse model (Sun et al., 2011). The complexity of GCase-substrate interactions is further increased by reports that GlcCer can directly influence the aggregation of α-synuclein, resulting in increased toxicity by a loss-of-function mechanism (Mazzulli et al., 2011). The possible relevance of altered ceramide levels caused by reduced GCase enzymatic activity has been supported by the identification of several genes related to ceramide that have been associated with LB pathology, suggesting that alterations in ceramide metabolism could also be associated with LB formation (Bras et al., 2008).

All the above described gain-and loss-of-function mechanisms have been proposed to explain the pathogenesis of homozygous *GBA* mutations associated with GD. How these mechanisms might translate into the context of heterozygous *GBA* mutations associated with PD is still very much unknown, mostly due to the lack of appropriate models of study. So far no *in vitro* human model is available to investigate this question, and the only mutant heterozygous models published are limited to some human post-mortem studies and a mouse model in which mutation (D409V) is not usually associated with PD. The first post-mortem study in brains from a limited number of PD patients carrying heterozygous mutations, showed that GCase protein was found associated with LBs, although this varied between patients. This suggests that heterozygous *GBA* mutations might contribute to aberrant aggregation of α-synuclein (Goker-Alpan et al., 2010). In 2011, a report on brain homogenates from human cerebral cortex of carriers of heterozygous *GBA* mutations diagnosed with PD or DLB showed a reduction of GCase activity (reduction of 41-56% compared to controls), and indications of α-synuclein aggregation, without apparent changes in GCase protein levels. A more recent study of several brain regions from multiple PD patients carrying heterozygous *GBA* mutations (Gegg et al., 2012) confirmed a 58% reduction in GCase activity which was most pronounced in the SNpc together with reduced GCase protein levels (Choi et al., 2011). In this same study increased expression of CHOP and BIP with occasional XBP1 splicing events were also observed, suggesting UPR activation. In addition, LC3-II levels were increased suggesting increased autophagy, while LIMP2 levels were unchanged. As mentioned previously, a heterozygous *GBA* mutant mouse model has also been published (Sardi et al., 2011), where GCase activity was reduced by 41% reduction, without signs of substrate accumulation (GlcCer and ClcSph) but with evidence of α-synuclein aggregation. However, because this mutation has not been reported in GD patients or in PD patients, the significance of these results has been questioned (Lopez and Sidransky,

2012). Overall, this limited number of studies in models of heterozygous *GBA* mutations not only gives some contradictory information, but also does not clearly define the impact of heteroygous *GBA* mutations in the development of PD. As human models are lacking in this field of research, we have developed hiPSC-derived dopaminergic cultures from PD patients carrying the heterozygous *GBA*-N370S mutation, together with idiopathic PD patients, and explored in more detail, in a human context and in a neuronal environment, the impact of this mutation in the progression of PD.

5.2 Results

5.2.1 *GBA*-N370S mutation leads to ER retention of GCase in dopaminergic neuronal cultures

The establishment of a human dopaminergic neuronal culture model was described in Chapter 3. Dopaminergic neuronal differentiation was shown to be consistent between the hiPSC lines used in this study (Chapter 4). The first goal was then to determine the effect of the heterozygous *GBA*-N370S mutation on GCase protein levels. In addition to the expected 60 kDa isoform corresponding to mature GCase (grey arrow, Figure 32A), the presence of an extra isoform of apparently higher molecular weight (black arrow, Figure 32A) was observed only in dopaminergic neuronal cultures derived from *GBA*-N370S PD patients. When quantified, this extra isoform represented up to 50% of total GCase in these cultures (Figure 32B).

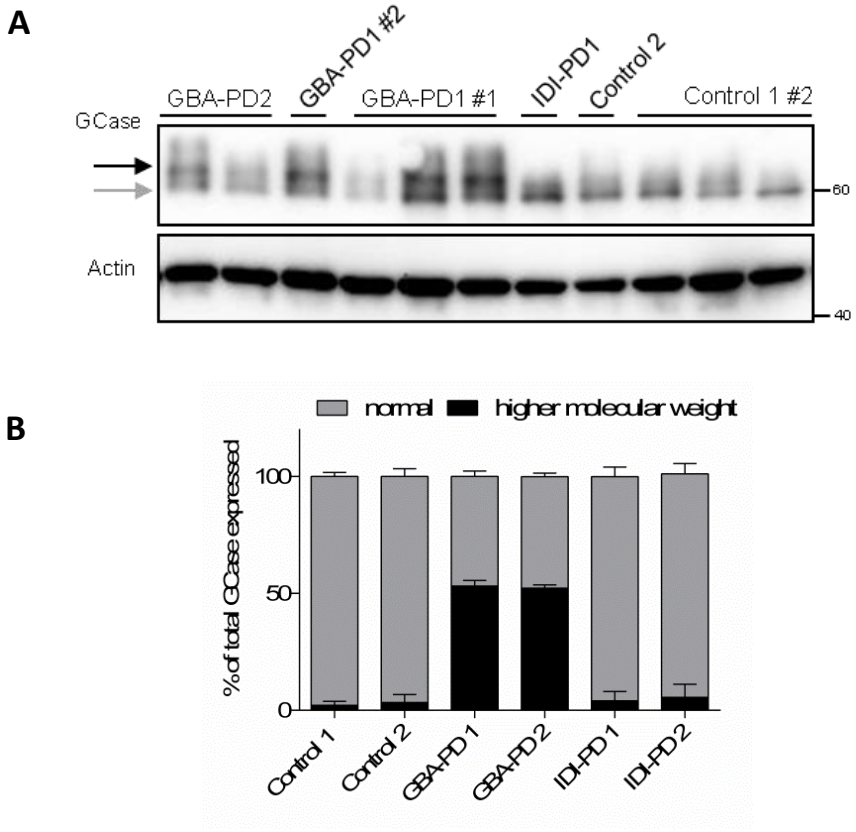

Figure 32 Heterozygous *GBA*-N370S mutation resulted in an extra GCase isoform in PD-derived dopaminergic neuronal cultures. (**A**) Representative Western blot for differentiated dopaminergic neuronal cultures demonstrated the presence of two isoforms for GCase protein specifically in *GBA*-N370S cultures. (**B**) Quantification of GCase isoforms by Western blot (as percentage of total GCase) confirmed that the higher molecular weight isoform (black bars) was specific to N370S dopaminergic neuronal cultures, representing up to 50% of total GCase levels. Data represent mean ± SEM. of at least 3 independent differentiations.

This N370S-specific isoform was found to be sensitive to treatment with Endoglycosidase H (EndoH), to yield a third, lower molecular weight isoform (blue arrow Figure 33A). Endo H is a glycosidase that cleaves high mannose oligosaccharides from N-linked glycoproteins. As glycoproteins are modified within the ER-Golgi complex, they are processed into EndoH-resistant complex oligosaccharides once in the Golgi. This indicates that a proportion of GCase in both *GBA*-N370S cell lines had retained high-mannose oligosaccharides, indicating failure to be processed in the Golgi, likely as a result of retention in the ER (Figure 33A). In *GBA* N370S-derived dopaminergic neuronal cultures, this EndoH-sensitive GCase isoform was significantly more abundant, representing 20% of total GCase (Figure 33B).

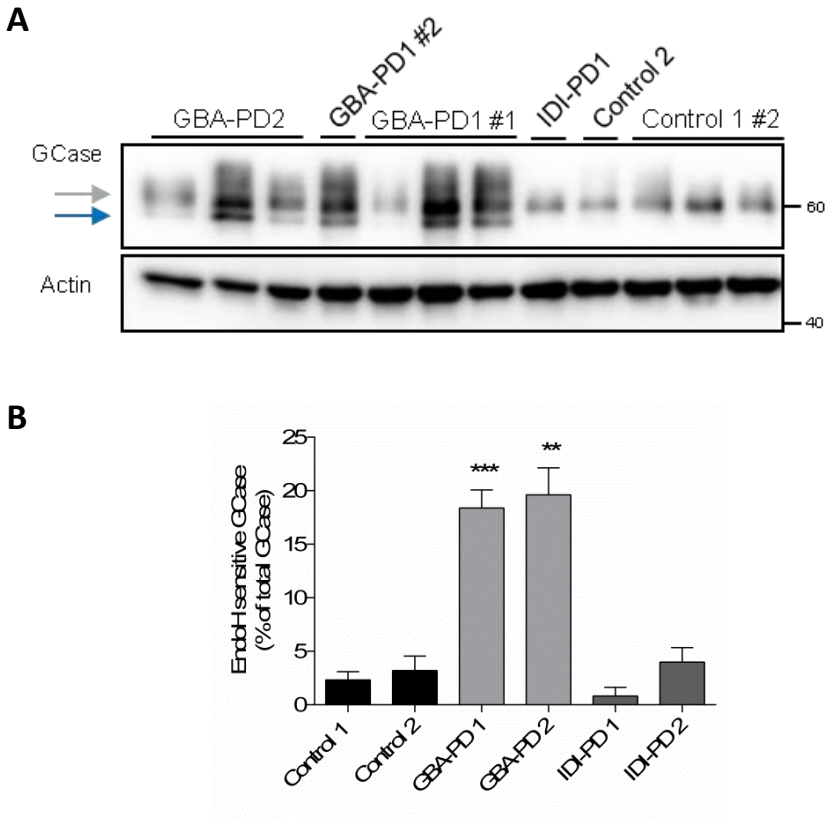

Figure 33 Heterozygous *GBA*-N370S mutation leads to retention of GCase in the ER in PD-derived dopaminergic neuronal cultures. (A) The GCase top isoform was sensitive to EndoH treatment; a representative Western blot is shown. **(B)** Quantification of the EndoH-sensitive band represented as a percentage of total GCase for each respective cell line. Data represent mean ± SEM. of at least 3 independent differentiations. Control 1 was used as an internal control within each differentiation. All statistical comparisons are with Control 2, **P < 0.01; ***P < 0.005 Student's t-test. Blue arrow represents EndoH sensitive GCase

Next we explored the impact of heterozygous *GBA*-N370S mutations in the total amount of GCase, as homozygous *GBA* mutant studies reported massive reduction in the enzyme levels caused by ER-associated degradation. In order to exclude the possible masking-effect of ER-retained GBA protein in the total quantification of the GCase, samples were treated with Peptide-N-Glycosidase F (PNGaseF) to remove almost all N-linked oligosaccharides from glycoproteins (high-mannose and complex N-linked glycans) (Maley et al., 1989). Under these conditions no significant differences in GCase protein levels were observed between N370S mutant, idiopathic-PD and control dopaminergic neuronal cultures (Figure 34). Overall, these results indicate that the N370S mutation likely prevents exit of GCase from the ER as a result of disrupting the structure and/or folding of the protein. However this blockage does not seems to result in degradation and consequent reduction of GCase levels.

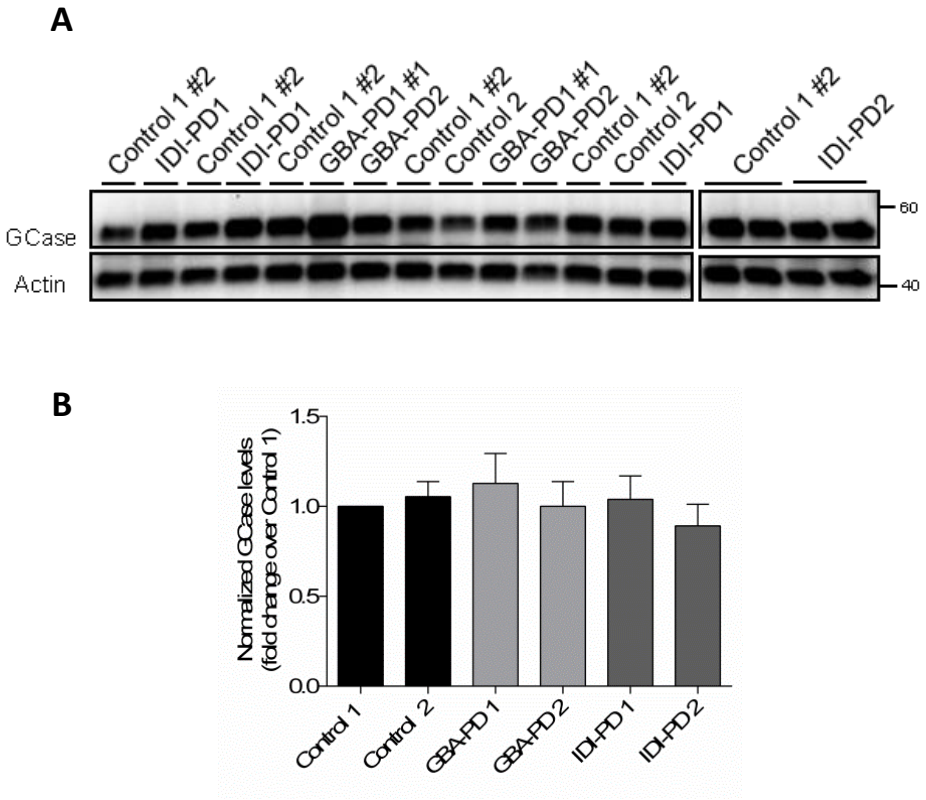

Figure 34 No differences for GCase protein levels in PD-derived dopaminergic neuronal cultures after PNGase F treatment. GCase expression levels after PNGase F treatment. (**A**) Representative Western blot. (**B**) Quantification of GCase as a fold change over control 1 is shown. Data represent mean ± SEM. of at least 3 independent differentiations. Control 1 was used as an internal control within each differentiation. All statistical comparisons are with Control 2, Student's t-test, not-significant

Furthermore, the levels of LIMP2, a GCase-specific lysosomal receptor, were also found increased in dopaminergic neuronal cultures derived from *GBA*-N370S mutant GBA patients when compared to controls, which was not observed in idiopathic-PD cultures (Figure 35).

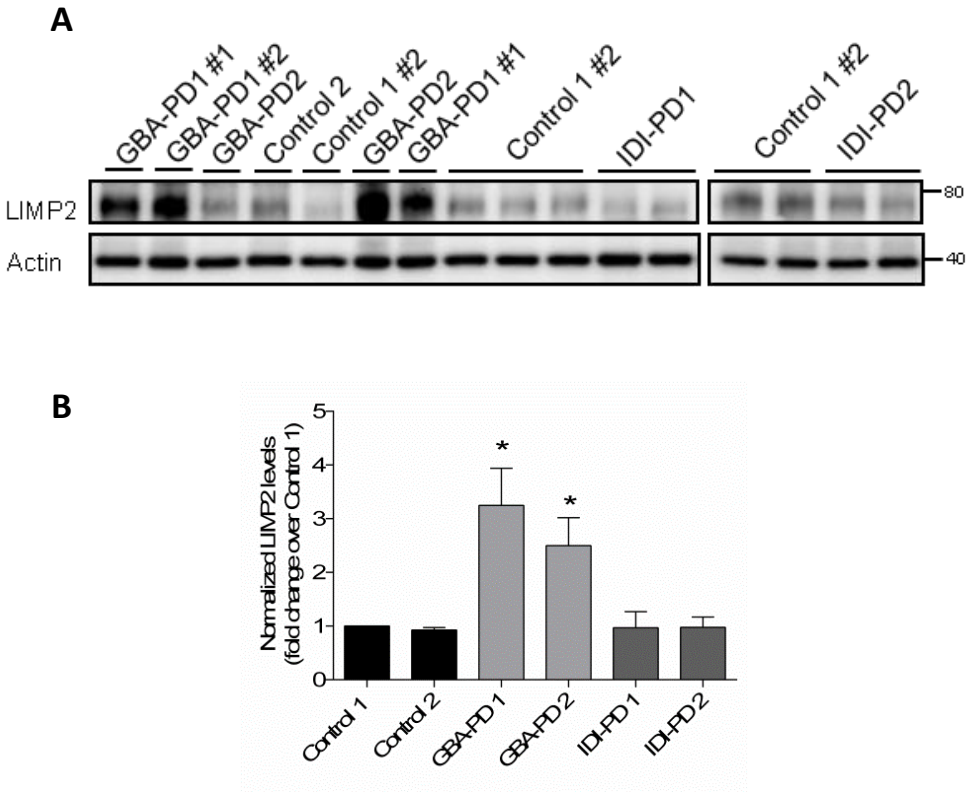

Figure 35 Heterozygous *GBA*-N370S mutation dopaminergic cultures had increased expression of LIMP2. **(A)** Representative Western blot for LIMP2 expression. (**B**) Quantification of LIMP2 expression as a fold change over control 1 is shown. Data represent mean ± SEM. of at least 3 independent differentiations. Control 1 was used as an internal control within each differentiation. All statistical comparisons made against Control 2, *P < 0.05 Student's t-test.

5.2.2 ER stress is induced in *GBA*-N370S dopaminergic neuronal cultures

Accumulation of misfolded GCase in the ER might have the potential to overload the cellular capacity for protein re-folding, activating ER stress and ultimately leading to activation of the UPR. Analysis of two main ER-resident chaperones showed significant upregulation of Bip/GRP78 and Calreticulin in *GBA*-N370S dopaminergic neuronal cultures which was not observed in idiopathic-PD or control-derived dopaminergic neuronal cultures (Figure 36A). Upregulation of other UPR mediators, namely Calnexin, PDI and IRE1alpha was also observed, confirming UPR activation (Figure 36B-D), although cleavage of XBP1 mRNA was not observed (Figure 37).

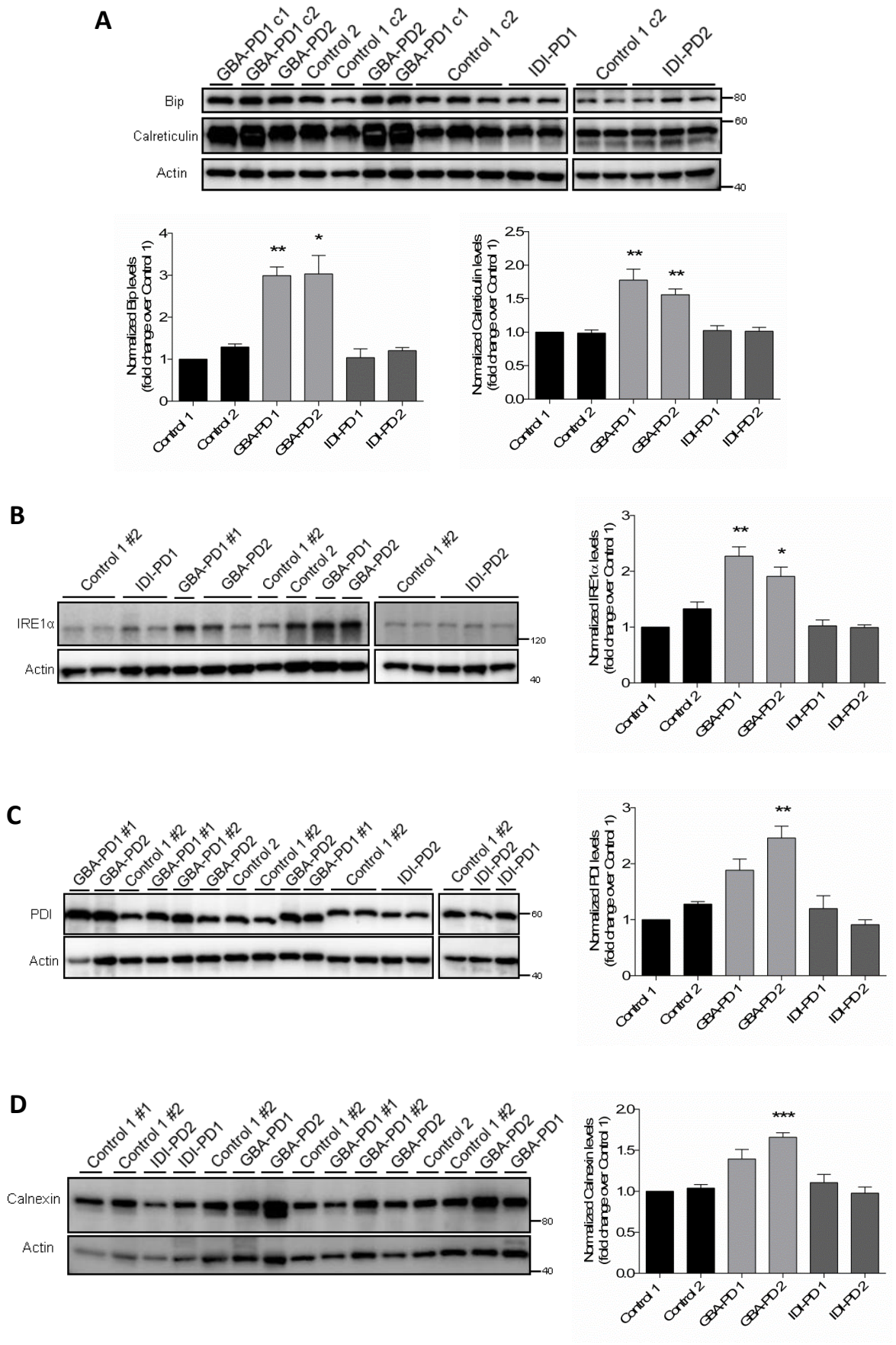
A
GBA-PD1 c1
GBA-PD1 c2
GBA-PD2
Control 2
Control 1 c2
GBA-PD2
GBA-PD1 c1
Control 1 c2
IDI-PD1
Control 1 c2
IDI-PD2
Bip
Calreticulin
Actin
80
60
40
Normalized Bip levels (fold change over Control 1)
Normalized Calreticulin levels (fold change over Control 1)
Control 1
Control 2
GBA-PD1
GBA-PD2
IDI-PD1
IDI-PD2
B
Control 1 #2
IDI-PD1
GBA-PD1 #1
GBA-PD2
Control 1 #2
Control 2
GBA-PD1
GBA-PD2
Control 1 #2
IDI-PD2
IRE1α
Actin
120
40
Normalized IRE1α levels (fold change over Control 1)
C
GBA-PD1 #1
GBA-PD2
Control 1 #2
GBA-PD1 #1
GBA-PD1 #2
GBA-PD2
Control 2
Control 1 #2
GBA-PD2
GBA-PD1 #1
Control 1 #2
IDI-PD2
Control 1 #2
IDI-PD2
IDI-PD1
PDI
Actin
60
40
Normalized PDI levels (fold change over Control 1)
D
Control 1 #1
Control 1 #2
IDI-PD2
IDI-PD1
Control 1 #2
GBA-PD1
GBA-PD2
Control 1 #2
GBA-PD1 #1
GBA-PD1 #2
GBA-PD2
Control 2
Control 1 #2
GBA-PD2
GBA-PD1
Calnexin
Actin
80
40
Normalized Calnexin levels (fold change over Control 1)

Figure 36 Dopaminergic neuronal cultures from heterozygous *GBA*-N370S PD patients show upregulation of ER stress markers. (A) Representative western blot analysis of the expression of the ER stress markers Bip and Calreticulin, in 35 day old dopaminergic neuronal cultures from controls, *GBA*-N370S mutant and idiopathic PD, and respective quantification as a fold change expression to Control 1. (**B-D**) Representative Western blots and quantification of expression (as fold change) of other ER stress markers, namely IRE1α (**B**), PDI (**C**) and Calnexin (**D**). For all analysis, data represent mean ± SEM. of at least 3 independent differentiations. Control 1 was used as an internal control within each differentiation. All statistical comparisons are with Control 2, *P < 0.05; **P < 0.01; ***P < 0.005 Student's t-test.

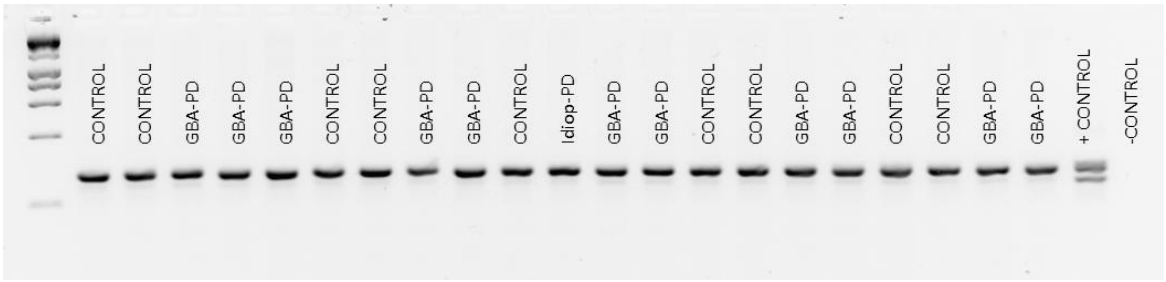

Figure 37 No activation of XBP1 mRNA splicing events for dopaminergic neuronal cultures. After dopaminergic neuronal differentiation, mRNA was extracted and screened for XBP1 splicing events by RT-PCR for Controls, Idiopathic-PD and *GBA-N370S* dopaminergic cultures

5.2.3 Autophagic demand is increased in *GBA*-N370S dopaminergic neuronal cultures

Activation of ER stress has previously been shown in other models to induce autophagy (Yorimitsu et al., 2006; Hart et al., 2012), which sometimes resulted from the accumulation of misfolded proteins (Iwata et al., 2005; Høyer-Hansen and Jäättelä, 2007). Therefore, autophagic induction and autophagic flux were investigated in hiPSC-derived dopaminergic neuronal cultures from PD patients. Western blot analysis of dopaminergic neuronal cultures showed significantly increased levels of LC3B-II (the lipidated form of the autophagosome marker, LC3/Atg8) in *GBA*-N370S and idiopathic cultures when compared to controls (Figure 38).

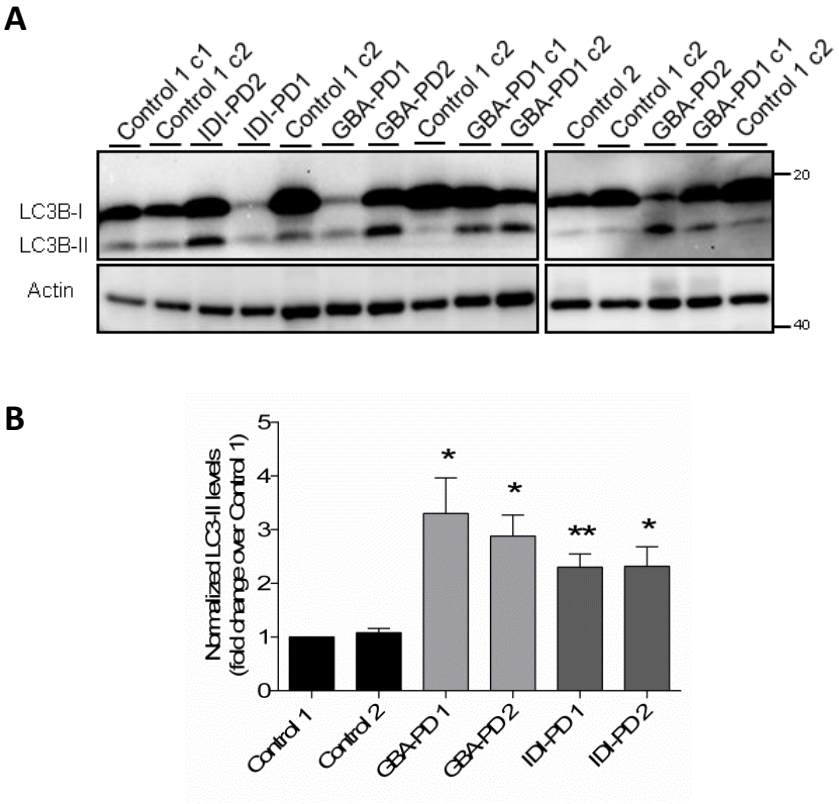

Figure 38 Dopaminergic neuronal cultures from heterozygous *GBA*-N370S PD and idiopathic PD patients show increased autophagosome levels. (A) Representative Western blot for LC3B-II expression. (**B**) Quantification (as fold change over Control 1) of LC3B-II expression in 35-day old dopaminergic neuronal cultures. Data represents mean ± SEM. of at least 3 independent differentiations. Control 1 was used as an internal control within each differentiation and all statistical comparisons are with Control 2, *P < 0.05; **P < 0.01 Student's t-test.

In collaboration with Dr Elizabeth Hartfield, increased levels of LC3, suggesting increased levels of autophagosomes were confirmed by immunofluorescence analysis. This confirmed an increased number of LC3 puncta per cell in *GBA*-N370S and idiopathic cultures suggesting increased number of autophagosomes and, critically, showed that this significant increase was specific to TH-positive neurons (Figure 39).

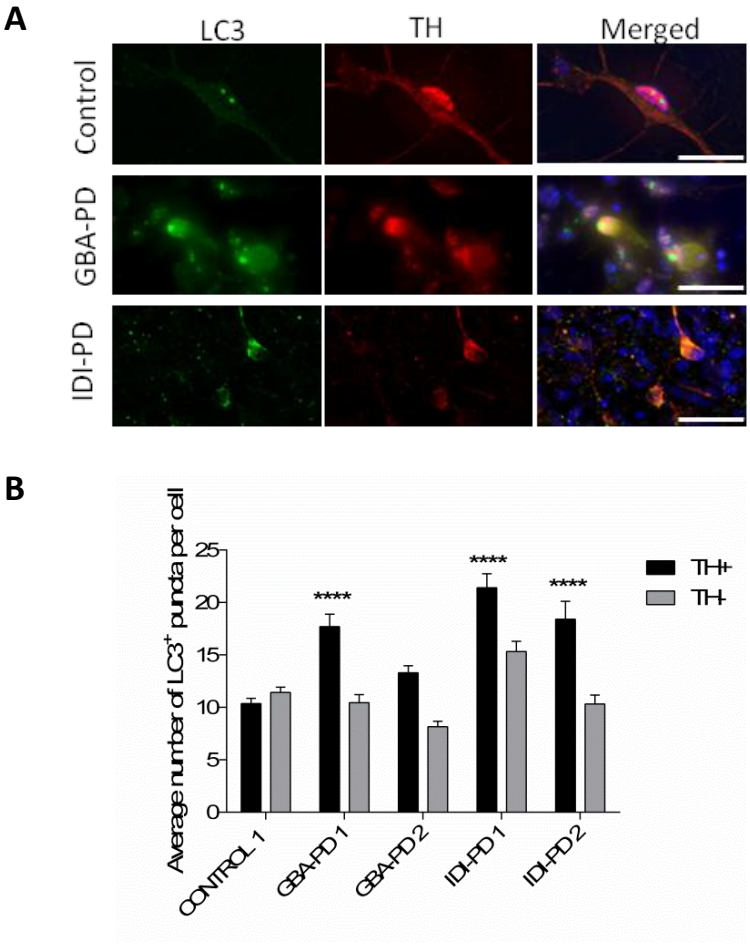

Figure 39 Increased number of autophagosomes in heterozygous *GBA*-N370S and idiopathic PD-derived dopaminergic neuronal cultures. (A) Immunofluorescence staining for LC3B (green) in dopaminergic TH positive neurons (red) in control and PD patient dopaminergic neuronal cultures (scale bar: 20 μm). (**B**) Average number of LC3B-positive puncta per cell, as represented in (A), in TH positive and TH negative cells. Data represents mean ± SEM. of at least 3 independent differentiations. Two-way ANOVA with Tukey post hoc analysis ****P < 0.001. Dopaminergic differentiation of all cell lines and corresponding immunostaining was performed by HF. Imaging of slides and puncta counting was performed by EH

To further study the initial steps of vesicle formation involved in the autophagic pathway and to discriminate between increase levels of autophagosomes resulting from autophagic induction or impaired vesicle degradation, the levels of Beclin1, a key regulator of autophagy used to study macroautophagy activation (Westbroek et al., 2011) were examined. In this assay, dopaminergic neuronal cultures from *GBA*-N370S patients were found to express increased levels of Beclin1 when compared to cultures derived from idiopathic PD patients or control individuals (Figure 40).

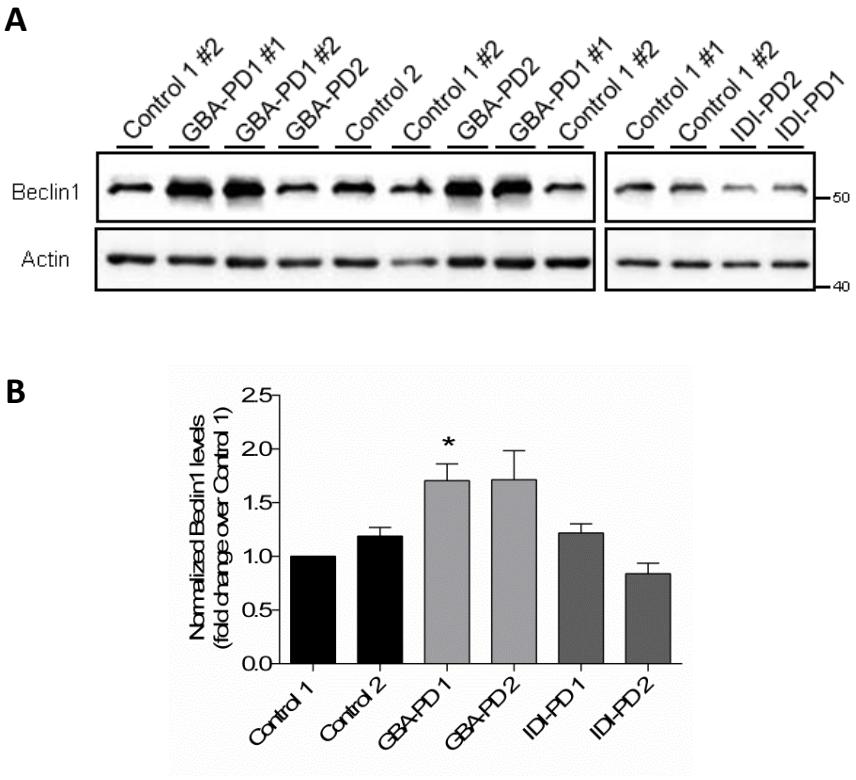

Figure 40 Increased expression of Beclin 1 in differentiated dopaminergic cultures from heterozygous *GBA*-N370S PD patients. (A) Representative Western blot for Beclin1 expression. (**B**) Quantification of Beclin1 expression as fold change over control 1 is shown. Data represents mean ± SEM. of at least 3 independent differentiations. Control 1 was used as an internal control within each differentiation. All statistical comparisons are with Control 2, *P < 0.05 Student's t-test.

To further evaluate autophagosome formation in *GBA*-N370S dopaminergic neuronal cultures, the turnover of LC3B-II was analysed by measuring autophagic flux, as described previously (Mizushima et al., 2010). Treatment with bafilomycin, which blocks the fusion of autophagic vesicles with lysosomes, resulted in increased levels of LC3B-II in control cells, as expected, demonstrating normal flux. In *GBA*-N370S dopaminergic neuronal cultures, a greater increase in LC3B-II was observed, indicating further autophagosome formation and consequent autophagic activation, compared to controls (Figure 41). Similar results were obtained when autophagic flux was determined by p62/SQSTM1 (p62) analysis using bafilomycin-treated samples and when LC3B-II and p62 levels were analysed after treatment with protease inhibitors (pepstatin A and E64d) (Figure 41).

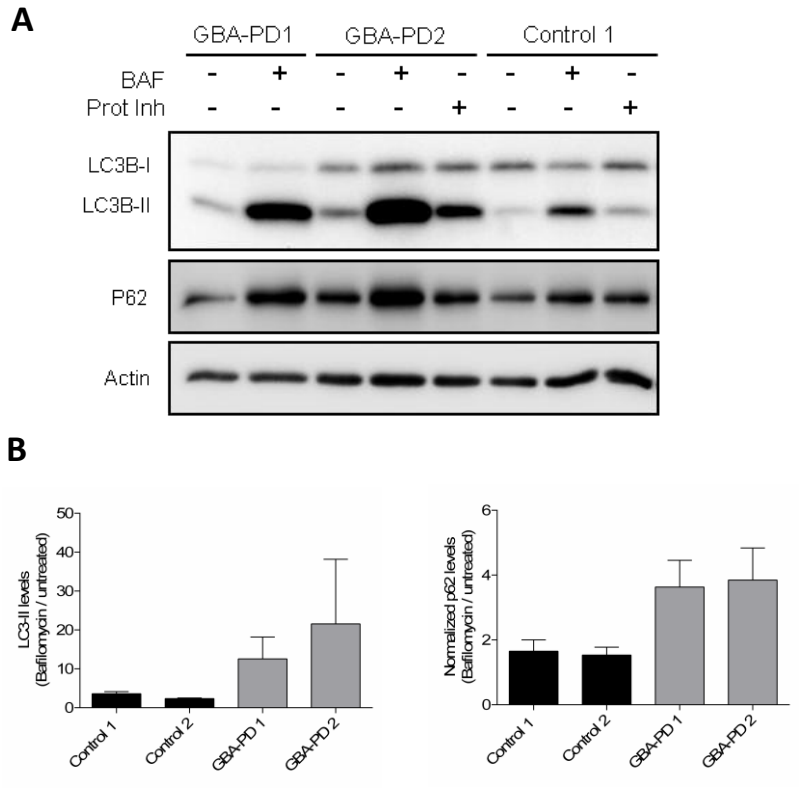

Figure 41 Dopaminergic neuronal cultures from heterozygous *GBA*-N370S PD patients show increased autophagic flux. (A) Autophagic flux analysis by Western blot of control and GBA N370S dopaminergic cultures in the presence or absence of Bafilomycin (10 nM for 6 hours) or proteasome inhibitors (pepstatin and E64d for 24hours). Both treatments led to increased expression of LC3B-II and p62 which were higher in both cases for GBA-N370S dopaminergic neuronal cultures. (**B**) Quantification of autophagic flux as a difference of expression of LC3B-II and p62, respectively, with and without bafilomycin treatment, represented in arbitrary units. For all analyses, data represent mean ± SEM. of at least 2 independent differentiations

5.2.4 Autophagic vacuole clearance is impaired in *GBA*-N370S dopaminergic neuronal cultures

As the *GBA*-N370S mutation is located in the catalytic domain of GCase (Wei et al., 2011), the impact of the heterozygous N370S *GBA* mutation on the activity of this lysosomal enzyme was determined. Both *GBA*-N370S PD patient neuronal cultures showed a ~45% reduction in GCase activity when compared to control individuals, while no significant difference was observed in dopaminergic neuronal cultures derived from patients with idiopathic PD (Figure 42).

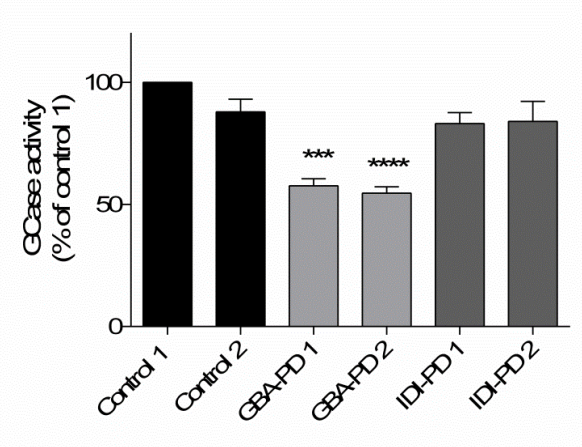

Figure 42 Reduced GCAse activity in dopaminergic neuronal cultures derived from heterozygous *GBA*-N370S PD patients. GCase enzyme activity assayed in differentiated dopaminergic neuronal cultures resulted in a 45% reduction in N370S GBA mutant PD cultures when compared to controls. No significant difference was observed for idiopathic patient cultures. Data represent mean ± SEM. of 3 independent differentiations. Control 1 was used as an internal control within each differentiation. All statistical comparisons are with Control 2, ***P < 0.005; ****P < 0.001 Student's t-test

Reduced GCase activity could potentially impair the overall dopaminergic cellular capacity for lysosomal degradation. This hypothesis was explored by analysis of p62/SQSTM1 as previously described (Bjørkøy et al., 2005; Klionsky et al., 2012). Western blot analysis revealed that p62 levels were increased in *GBA*-N370S dopaminergic neuronal cultures (Figure 43), which supports a deficit in these cells for the clearance of autophagic vacuoles.

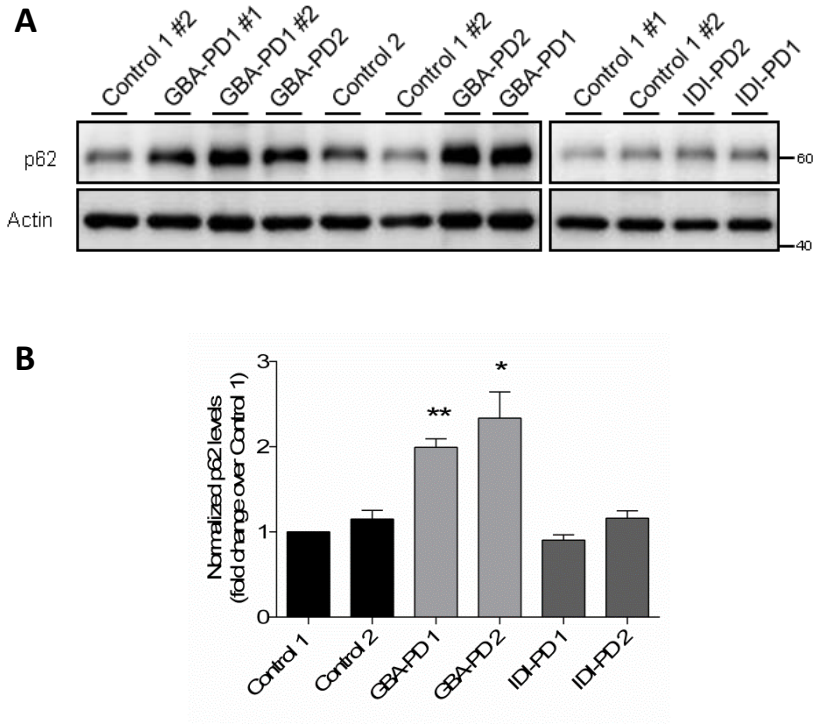

Figure 43 Dopaminergic neuronal cultures from heterozygous *GBA*-N370S PD show increased p62 levels. (A) Representative Western blot for p62 expression. (**B**) Quantification of p62 expression as fold change over control 1 is shown. Data represents mean ± SEM. of at least 3 independent differentiations. Control 1 was used as an internal control within each differentiation. All statistical comparisons are with Control 2, *P < 0.05; **P < 0.01 Student's t-test.

To follow-up the findings in *GBA*-N370S cultures, we next compared *GBA*-N370S and control dopaminergic neurons for ultra-structural alterations by electron microscopy (EM) specifically in identified TH-positive neurons, in collaboration with Dr Helen Christian. This examination revealed an accumulation, in TH immunogold-labelled cells, of electron-dense debris within lysosomal structures in GBA-N370S mutant dopaminergic neurons which was not present in control lines (Figure 44, arrows). This likely represents un-degraded cargo in these N370S dopaminergic neurons (Figure 44, arrowheads)

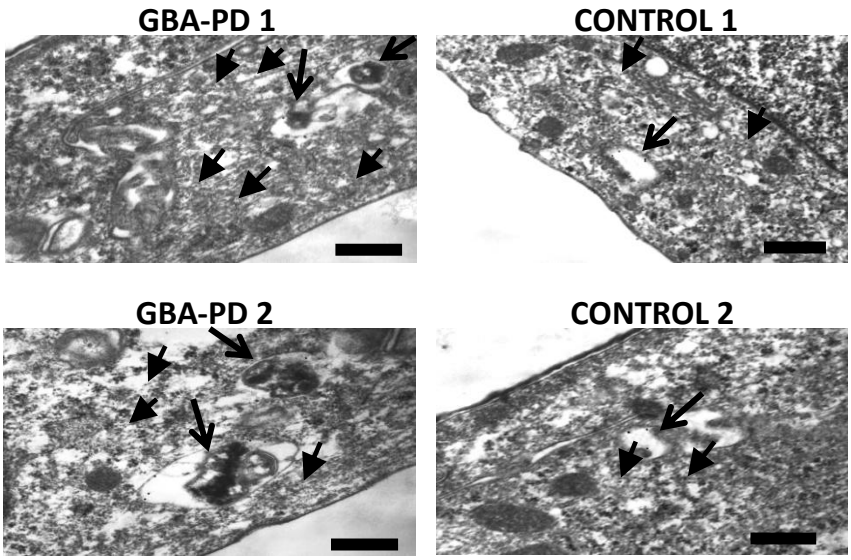

Figure 44 Accumulation of electron-dense material in dopaminergic neurons derived from PD patients carrying a heterozygous *GBA*-N370S mutation. Electron micrographs showing representative examples of un-degraded cargo observed within lysosomal structures in TH-immunogold-positive GBA-N370S neurons. Arrows indicate LAMP1 positive structures of the lysosomal pathway; arrow heads indicate TH immunogold (5 nm). Scale bar =200 nm. Top left GBA-PD2; Bottom left GBA-PD1; Top right Control 1; Bottom right Control 2.

5.2.5 *GBA*-N370S dopaminergic neurons have an enlarged lysosomal compartment

Following on the observation of a possible impairment in lysosomal degradation, as shown by accumulation of electron-dense material by EM and reduced GCase activity, expression of multiple lysosomal markers was examined. Dopaminergic neuronal cultures derived from GBA N370S PD patients showed increased protein expression of the lysosomal markers LAMP1 (Figure 45A) and LAMP2A (Figure 45B). To further confirm aberrant lysosomal compartment, the levels of CathepsinD were analysed. This major lysosomal enzyme was also found increased in dopaminergic neuronal cultures from N370S patients but not in idiopathic PD when compared to controls (Figure 45C).

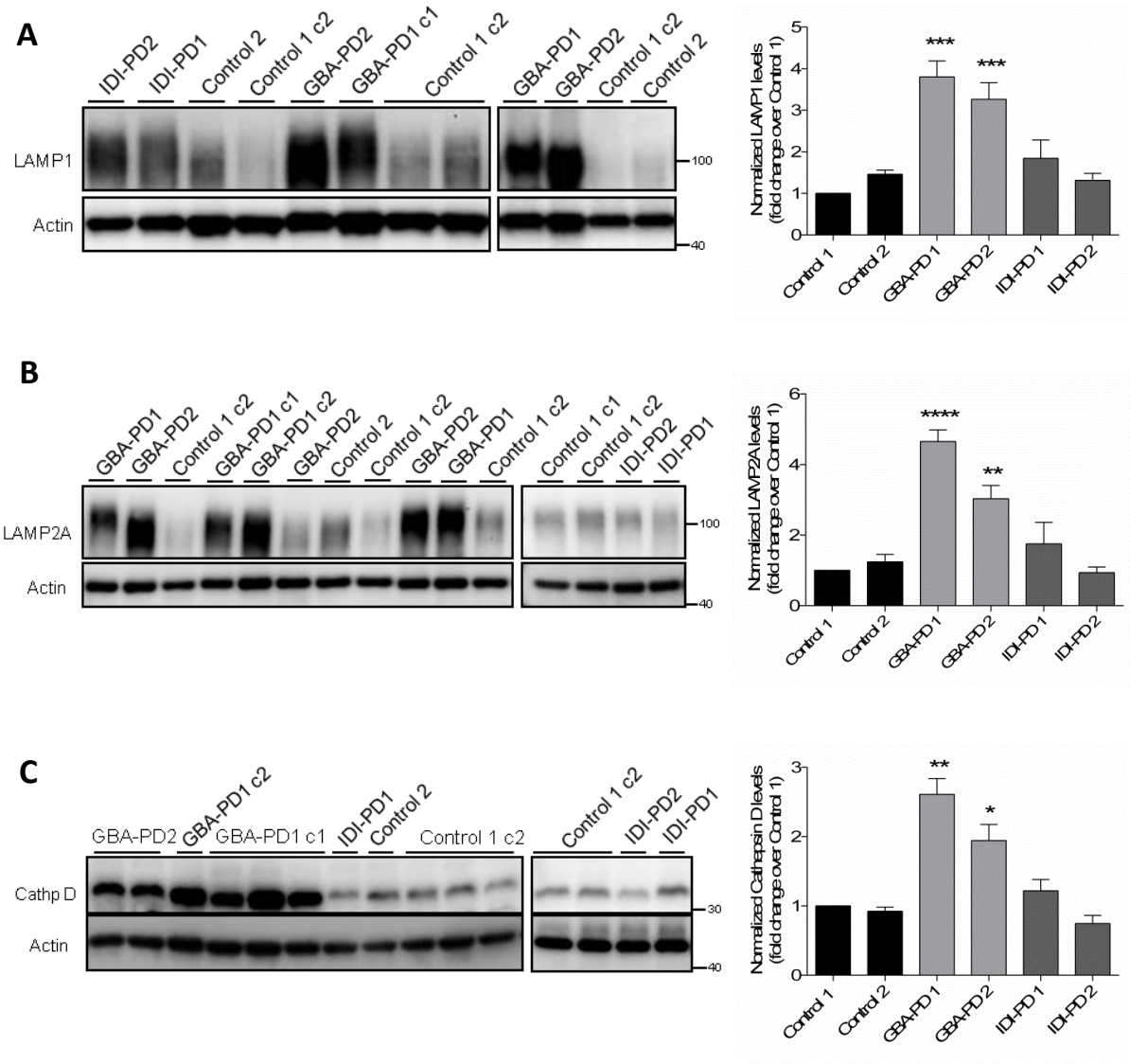

Figure 45 Dopaminergic neuronal cultures from heterozygous GBA-N370S PD show increased expression of multiple lysosomal markers. Differentiated dopaminergic neuronal cultures (35 days old) were analysed for the expression of lysosomal markers. (**A**) Representative Western blot and respective quantification of LAMP1 expression levels (**B**) Representative Western blot and respective quantification of LAMP2A expression levels. (**C**) Representative Western blot and respective quantification of CathepsinD expression levels. Data represent mean ± SEM. of at least 3 independent differentiations. Control 1 was used as an internal control within each differentiation. All statistical comparisons are with Control 2, *P < 0.05; **P < 0.01; ***P < 0.005; ****P < 0.001 Student's t-test

The likely enlargement of the lysosomal compartment in *GBA*-N370S dopaminergic neurons was further confirmed by EM in collaboration with Dr Helen Christian which showed an increase in the number of lysosomes in TH immunogold-labelled cells (Figure 46A, B). These data highlighted that the enlargement of the lysosomal compartment was specific to TH-positive dopaminergic neurons, as no difference was found in TH-negative cells (Figure 46B). In addition, increased size of lysosomes was also detected (Figure 46A, C). This was determined by the quantification of the cell area of TH-positive neurons occupied by lysosomal organelles detected by EM, which was significantly increased in *GBA*-N370S cells compared to controls (Figure 46C). This increase in the size of lysosomes was also found to be specific to dopaminergic neurons as no alterations in size were found for TH-negative cells (Figure 46C).

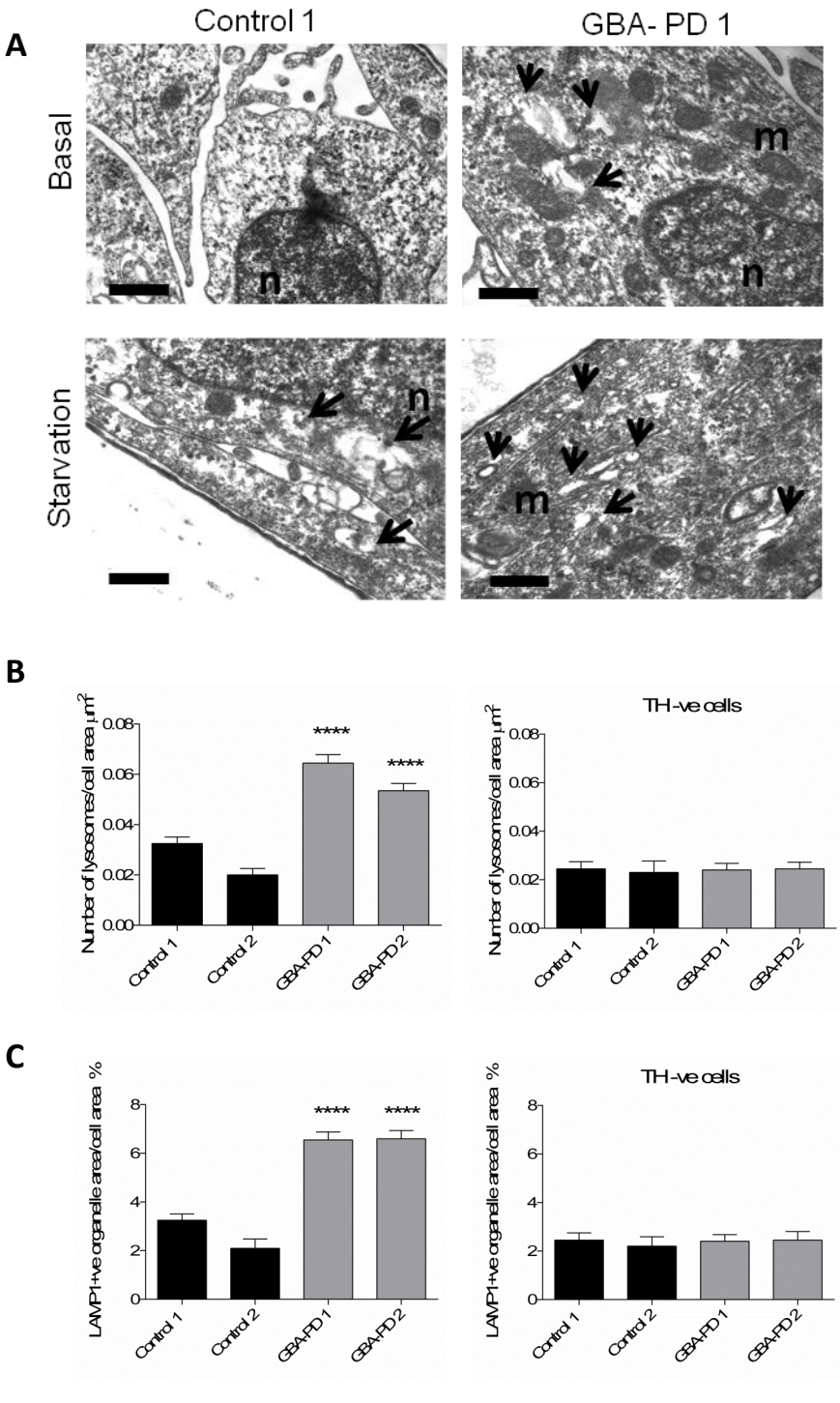
A
Control 1
GBA- PD 1
Basal
Starvation
n
m
B
Number of lysosomes/cell area µm²
0.08
0.06
0.04
0.02
0.00
****
****
Control 1
Control 2
GBA-PD 1
GBA-PD 2
TH-ve cells
C
LAMP1+ve organelle area/cell area %
8
6
4
2
0

Figure 46 Enlargement of the lysosomal compartment in dopaminergic neurons derived from PD patients carrying a heterozygous GBA-N370S mutation. (A) Electron micrographs showing representative images of immunogold-labelled TH-positive neurons for differentiated controls and GBA N370S neurons in basal and under starvation conditions. Arrows indicate LAMP1 positive structures of the lysosomal pathway. Scale bar =200 nm. (**B**) Quantification of EM data shows increased number of lysosomes under basal conditions for TH labelled neurons in both GBA-N370S cell lines compared to controls (left). Identical quantification in TH-negative cells is shown (right) (**C**) Size of lysosomes, represented as percentage of cell area occupied by LAMP1 labelled organelles, was significantly increased in TH neurons for GBA N370S derived dopaminergic cultures (left), while no differences were observed in TH-negative cells (right). Representative images are from cultures from Control 1 and GBA-PD1. Data represent mean ± SEM. n=20 cells for each cell line from 2 independent differentiations. Comparisons are with Control 1 and Control 2 ****$P < 0.001$ Student's t-test.

Since increased number of lysosomes could also be a consequence of upregulated lysosomal synthesis, the levels of transcription factor EB (TFEB), a master regulator of lysosomal biogenesis and function (Song et al., 2013) was analysed. After differentiation into dopaminergic neuronal cultures, no significant alterations of TFEB expression were observed for *GBA*-N370S or idiopathic PD patient derived cultures, when compared to controls (Figure 47).

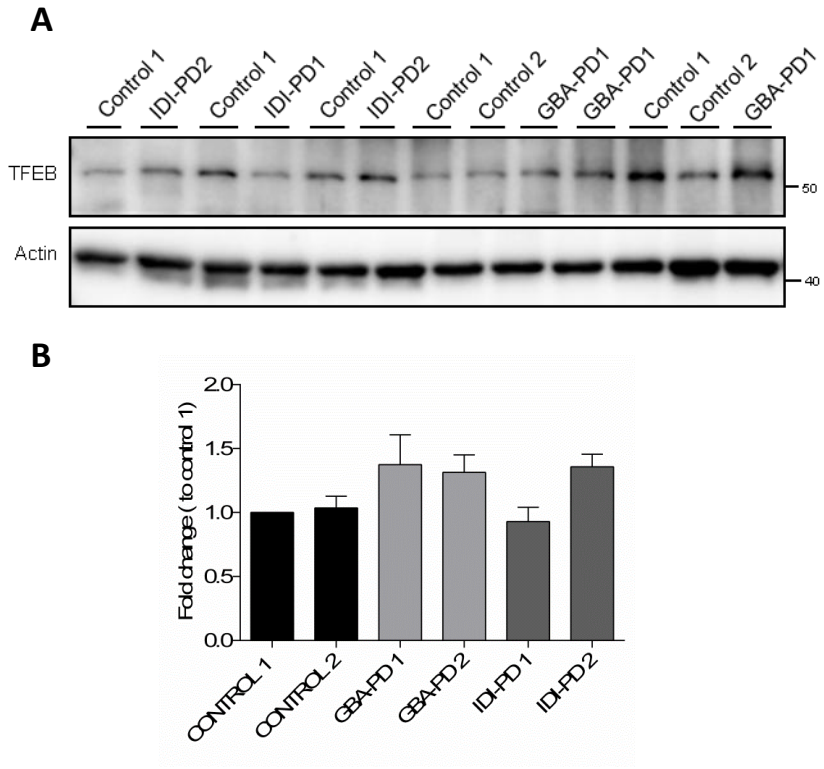

Figure 47 No alterations for TFEB expression levels in dopaminergic neuronal cultures from heterozygous GBA-N370S or idiopathic PD patients. (A) Representative Western blot for TFEB expression. (**B**) Quantification of TFEB expression as fold change over control 1 is shown. Data represents mean ± SEM. of at least 3 independent differentiations. Control 1 was used as an internal control within each differentiation. All statistical comparisons are with Control 2, Student's t-test, not-significant

Furthermore, it is important to notice that although the numbers of lysosomes were increased even in basal conditions in *GBA*-N370S cells, these dopaminergic cultures were still capable of responding efficiently to situations of increased autophagic demand, as demonstrated by increased number of lysosomes under starvation conditions by EM analysis (Figure 48). Blocking the fusion of lysosomes with autophagosomes using Bafilomycin A, resulted in a similar increase in the number of lysosomes in dopaminergic neurons across all cell lines, which further demonstrates that the process of lysosomal biogenesis is probably primarily unaffected in PD derived dopaminergic neurons.

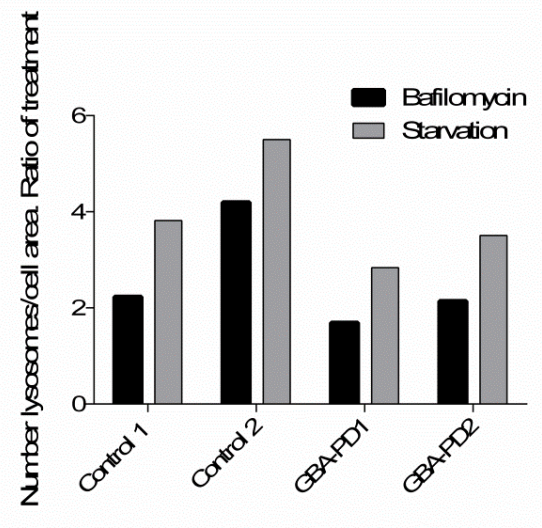

Figure 48 Efficient lysosomal biogenesis in dopaminergic neurons determined by EM. 24h starvation or 6h Bafilomycin A treatment resulted in increased number of lysosomes in TH-positive neurons relative to basal condition for both control and N370S dopaminergic cultures, as determined by EM quantification of LAMP1 labelled structures. Data represent mean of n=20 cells for each cell line for each condition from 2 independent differentiations.

5.2.6 *GBA*-N370S dopaminergic neuronal cultures have increased α-synuclein release

Accumulation of α-synuclein is a characteristic pathological marker of PD which has been proposed to possibly result from defective clearance mechanisms. Therefore, in light of our previous results the modulation of a-synuclein levels in dopaminergic cultures was further explored. The intracellular α-synuclein content in dopaminergic neuronal cultures from *GBA*-N370S PD showed no significant differences when compared to controls (Figure 49).

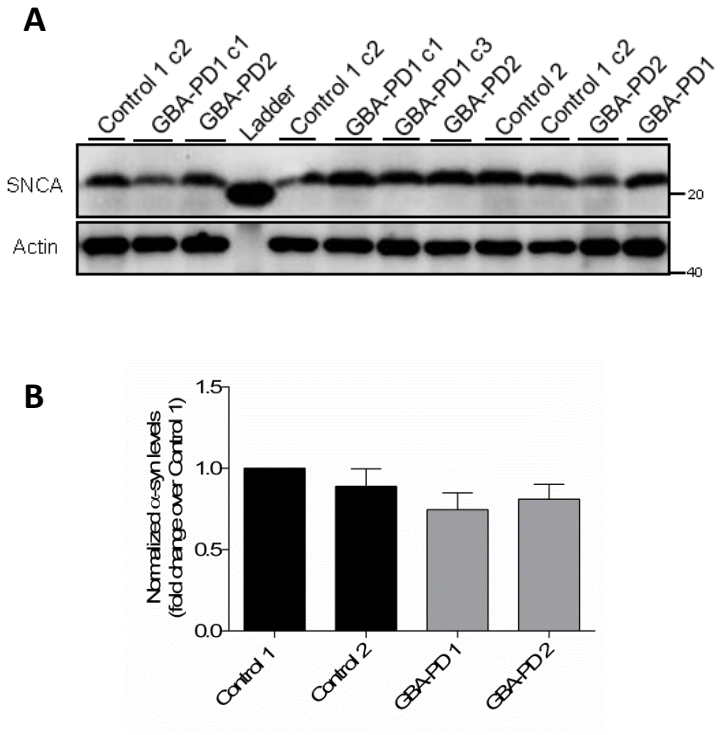

Figure 49 No alterations in α-synuclein content in dopaminergic neuronal cultures from heterozygous *GBA*-N370S mutation when compared to controls. (A) Representative Western blot of α-synuclein intercellular levels in differentiated dopaminergic neuronal cultures after 35 days from controls and *GBA*-N370S PD lines. (**B**) Quantification of α-synuclein levels represented as a fold change over control 1 is shown. Data represent mean ± SEM. of at least 3 independent differentiations. All statistical comparisons are with Control 2, Student's t-test, not-significant.

Recently however, other laboratories have shown that impairments in the autophagic system might lead to extracellular secretion of α-synuclein (Alvarez-Erviti et al., 2011; Ejlerskov et al., 2013; Lee et al., 2013). In collaboration with Dr Kostas Vrekelis, University of Athens, the culture media of dopaminergic cultures undergoing differentiation was analysed. Analysis of α-synuclein released into the culture media was determined by ELISA and showed not only increased secretion as cells matured in culture, but, more interestingly, that higher amounts of α-synuclein were secreted in dopaminergic neuronal cultures differentiated from *GBA*-N370S patients compared to controls (Figure 50).

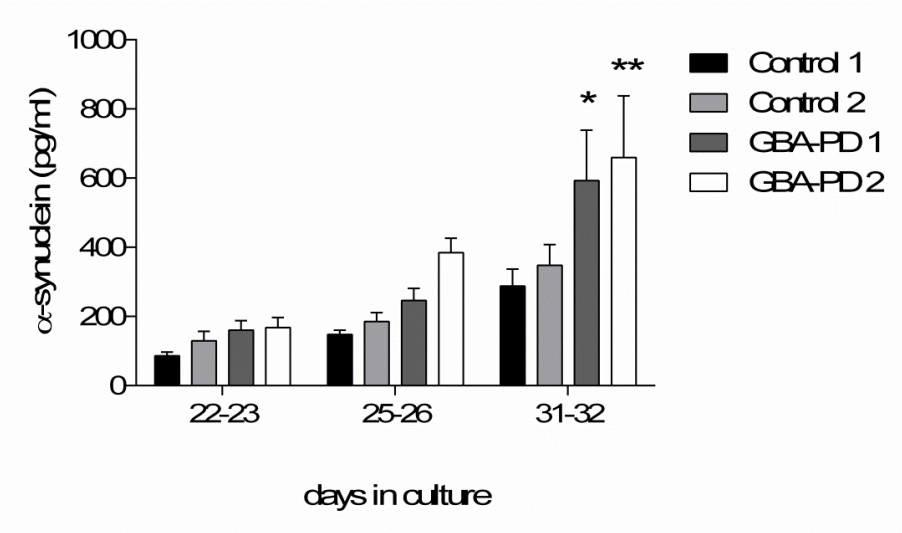

Figure 50 Increased extracellular α-synuclein levels in the culture media from dopaminergic neuronal cultures derived from PD patients carrying a heterozygous *GBA*-N370S mutation. Culture media from cells undergoing dopaminergic differentiation was assayed by ELISA for the presence of α-syn. X axis represents total days in culture from the EB stage. Data represent mean ± SEM. of an n=6 per line from 2 independent differentiations, with each sample analysed in triplicate. Two-way ANOVA with Tukey post hoc analysis; *$P < 0.05$; **$P < 0.01$ when compared to control 1.

5.2.7 GCase inhibition does not cause ER stress, UPR activation nor increased induction of autophagy

Analyses thus far seem to suggest that the *GBA*-N370S mutation affects dopaminergic neuron protein homeostasis, leading to ER stress and increased autophagic demand combined with reduced lysosomal degradation capacity. To investigate *GBA*-related mechanisms in PD which may be distinct from GD, we asked if our observations may derive directly from reduced GCase activity. Dopaminergic neuronal cultures from healthy control individuals were subjected to an acute treatment (4 days) with Conduritol B-Epoxide (CBE), a GCase inhibitor. This treatment resulted in an enzymatic activity reduction of >98% (Figure 51A). Protein expression analyses from control differentiated dopaminergic neuronal cultures showed no alteration in the levels of ER stress markers Bip/GRP78, Calnexin, and Calreticulin, no changes in LIMP2 expression, and no alteration in the levels of LC3B-II, after CBE treatment (Figure 51B-D). However, the lysosomal compartment may be perturbed as determined by LAMP2A and p62 levels after CBE treatment (Figure 51B, C, E).

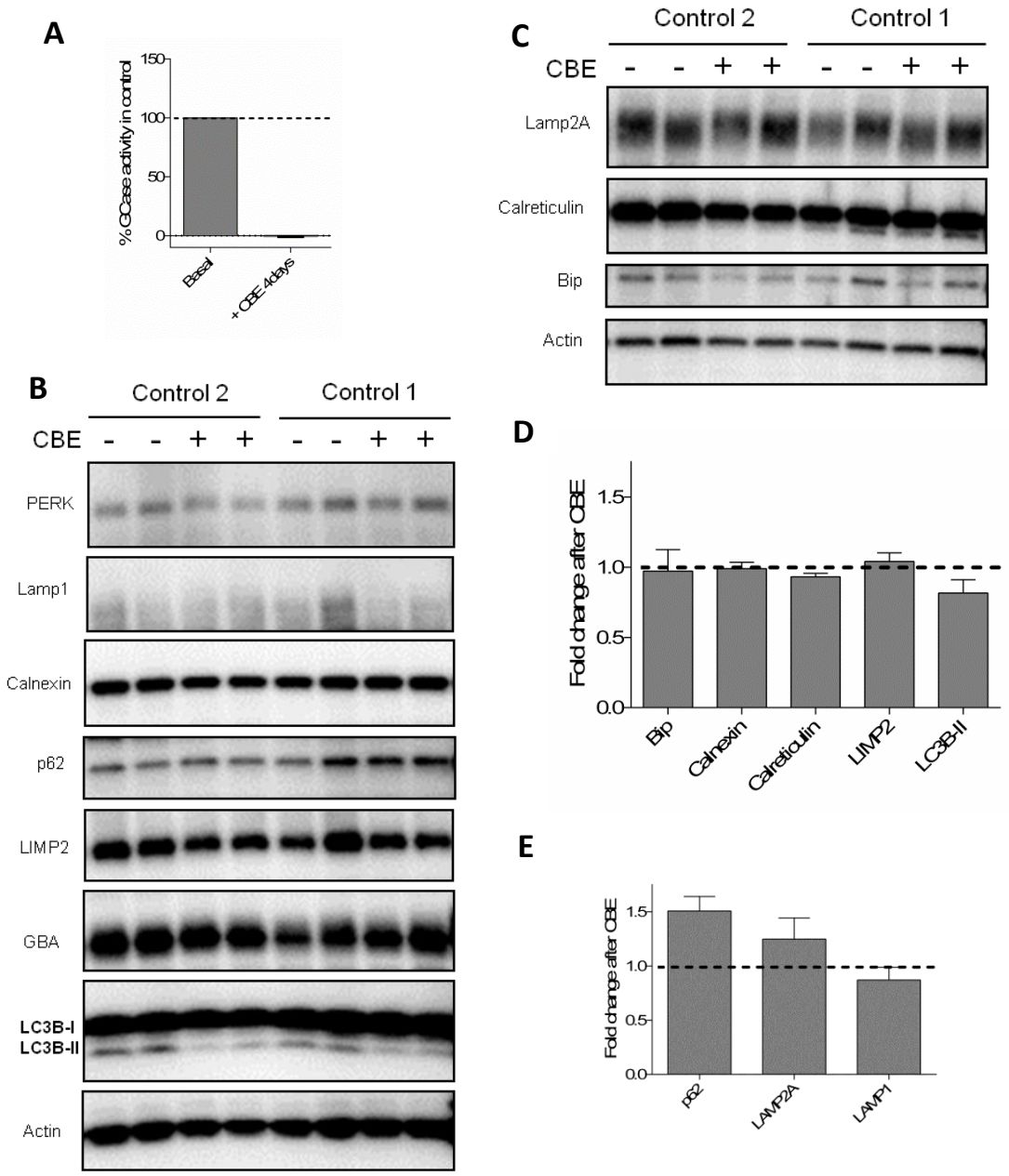

Figure 51 Inhibiting GCase activity with CBE does not lead to ER stress, UPR or increased autophagy in dopaminergic neuronal cultures derived from control individuals. (A) CBE treatment (4 days) reduced GCase activity in dopaminergic neuronal cultures derived from control hiPS lines by >98%. (B and C) Representative Western blots for lysosomal and autophagic markers on dopaminergic neuronal cultures derived from Control 1 and Control 2 hiPSC lines treated with CBE. (D and E) Quantification of results obtained in (B and C), data shown as a fold change in expression for each marker after CBE treatment. For simplicity in interpretation of results, data from differentiated cultures from Control 1 and Control 2 were pooled together for graphical representation. Data represent mean ± SEM. of at least 2 independent differentiations.

5.3 Discussion

In this chapter, phenotypic differences between heterozygous *GBA*-N370S, idiopathic PD and control derived dopaminergic neuronal cultures were explored. The goal was to obtain novel insights in how heterozygous *GBA* mutations might contribute to the development and progression of PD.

Initial analysis at the protein level revealed the presence of an extra, higher molecular weight isoform of the GCase protein specific for *GBA*-N370S derived dopaminergic neuronal cultures. This isoform represented up to 50% of total expressed GCase and was found to be sensitive to EndoH treatment. These observations suggest that the heterozygous *GBA*-N370S mutation was sufficient to cause the retention of GCase within the ER, similar to what has previously been observed for homozygous *GBA* mutant models (Ron and Horowitz, 2005; Wang et al., 2011). However, contradictory to reported homozygous mutant studies, no differences on total GCase levels in *GBA*-N370S PD lines were found. This indicates that GCase is probably not targeted for degradation as a result of ER retention, which is the usual consequence of homozygous *GBA* mutations; ER-associated degradation of GCase leading to a reduction in GCase levels (Ron and Horowitz, 2005; Choi et al., 2011; Mazzulli et al., 2011; Sun et al., 2011; Panicker et al., 2012; Tiscornia et al., 2013). This major difference in our PD model, compared with GD models highlights the importance of studying the exact type of genetic alteration associated with a specific pathology.

LIMP2 is a GCase-specific lysosomal receptor that mediates the transport of GCase from the ER to the lysosome (Reczek et al., 2007). In our study, expression of LIMP2 was found increased specifically for *GBA*-N370S derived dopaminergic neuronal cultures, which supports a possible role for LIMP2 in trafficking ER-retained mutant or WT GCase from the ER to the lysosome as a compensatory mechanism (Reczek et al., 2007). Of note, a recent

post-mortem analysis of PD brains carrying different types of heterozygous *GBA* mutations suggests no alteration in the protein levels of LIMP2. However the data was very variable and post-mortem results represent an end-stage of the disease which might not reflect the early-stage of neuronal dysfunction we are trying to replicate using hiPSC-derived dopaminergic cultures (Gegg et al., 2012).

ER stress activation has been shown to result from accumulation of misfolded proteins, ultimately resulting in UPR activation (Høyer-Hansen and Jäättelä, 2007). The relevance of this mechanism in the context of PD has been previously highlighted in studies showing activation of the UPR in the SNpc of PD patients (Hoozemans et al., 2007). Here, in dopaminergic neuronal cultures from *GBA*-N370S patients, the expression of multiple ER chaperones was found upregulated, which likely reflects a dysregulation of the ER homeostatic environment induced by accumulation of misfolded GCase protein. This comes in agreement with a recent post-mortem analysis of brain from PD patients carrying multiple heterozygous *GBA* mutations showing UPR activation (Gegg et al., 2012). Another recent study reports accumulation of GCase in the ER and upregulation of ER stress in hiPSC-derived neurons from PD patients carrying the A53T mutation in the SNCA gene and a α-synuclein triplication patient (Chung et al., 2013), highlighting the relevance of this phenotype in a variety of PD cases. Furthermore, these results come in agreement with multiple reports from GD models where homozygous mutations also resulted in ER stress activation, likely reflecting common dysregulations between these two pathologies based on protein misfolding events (Wei et al., 2008; Lee et al., 2011; Wang et al., 2011; Maor et al., 2013). Of note, cleavage of XBP1 mRNA, another marker or ER stress, was not observed in our differentiated dopaminergic neuronal cultures. This could mean that XBP1 splicing is not a crucial transducer in this context as it also has been previously detected in the brains of only one third of GBA mutant PD patients analysed (Gegg et al., 2012).

In studies from other unrelated pathologies, ER stress has been shown to trigger autophagy (reviewed in (Høyer-Hansen and Jäättelä, 2007)). However this possibility has not yet been explored in the context of PD-related *GBA* mutations. We show here multiple lines of evidence for autophagy activation in PD dopaminergic neuronal cultures, including increased expression levels of autophagosomes in TH-positive neurons derived from both idiopathic and *GBA*-N370S PD patients. Beclin1 expression was also found increased in *GBA*-N370S cultures, together with increased autophagic flux. Overall, these combined data support an increased autophagic demand in *GBA*-N370S PD lines which could represent a response to ER stress caused by retention of misfolded mutant GCase in the ER. These results come in agreement with a recent PD-hiPSC study where induction of autophagy was also shown, reporting increased autophagosome levels detected in dopaminergic cultures derived from idiopathic and LRRK2-G2019S patients, although autophagic flux levels were found decreased in this report (Sánchez-Danés et al., 2012). Furthermore, increased levels of LC3-II have also been shown to be increased in the putamen of PD patients carrying heterozygous *GBA* mutations (Gegg et al., 2012), and in the SNpc and amygdala of PD brains, all suggesting that an increase in autophagy is related with the pathological process of PD (Alvarez-Erviti et al., 2010).

When the impact of the heterozygous *GBA*-N370S mutation on GCase activity was analysed in our model, a 45% reduction in activity was observed in differentiated dopaminergic neuronal cultures, which is in agreement with the results obtained from post-mortem analyses of the SNpc from PD patients carrying diverse heterozygous *GBA* mutations (Gegg et al., 2012). In cultures from idiopathic patients no differences were found in our study which contrasts with the results from the previously mentioned post-mortem report. Interestingly, a 25% reduction of GCase activity in post-mortem brain tissue was also found in patients carrying heterozygous *GBA* mutations who developed Lewy body disease (LBD),

an α-synucleinopathy related to PD (Kurzawa-Akanbi et al., 2012). Reduced GCase activity may contribute to a more general decreased lysosomal degradation capacity of neurons. Exploring this possibility lead to the observation of increased protein levels of p62 and accumulation of electron-dense debris inside lysosomal structures which were observed specifically in dopaminergic neurons derived from *GBA*-N370S PD patients. These observations likely reflect the accumulation of un-degraded cargo within dopaminergic neurons, supporting a defect in the clearance of autophagic vacuoles. These results come in agreement with previous reports of reduced lysosomal degradation in a mouse model of PD (Dehay et al., 2010) and confirmed in post-mortem analysis of PD patients (Anglade et al., 1997; Dehay et al., 2010) and in related Lewy body disorders (Klucken et al., 2012; Kurzawa-Akanbi et al., 2012). Reduced autophagic clearance was also detected in a previous study using hiPSC-derived dopaminergic cultures from PD patients carrying a G2019S LRRK2 mutation, which was also observed in cultures from idiopathic patients (Sánchez-Danés et al., 2012).

To explore the possibility that impaired lysosomal degradation might lead to downstream defects along the autophagic pathway, expression of multiple lysosomal markers in differentiated dopaminergic neuronal cultures was further examined. *GBA*-N370S cultures showed increased protein expression of the lysosomal markers LAMP1 and LAMP2A. Also increased were the levels of Cathepsin D, a major lysosomal enzyme involved in a-synuclein degradation (Sevlever et al., 2008) which is found increased in primate models of PD (Yelamanchili et al., 2011) and in models of GCase deficiency associated with areas of neuronal loss (Vitner et al., 2010). These results reflect an enlargement of the lysosomal compartment which was confirmed to correspond to both an increase in the number and the size of lysosomes as detected by EM analysis. Crucially EM analysis showed that this increase was specific for dopaminergic neurons, emphasising once again the importance of

studying a disease-relevant cell type. We propose that although the increased number of lysosomes could be caused in part by an increased autophagic demand (as described earlier), it is also likely caused by a reduced lysosomal degradation capacity brought about by reduced GCase activity as supported also by the increased size of the lysosomes in dopaminergic neurons detected by EM analysis.

One of the main pathological hallmarks of PD involves the accumulation of α-synuclein. α-synuclein has previously been shown to be degraded by the autophagy-lysosome pathway (ALP) (Cuervo et al., 2004) and to be altered in response to autophagic impairments (Klucken et al., 2012) and ER stress (Hoepken et al., 2008). Furthermore, impairments to the autophagic system have been shown to result in α-synuclein secretion (Alvarez-Erviti et al., 2011; Ejlerskov et al., 2013; Lee et al., 2013). Therefore, the possible modulation of a-synuclein levels by the previously observed impaired lysosomal degradation and autophagy induction was further explored. After differentiation, increased levels of secreted α-synuclein were found in the culture media from *GBA*-N370S dopaminergic neuronal cultures. This is likely a consequence of the lysosomal/autophagic defects described above for these cultures, and is consistent with a previous study showing increased α-synuclein release into the media by neurons derived from a patient carrying an α-synuclein triplication (Devine et al., 2011). α-synuclein release could be an early event in the pathology of PD, as a potential compensation mechanism to remove excess intracellular α-synuclein. Secreted α-synuclein can also become pathogenic as it has been shown that uptake of α-synuclein by neurons can result in impaired cellular proteostasis (Desplats et al., 2009; Hansen et al., 2011), including GCase accumulation in the ER (Mazzulli et al., 2011). α-synuclein has also been shown to induce ER stress, block ER-Golgi trafficking (Cooper et al., 2006), induce lysosomal rupture (Freeman et al., 2013) decrease lysosomal function (Cuervo et al., 2004; Winslow et al., 2010) and inhibit the lysosomal activity of normal GCase (Mazzulli et al., 2011).

Furthermore, CMA uses LAMP2A to transport α-synuclein to the lysosomes (Dawson and Dawson, 2011) and in transgenic mice overexpressing α-synuclein, LAMP2A was upregulated to increase the elimination of α-synuclein via lysosomal degradation (Mak et al., 2010). Our previously observed increase in expression of LAMP2A in dopaminergic cultures from *GBA*-N370S patients could also be involved in a similar cellular response against α-synuclein accumulation.

It has been suggested that in neuronal cells, pharmacological inhibition of GCase is not sufficient to disturb α-synuclein levels or to impair lysosomal function (Dermentzaki et al., 2013). Using a similar approach of GCase inhibition with CBE in control cell lines, we aimed to determine whether inhibition of GCase is sufficient to recapitulate the autophagic/lysosomal deficits observed in *GBA*-N370S PD dopaminergic neuronal cultures. No alterations were observed for these mechanisms which we consider to be dependent primarily on misfolded N370S GCase, namely ER stress upregulation and autophagic activation. On the other hand, CBE treatment resulted in a mild perturbation of lysosomal degradation-related events, such as increased expression of LAMP2A and p62, although there was no change in LAMP1. Overall, the results obtained after CBE treatment support the hypothesis that the phenotypes of ER stress upregulation and autophagy activation observed in *GBA*-N370S dopaminergic cultures were likely driven by *GBA*-N370S dependent GCase protein retention, whereas the overall cellular lysosomal degradation capacity might be affected by GCase activity.

Taken together, the findings from this chapter suggest that in PD-derived hiPSCs, the heterozygous *GBA*-N370S mutation impairs the lysosomal degradation capacity of dopaminergic neurons. In addition, it also leads to the accumulation of unfolded GCase within the ER resulting in ER stress activation, which likely increases the demand for autophagic degradation. This overall impairment to the autophagy pathway might further

disrupt the degradation of other cellular components by this pathway, including α-synuclein. We propose that this combination of increased autophagic activation and reduced lysosomal degradation capacity exerts a dual protein homeostasis impairment specific for dopaminergic neurons that might be relevant to the initial stages of PD pathology in susceptible dopaminergic neuronal populations.

Chapter 6

Conclusion

Increased population aging has resulted in an increased impact of age related disorders in current society. PD, the second most common neurodegenerative disorder is a good example of such a disease. Despite all the research which has been done, age is still the best known risk factor for PD. As populations age, the impact of similar disorders will increase, requiring a better understanding of the underlying causes of age-related pathologies. Scientific progress over the last decades has elucidated multiple aspects of PD, with a dramatic change in the understanding of this disease. Initially considered an idiopathic pathology without a genetic origin, the development of genetic analysis technologies has resulted in the identification of important genetic predispositions for PD. Overall, PD is currently known to have an important genetic background, and a lot of effort has been invested in understanding the molecular mechanisms by which specific PD-associated genetic alterations result in PD. However, it is important to note that we have not been able to identify a genetic cause to the vast majority of PD cases and despite extensive progress in research, treatment options available are still very limited and mostly symptomatic. An unexpected association of PD with mutations in *GBA* has recently emerged, and represents to date the most common genetic risk factor identified for PD. However most of these studies are epidemiologic and

the mechanisms by which *GBA* mutations might result in PD are still mostly unknown. In response, the central role of this thesis was to elucidate the role of GBA mutations in the context of a PD relevant human model of disease.

One of the major limitations for a better understanding of the impact of *GBA* mutations, and other relevant genes, in the pathology of PD has been the lack of highly relevant human cell disease models. In the context of *GBA*, mutations associated with PD are mostly heterozygous. Models to recapitulate such genetic alteration are more difficult to recapitulate *in vitro* and are in clear need. Furthermore, some unproven mechanisms have been postulated following results obtained from distinct homozygous *GBA* mutations models, which clearly do not recapitulate the heterozygous variants associated with PD. To overcome these limitations, our approach was based on the establishment of dopaminergic neuronal cultures from PD patients identified as carriers of heterozygous *GBA* mutations as a model of study. For the generation of patient derived dopaminergic neurons, we took advantage of the current developments offered by hiPSC technology. This allowed us to obtain pluripotent stem cells from multiple individuals which could then be differentiated into human dopaminergic neurons, a brain cell type not previously available by other methods.

Our initial goal was then to derive dopaminergic neurons from hiPSCs. Since at the time this project was started protocols available were still limited, we aimed at developing an efficient protocol for the differentiation of hiPSCs into dopaminergic neuronal cultures. Multiple strategies were employed, and improvements implemented starting from mESCs and hESCs. Ultimately we were able to develop a robust protocol which was efficient in generating functional dopaminergic neurons across several hiPSC lines. Cells obtained using this protocol were extensively characterized and confirmed to express multiple putative midbrain markers, to produce dopamine and present DAT activity. Using this protocol we were able to generate 40% of neurons, of which around 35% expressed TH. Although these

values are comparable to the results from some other protocols published in the meantime, we were able to do it in a short period of time (5 weeks) and to characterize in depth the dopaminergic neurons present in culture. However, we recognize that cultures obtained using this and other protocols are still highly heterogeneous and further improvements in efficiency are expected to further purify the population of interest in culture.

Once a differentiation protocol was established, we set to identify PD patients of interest to be recruited for the current study. All individuals screened for this study were part of a clinical cohort established by the OPDC at the start of this project. N370S and L444P represent the two most common heterozygous *GBA* mutations found associated with PD (up to 70% of total cases), and were therefore the focus of our mutation screening. N370S mutations were found in 1.65 % of PD patients in this cohort, while L444P mutations were found in 1.26 % of PD patients. In the control population only one positive case (N370S) was found overall. Together, these mutations were present in 2.83% of PD patients, which comes in agreement with the results reported by other studies. No differences were observed for the age of onset between idiopathic patients and carriers of *GBA* mutations in our study. This observation does not come in agreement with the results obtained by a multicenter study where the examination of over 5000 PD patients identified an earlier age of onset (4 years compared to idiopathic) in carriers of *GBA* mutations. The low number of positive cases identified in our current cohort, and the fact that we screened for only two *GBA* mutations could at least in part explain this different observations. Increasing the number of PD patients recruited for this cohort and complete screening of *GBA* exons would likely help elucidating this question. Within the "at-risk" group, a higher frequency of *GBA*-N370S mutations was found (5.3%) when compared to controls. This group is mostly composed of relatives of PD patients with a strong family history of PD and individuals with idiopathic REM sleep disorder. This potentially relevant observation should be followed up in the future, by

determining if these individuals will have an increased predisposition to develop PD. This could help to clarify the relevance of *GBA* as a risk factor for PD.

After the identification of PD patients of interest, hiPSC lines were generated by our collaborators from control individuals, idiopathic PD patients and PD patients carrying *GBA*-N370S heterozygous mutations. Most PD-hiPSCs reports available have focused almost exclusively on monogenic forms of PD, with idiopathic cases, the most common form of PD, being vastly neglected. For a better understanding of possible *GBA* related mechanism in the context of the more common cases of PD, the inclusion of idiopathic cases in this study was determined as essential. Also important was the inclusion of cell lines derived from more than one individual within each group, which is an improvement when compared to multiple reports available using lines from single PD patients. However, overall we recognize the limitation in the sample size of our study. Ideally, multiple clonal lines from multiple individuals within each group would favour a more accurate representation of the pathologic mechanisms across individuals. This would account for intra-individual variability resulting from the already reported variability along clonal lines derived from the same individual, and for inter-patient variability, as multiple patients likely present a certain degree of pathological variation which might be relevant for the global understanding of the disease.

After confirming a similar efficiency in dopaminergic differentiation across all lines included in this study, we could proceed with investigating the role of heterozygous *GBA*-N370S mutations in PD using a highly relevant human model of disease. Initial observations in differentiated dopaminergic cultures of an extra GCase protein isoform which was sensitive to EndoH treatment suggested that the the *GBA*-N370S heterozygous mutation results in retention of GCase within the ER. This result comes in agreement with previous reports on the impact of homozygous *GBA* mutations. However, unlike in studies of homozygous GD mutations, no differences were observed for total amounts of GCase protein

in differentiated dopaminergic cultures from *GBA*-N370S heterozygous mutations. In homozygous *GBA* mutations, ER retention of GCase leads to degradation of the protein resulting in a significant decrease of the total amount of GCase. No evidences of a similar reduction was observed in our heterozygous cultures indicating a clear and important difference, that could not be accounted for based on homozygous studies, suggesting different mechanisms of action. The levels of LIMP2, a GCase specific lysosomal receptor were found increased specifically for dopaminergic neuronal cultures from *GBA*-N370S cultures, suggesting a possible role of LIMP2 in the trafficking of ER-retained GCase. Dopaminergic neuronal cultures from *GBA*-N370S heterozygous lines were also found to have increased expression of multiple markers of ER stress. This observation was also *GBA* specific as no alterations were found in idiopathic cases. We propose that this alteration could be a consequence of excessive GCase accumulation within the ER, in a similar way to what has been observed for homozygous *GBA* mutant models. In other models of unrelated pathologies, ER stress was shown to result in autophagy activation, and has not yet been explored in the context of *GBA* mutant models. When explored in the context of differentiated dopaminergic cultures, we found multiple evidences suggesting autophagy activation in *GBA*-N370S mutation lines. These included increased expression of Beclin 1, increased autophagic flux and increased levels of autophagosomes. For the latter, an apparent increase was also observed for idiopathic cultures, suggesting a common phenotype across the two groups, which might be explained, at least in part, by a different mechanism of action.

When exploring the potential effects of the heterozygous *GBA*–N370S mutation at the lysosomal level we observed a ~45% reduction in the activity of GCase when compared to controls, while no difference was observed for dopaminergic neuronal cultures from idiopathic individuals. As the N370S mutation is located in the catalytic domain of GCase

this impairment was not surprising, but was not yet previously confirmed. Next we explored the hypothesis that the reduced GCase activity could interfere with the general lysosomal degradation capacity of these cells. An impaired lysosomal degradation was observed, with increased p62 levels and accumulation of debris within lysosomal structures which was, importantly, only observed within TH positive cells. To follow on possible downstream impairments caused by this potential impaired lysosomal degradation, further lysosomal aspects were analysed. The levels of multiple lysosomal markers were found increased in dopaminergic cultures from *GBA*-N370S mutation lines reflecting an enlargement of the lysosomal compartment which was then confirmed by EM to correspond to an increased number and size of lysosomes. Importantly, this enlargement was found to be specific for TH positive cells, suggesting a mechanistic cellular specificity relevant for the context of PD.

The pathological hallmark of PD is represented by the accumulation of α-synuclein, which can be degraded by the autophagic-lysosomal pathway. Next we explored the hypothesis that the previously described autophagic-lysosomal deregulation observed for *GBA*-N370S cultures could potentially impair α-synuclein levels. Importantly we observed that the levels of α-synuclein present in the culture media increased over the course of differentiation and that those levels were higher in *GBA*-N370S dopaminergic cultures when compared to controls, suggesting a possible increased secretion of α-synuclein in *GBA*-N370S cultures.

Finally, we tried to distinguish between phenotypes caused by accumulation of unfolded GCase in the ER and phenotypes that were related to decreased GCase activity. For that, dopaminergic cultures differentiated from control individual lines were treated with CBE, a GCase inhibitor. After acute GCase inhibition (>95%) over four days, no alterations were found for the mechanisms we had hypothesised to be dependent mostly on ER retention of misfolded GCase, namely ER stress activation and autophagy activation. On the other

hand, CBE treatment resulted in a mild alteration of the levels of markers mostly related to lysosomal degradation.

Taken together, our findings suggest that in PD the heterozygous *GBA*-N370S mutation impairs the lysosomal degradation capacity in dopaminergic neurons but, critically, also leads to the accumulation of unfolded GCase within the ER and consequent ER stress, which likely increases the demand for autophagic degradation. We propose that this combination of increased autophagic demand and reduced lysosomal degradation capacity exerts a dual protein homeostasis impairment specific for dopaminergic neurons, which ultimately might disrupt the α-synuclein pathway (Figure 52).

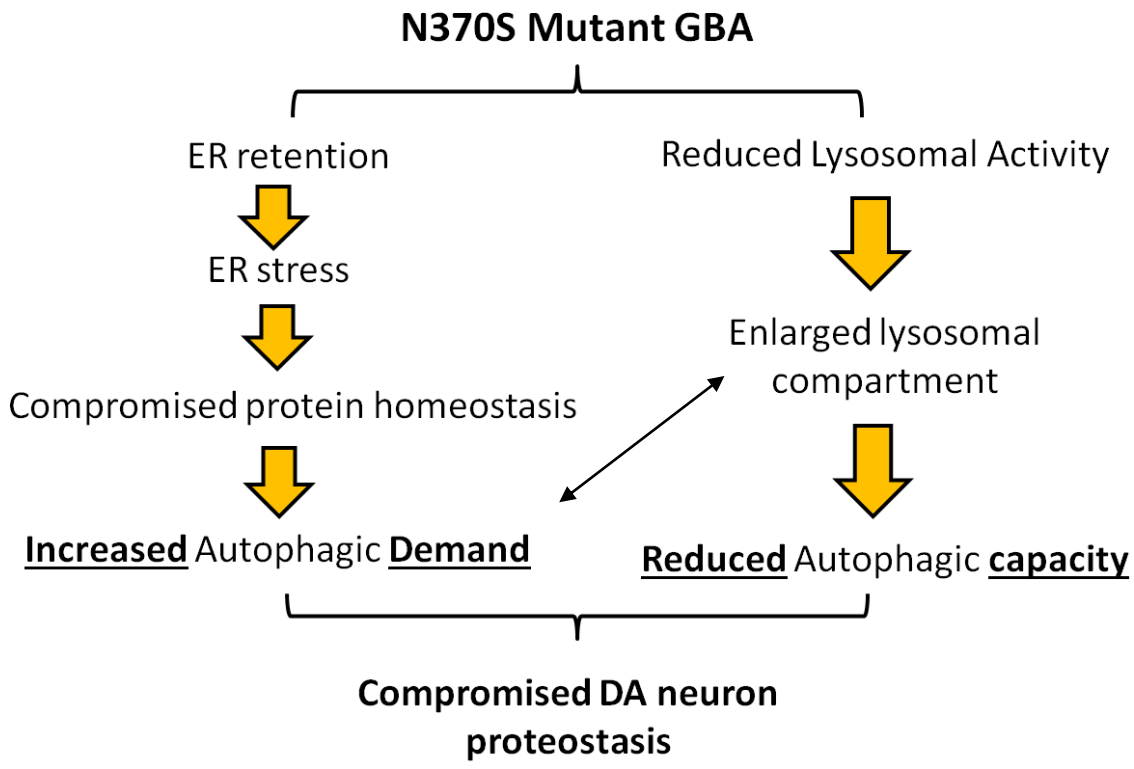

Figure 52 Schematic of the proposed mechanisms of action by which the GBA-N370S mutation might impair dopaminergic cultures derived from PD patients

In summary, this work is the first study to examine cellular mechanism of PD pathology in heterozygous *GBA* mutant PD iPSC lines. We uncover disease mechanisms that are distinct from homozygous *GBA* mutations that usually result in GD, and would not be expected from such models (Table 12).

To further dissect the differences between heterozygous *GBA* mutant-PD and GD (caused by homozygous *GBA* mutations) it will be important to examine in detail the impact of these mutations in the lipid metabolism of differentiated dopaminergic cultures. GD, a lysosomal storage disease, presents with accumulation of GlcCer, resulting in further changes in lipid homeostasis. We have differentiated multiple hiPSC lines from PD patients and controls, and cells were collected for a lipid profiling analysis that is currently ongoing at Fran Platt's laboratory (Department of Pharmacology, University of Oxford). It will be also important to examine next in detail dopaminergic neuronal cultures derived from PD patients-hiPSC lines carrying other PD relevant *GBA* mutations including the heterozygous *GBA*-L444P mutation. Recently the *GBA* E326K variant has also been proposed as a risk factor for PD, being commonly found in PD populations (Duran et al., 2013) and reaching GWAS significance (Pankratz et al., 2012). Interestingly, E326K mutations have not been reported as a causative mutation for GD and been found both in heterozygous and homozygous context in PD, increasing the complexity of the association of *GBA* mutations with PD. Determining the similarities and differences of the impact of these different mutations in the context of PD derived dopaminergic neurons will allow a better understanding of the mechanism by which *GBA* mutations contribute to the pathology of PD.

Table 12 Overview of the phentoypes observed in our PD *GBA*-N370S model compared to available GD homozygous models

	GD models	Our hiPSC model
***GBA* mutation**	Homozygous	Heterozygous
Human cell models available (excluding post-mortem**)**	Many (fibroblast; iPSCs; iPSCs derived macrophages, neurons and DA populations)	None reported
GCase Protein levels	Reduced (slightly variable but up to 90% reduction)	No change
ER-associated degradation	Yes	No
LIMP2 modulation	Not explored	Increased expression
ER stress activation	Confirmed	Confirmed
Autophagy induction	No change or reduced (only 2 short studies done	Increased
GBA activity	Reduced (80-95% reduction)	Reduced (45% reduction)
Lysosomal degradation capacity	Reduced lysosomal degradation, reduced proteolysis of long-lived proteins; delayed clearance of phagocytosed RBCs	Reduced
Other lysosomal defects	LAMP1 accumulation in a GCase KD model only – not a disease model	Increased number and size of lysosomes
SNCA	Increased accumulation	Increased secretion
Underlying cause	GCase protein loss/or enzyme inactivation	Protein misfolding and enzyme deficiency

References

Aboud, A.A., Tidball, A.M., Kumar, K.K., Neely, M.D., Ess, K.C., Erikson, K.M., et al. (2012). Genetic risk for Parkinson's disease correlates with alterations in neuronal manganese sensitivity between two human subjects. Neurotoxicology *33*: 1443–9.

Abou-Sleiman, P.M., Healy, D.G., Quinn, N., Lees, A.J., and Wood, N.W. (2003). The role of pathogenic DJ-1 mutations in Parkinson's disease. Annals of Neurology *54*: 283–6.

Abou-Sleiman, P.M., Muqit, M.M.K., McDonald, N.Q., Yang, Y.X., Gandhi, S., Healy, D.G., et al. (2006a). A heterozygous effect for PINK1 mutations in Parkinson's disease? Annals of Neurology *60*: 414–9.

Abou-Sleiman, P.M., Muqit, M.M.K., and Wood, N.W. (2006b). Expanding insights of mitochondrial dysfunction in Parkinson's disease. Nature Reviews. Neuroscience *7*: 207–19.

Aharon-Peretz, J., Rosenbaum, H., and Gershoni-Baruch, R. (2004). Mutations in the glucocerebrosidase gene and Parkinson's disease in Ashkenazi Jews. The New England Journal of Medicine *351*: 1972–1977.

Alegre-Abarrategui, J., Christian, H., Lufino, M.M.P., Mutihac, R., Venda, L.L., Ansorge, O., et al. (2009). LRRK2 regulates autophagic activity and localizes to specific membrane microdomains in a novel human genomic reporter cellular model. Human Molecular Genetics *18*: 4022–4034.

Alvarez-Erviti, L., Rodriguez-Oroz, M.C., Cooper, J.M., Caballero, C., Ferrer, I., Obeso, J. a, et al. (2010). Chaperone-mediated autophagy markers in Parkinson disease brains. Archives of Neurology *67*: 1464–1472.

Alvarez-Erviti, L., Seow, Y., Schapira, A.H., Gardiner, C., Sargent, I.L., Wood, M.J. a, et al. (2011). Lysosomal dysfunction increases exosome-mediated alpha-synuclein release and transmission. Neurobiology of Disease *42*: 360–367.

Andersson, E., Tryggvason, U., Deng, Q., Friling, S., Alekseenko, Z., Robert, B., et al. (2006). Identification of intrinsic determinants of midbrain dopamine neurons. Cell *124*: 393–405.

Anglade, P., Vyas, S., Javoy-Agid, F., Herrero, M.T., Michel, P.P., Marquez, J., et al. (1997). Apoptosis and autophagy in nigral neurons of patients with Parkinson's disease. Histology and Histopathology *12*: 25–31.

Ascherio, A., Zhang, S.M., Hernan, M.A., Kawachi, I., Colditz, G.A., Speizer, F.E., et al. (2001). Prospective study of caffeine consumption and risk of Parkinson's disease in men and women. Ann Neurol *50*: 56–63.

Badano, J.L., and Katsanis, N. (2002). Beyond Mendel: an evolving view of human genetic disease transmission. Nature Reviews. Genetics *3*: 779–89.

Badger, J.L., Cordero-Llana, O., Hartfield, E.M., and Wade-Martins, R. (2014). Parkinson's disease in a dish - Using stem cells as a molecular tool. Neuropharmacology *76 Pt A*: 88–96.

Balducci, C., Pierguidi, L., Persichetti, E., Parnetti, L., Sbaragli, M., Tassi, C., et al. (2007). Lysosomal hydrolases in cerebrospinal fluid from subjects with Parkinson's disease. Movement Disorders : Official Journal of the Movement Disorder Society *22*: 1481–1484.

Beavan, M.S., and Schapira, A.H. V (2013). Glucocerebrosidase mutations and the pathogenesis of Parkinson disease. Annals of Medicine *45*: 511–21.

Bekris, L.M., Mata, I.F., and Zabetian, C.P. (2010). The genetics of Parkinson disease. Journal of Geriatric Psychiatry and Neurology *23*: 228–42.

Bembi, B., Zambito Marsala, S., Sidransky, E., Ciana, G., Carrozzi, M., Zorzon, M., et al. (2003). Gaucher's disease with Parkinson's disease: clinical and pathological aspects. Neurology *61*: 99–101.

Bendikov-Bar, I., Maor, G., and Horowitz, M. (2013). Processing and maturation of human glucocerebrosidase. In Advances in Gaucher Disease: Basic and Clinical Perspectives, (Future Medicine Ltd), pp 140–157.

Benito-León, J., Porta-Etessam, J., and Bermejo, F. (1998). [Epidemiology of Parkinson disease]. Neurología (Barcelona, Spain) *13 Suppl 1*: 2–9.

Betarbet, R., Sherer, T.B., MacKenzie, G., Garcia-Osuna, M., Panov, A. V, and Greenamyre, J.T. (2000). Chronic systemic pesticide exposure reproduces features of Parkinson's disease. Nature Neuroscience *3*: 1301–6.

Bjørkøy, G., Lamark, T., Brech, A., Outzen, H., Perander, M., Overvatn, A., et al. (2005). p62/SQSTM1 forms protein aggregates degraded by autophagy and has a protective effect on huntingtin-induced cell death. The Journal of Cell Biology *171*: 603–14.

Bonifati, V. (2014). Genetics of Parkinson's disease - state of the art, 2013. Parkinsonism & Related Disorders *20 Suppl 1*: S23–8.

Bonifati, V., Rizzu, P., Baren, M.J. van, Schaap, O., Breedveld, G.J., Krieger, E., et al. (2003). Mutations in the DJ-1 gene associated with autosomal recessive early-onset parkinsonism. Science (New York, N.Y.) *299*: 256–9.

Bonifati, V., Rohé, C.F., Breedveld, G.J., Fabrizio, E., Mari, M. De, Tassorelli, C., et al. (2005). Early-onset parkinsonism associated with PINK1 mutations: frequency, genotypes, and phenotypes. Neurology *65*: 87–95.

Braak, H., and Tredici, K. Del (2008). Invited Article: Nervous system pathology in sporadic Parkinson disease. Neurology *70*: 1916–25.

Braak, H., Tredici, K. Del, Rüb, U., Vos, R.A.I. de, Jansen Steur, E.N.H., and Braak, E. (2003). Staging of brain pathology related to sporadic Parkinson's disease. Neurobiology of Aging *24*: 197–211.

Bras, J., Paisan-Ruiz, C., Guerreiro, R., Ribeiro, M.H., Morgadinho, A., Januario, C., et al. (2009). Complete screening for glucocerebrosidase mutations in Parkinson disease patients from Portugal. Neurobiology of Aging *30*: 1515–1517.

Bras, J., Singleton, A., Cookson, M., and Hardy, J. (2008). Emerging pathways in genetic Parkinson's disease: Potential role of ceramide metabolism in Lewy body disease. FEBS Journal *275*: 5767–5773.

Braulke, T., and Bonifacino, J.S. (2009). Sorting of lysosomal proteins. Biochimica Et Biophysica Acta *1793*: 605–14.

Brockmann, K., Srulijes, K., Hauser, A.K., Schulte, C., Csoti, I., Gasser, T., et al. (2011). GBA-associated PD presents with nonmotor characteristics. Neurology *77*: 276–80.

Byers, B., Cord, B., Nguyen, H.N., Schüle, B., Fenno, L., Lee, P.C., et al. (2011). SNCA triplication Parkinson's patient's iPSC-derived DA neurons accumulate α-synuclein and are susceptible to oxidative stress. PloS One *6*: e26159.

Cai, J., Yang, M., Poremsky, E., Kidd, S., Schneider, J.S., and Iacovitti, L. (2010). Dopaminergic neurons derived from human induced pluripotent stem cells survive and integrate into 6-OHDA-lesioned rats. Stem Cells Dev *19*: 1017–1023.

Caiazzo, M., Dell'Anno, M.T., Dvoretskova, E., Lazarevic, D., Taverna, S., Leo, D., et al. (2011). Direct generation of functional dopaminergic neurons from mouse and human fibroblasts. Nature *476*: 224–7.

Canet-Avilés, R.M., Wilson, M.A., Miller, D.W., Ahmad, R., McLendon, C., Bandyopadhyay, S., et al. (2004). The Parkinson's disease protein DJ-1 is neuroprotective due to cysteine-sulfinic acid-driven mitochondrial localization. Proceedings of the National Academy of Sciences of the United States of America *101*: 9103–8.

Chambers, S.M., Fasano, C. a, Papapetrou, E.P., Tomishima, M., Sadelain, M., and Studer, L. (2009). Highly efficient neural conversion of human ES and iPS cells by dual inhibition of SMAD signaling. Nature Biotechnology *27*: 275–280.

Chartier-Harlin, M.C., Dachsel, J.C., Vilariño-Güell, C., Lincoln, S.J., Leprêtre, F., Hulihan, M.M., et al. (2011). Translation initiator EIF4G1 mutations in familial parkinson disease. American Journal of Human Genetics *89*: 398–406.

Chen, Y., McMillan-Ward, E., Kong, J., Israels, S.J., and Gibson, S.B. (2007). Mitochondrial electron-transport-chain inhibitors of complexes I and II induce autophagic cell death mediated by reactive oxygen species. Journal of Cell Science *120*: 4155–66.

Chiba, Y., Komori, H., Takei, S., Hasegawa-Ishii, S., Kawamura, N., Adachi, K., et al. (2014). Niemann-Pick disease type C1 predominantly involving the frontotemporal region, with cortical and brainstem Lewy bodies: an autopsy case. Neuropathology : Official Journal of the Japanese Society of Neuropathology *34*: 49–57.

Cho, H.-J., Lee, C.-S., Kwon, Y.-W., Paek, J.S., Lee, S.-H., Hur, J., et al. (2010). Induction of pluripotent stem cells from adult somatic cells by protein-based reprogramming without genetic manipulation. Blood *116*: 386–395.

Choi, J.H., Stubblefield, B., Cookson, M.R., Goldin, E., Velayati, A., Tayebi, N., et al. (2011). Aggregation of α-synuclein in brain samples from subjects with glucocerebrosidase mutations. Molecular Genetics and Metabolism *104*: 185–8.

Chu, Y., Dodiya, H., Aebischer, P., Olanow, C.W., and Kordower, J.H. (2009). Alterations in lysosomal and proteasomal markers in Parkinson's disease: relationship to alpha-synuclein inclusions. Neurobiology of Disease *35*: 385–98.

Chung, C.Y., Khurana, V., Auluck, P.K., Tardiff, D.F., Mazzulli, J.R., Soldner, F., et al. (2013). Identification and rescue of α-synuclein toxicity in Parkinson patient-derived neurons. Science (New York, N.Y.) *342*: 983–7.

Chung, S., Leung, A., Han, B., and Chang, M. (2009). Wnt1-lmx1a forms a novel autoregulatory loop and controls midbrain dopaminergic differentiation synergistically with the SHH-FoxA2 pathway. Cell Stem Cell *5*: 646–658.

Clark, I.E., Dodson, M.W., Jiang, C., Cao, J.H., Huh, J.R., Seol, J.H., et al. (2006). Drosophila pink1 is required for mitochondrial function and interacts genetically with parkin. Nature *441*: 1162–6.

Clark, L.N., Kartsaklis, L.A., Wolf Gilbert, R., Dorado, B., Ross, B.M., Kisselev, S., et al. (2009). Association of glucocerebrosidase mutations with dementia with lewy bodies. Archives of Neurology *66*: 578–83.

Clark, L.N., Nicolai, A., Afridi, S., Harris, J., Mejia-Santana, H., Strug, L., et al. (2005). Pilot association study of the beta-glucocerebrosidase N370S allele and Parkinson's disease in subjects of Jewish ethnicity. Movement Disorders : Official Journal of the Movement Disorder Society *20*: 100–103.

Clark, L.N., Ross, B.M., Wang, Y., Mejia-Santana, H., Harris, J., Louis, E.D., et al. (2007). Mutations in the glucocerebrosidase gene are associated with early-onset Parkinson disease. Neurology *69*: 1270–1277.

Cleeter, M.W.J., Chau, K.-Y., Gluck, C., Mehta, A., Hughes, D.A., Duchen, M., et al. (2013). Glucocerebrosidase inhibition causes mitochondrial dysfunction and free radical damage. Neurochemistry International *62*: 1–7.

Cooper, A. a, Gitler, A.D., Cashikar, A., Haynes, C.M., Hill, K.J., Bhullar, B., et al. (2006). Alpha-synuclein blocks ER-Golgi traffic and Rab1 rescues neuron loss in Parkinson's models. Science (New York, N.Y.) *313*: 324–8.

Cooper, O., Hargus, G., Deleidi, M., Blak, A., Osborn, T., Marlow, E., et al. (2010). Differentiation of human ES and Parkinson's disease iPS cells into ventral midbrain dopaminergic neurons requires a high activity form of SHH, FGF8a and specific regionalization by retinoic acid. Molecular and Cellular Neurosciences *45*: 258–266.

Cooper, O., Seo, H., Andrabi, S., Guardia-Laguarta, C., Graziotto, J., Sundberg, M., et al. (2012). Pharmacological rescue of mitochondrial deficits in iPSC-derived neural cells from patients with familial Parkinson's disease. Science Translational Medicine *4*: 141ra90.

Corti, O., Lesage, S., and Brice, A. (2011). What genetics tells us about the causes and mechanisms of Parkinson's disease. Physiological Reviews *91*: 1161–1218.

Cowan, C.A., Klimanskaya, I., McMahon, J., Atienza, J., Witmyer, J., Zucker, J.P., et al. (2004). Derivation of embryonic stem-cell lines from human blastocysts. The New England Journal of Medicine *350*: 1353–6.

Cranmer, J.M., Lein, P.J., Pessah, I.N., Aboud, A.A., Tidball, A.M., Kumar, K.K., et al. (2012). Genetic risk for Parkinson's disease correlates with alterations in neuronal manganese sensitivity between two human subjects. NeuroToxicology *33*: 1443–1449.

Crews, L., Spencer, B., Desplats, P., Patrick, C., Paulino, A., Rockenstein, E., et al. (2010). Selective molecular alterations in the autophagy pathway in patients with Lewy body disease and in models of alpha-synucleinopathy. PloS One *5*: e9313.

Cuervo, A.M., Stefanis, L., Fredenburg, R., Lansbury, P.T., and Sulzer, D. (2004). Impaired degradation of mutant alpha-synuclein by chaperone-mediated autophagy. Science (New York, N.Y.) *305*: 1292–5.

Cullen, V., Lindfors, M., Ng, J., Paetau, A., Swinton, E., Kolodziej, P., et al. (2009). Cathepsin D expression level affects alpha-synuclein processing, aggregation, and toxicity in vivo. Molecular Brain *2*: 5.

Cullen, V., Sardi, S.P., Ng, J., Xu, Y.-H., Sun, Y., Tomlinson, J.J., et al. (2011). Acid β-glucosidase mutants linked to Gaucher disease, Parkinson disease, and Lewy body dementia alter α-synuclein processing. Annals of Neurology *69*: 940–953.

Dagda, R.K., Zhu, J., Kulich, S.M., and Chu, C.T. (2008). Mitochondrially localized ERK2 regulates mitophagy and autophagic cell stress: implications for Parkinson's disease. Autophagy *4*: 770–82.

Davis, C.A., and Joyner, A.L. (1988). Expression patterns of the homeo box-containing genes En-1 and En-2 and the proto-oncogene int-1 diverge during mouse development. Genes & Development *2*: 1736–44.

Dawson, T., and Dawson, V. (2011). A Lysosomal Lair for a Pathogenic Protein Pair. Science Translational Medicine *3*: 91ps28.

Dehay, B. (2012). Loss of P-type ATPase ATP13A2/PARK9 function induces general lysosomal deficiency and leads to Parkinson disease neurodegeneration. Proceedings of the … *109*: 9611–9616.

Dehay, B., Bové, J., Rodríguez-Muela, N., Perier, C., Recasens, A., Boya, P., et al. (2010). Pathogenic lysosomal depletion in Parkinson's disease. The Journal of Neuroscience : the Official Journal of the Society for Neuroscience *30*: 12535–12544.

Dehay, B., Martinez-Vicente, M., Caldwell, G. a, Caldwell, K. a, Yue, Z., Cookson, M.R., et al. (2013). Lysosomal impairment in Parkinson's disease. Movement Disorders : Official Journal of the Movement Disorder Society *28*: 725–732.

Dehay, B., Ramirez, A., Martinez-Vicente, M., Perier, C., Canron, M.-H., Doudnikoff, E., et al. (2012). Loss of P-type ATPase ATP13A2/PARK9 function induces general lysosomal deficiency and leads to Parkinson disease neurodegeneration. Proceedings of the National Academy of Sciences of the United States of America *109*: 9611–6.

Dekker, N., Dussen, L. van, Hollak, C.E.M., Overkleeft, H., Scheij, S., Ghauharali, K., et al. (2011). Elevated plasma glucosylsphingosine in Gaucher disease: relation to phenotype, storage cell markers, and therapeutic response. Blood *118*: e118–27.

Dermentzaki, G., Dimitriou, E., Xilouri, M., Michelakakis, H., and Stefanis, L. (2013). Loss of β-glucocerebrosidase activity does not affect alpha-synuclein levels or lysosomal function in neuronal cells. PloS One *8*: e60674.

Desplats, P., Lee, H.-J., Bae, E.-J., Patrick, C., Rockenstein, E., Crews, L., et al. (2009). Inclusion formation and neuronal cell death through neuron-to-neuron transmission of alpha-synuclein. Proceedings of the National Academy of Sciences of the United States of America *106*: 13010–5.

Devine, M.J., Ryten, M., Vodicka, P., Thomson, A.J., Burdon, T., Houlden, H., et al. (2011). Parkinson's disease induced pluripotent stem cells with triplication of the α-synuclein locus. Nature Communications *2*: 440.

Dexter, D.T., Wells, F.R., Lees, A.J., Agid, F., Agid, Y., Jenner, P., et al. (1989). Increased nigral iron content and alterations in other metal ions occurring in brain in Parkinson's disease. Journal of Neurochemistry *52*: 1830–1836.

Dickson, D.W., Braak, H., Duda, J.E., Duyckaerts, C., Gasser, T., Halliday, G.M., et al. (2009). Neuropathological assessment of Parkinson's disease: refining the diagnostic criteria. Lancet Neurology *8*: 1150–7.

Dimos, J.T., Rodolfa, K.T., Niakan, K.K., Weisenthal, L.M., Mitsumoto, H., Chung, W., et al. (2008). Induced pluripotent stem cells generated from patients with ALS can be differentiated into motor neurons. Science (New York, N.Y.) *321*: 1218–21.

Duran, R., Mencacci, N.E., Angeli, A. V, Shoai, M., Deas, E., Houlden, H., et al. (2013). The glucocerobrosidase E326K variant predisposes to Parkinson's disease, but does not cause Gaucher's disease. Movement Disorders : Official Journal of the Movement Disorder Society *28*: 232–6.

Dvir, H., Harel, M., McCarthy, A. a, Toker, L., Silman, I., Futerman, A.H., et al. (2003). X-ray structure of human acid-beta-glucosidase, the defective enzyme in Gaucher disease. EMBO Reports *4*: 704–709.

Ebert, A.D., Yu, J., Rose, F.F., Mattis, V.B., Lorson, C.L., Thomson, J. a, et al. (2009). Induced pluripotent stem cells from a spinal muscular atrophy patient. Nature *457*: 277–80.

Eblan, M.J., Scholz, S., Stubblefield, B., Gutti, U., Goker-Alpan, O., Hruska, K.S., et al. (2006). Glucocerebrosidase mutations are not found in association with LRRK2 G2019S in subjects with parkinsonism. Neuroscience Letters *404*: 163–165.

Edvardson, S., Cinnamon, Y., Ta-Shma, A., Shaag, A., Yim, Y.-I., Zenvirt, S., et al. (2012). A deleterious mutation in DNAJC6 encoding the neuronal-specific clathrin-uncoating co-chaperone auxilin, is associated with juvenile parkinsonism. PloS One *7*: e36458.

Ejlerskov, P., Rasmussen, I., Nielsen, T.T., Bergström, A.-L., Tohyama, Y., Jensen, P.H., et al. (2013). Tubulin polymerization-promoting protein (TPPP/p25α) promotes unconventional secretion of α-synuclein through exophagy by impairing autophagosome-lysosome fusion. The Journal of Biological Chemistry *288*: 17313–35.

Emelyanov, A., Boukina, T., Yakimovskii, A., Usenko, T., Drosdova, A., Zakharchuk, A., et al. (2012). Glucocerebrosidase gene mutations are associated with Parkinson's disease in Russia. Movement Disorders : Official Journal of the Movement Disorder Society *27*: 158–9.

Emmanouilidou, E., Elenis, D., Papasilekas, T., Stranjalis, G., Gerozissis, K., Ioannou, P.C., et al. (2011). Assessment of α-synuclein secretion in mouse and human brain parenchyma. PloS One *6*: e22225.

Erickson, A.H., Ginns, E.I., and Barranger, J.A. (1985). Biosynthesis of the lysosomal enzyme glucocerebrosidase. The Journal of Biological Chemistry *260*: 14319–24.

Eyal, N., Wilder, S., and Horowitz, M. (1990). Prevalent and rare mutations among Gaucher patients. Gene *96*: 277–83.

Farrer, M.J., Williams, L.N., Algom, A.A., Kachergus, J., Hulihan, M.M., Ross, O.A., et al. (2009). Glucosidase-beta variations and Lewy body disorders. Parkinsonism & Related Disorders *15*: 414–6.

Fasano, C.A., Chambers, S.M., Lee, G., Tomishima, M.J., and Studer, L. (2010). Efficient Derivation of Functional Floor Plate Tissue from Human Embryonic Stem Cells. Cell Stem Cell *6*: 336–347.

Findley, L., Aujla, M., Bain, P.G., Baker, M., Beech, C., Bowman, C., et al. (2003). Direct economic impact of Parkinson's disease: a research survey in the United Kingdom. Movement Disorders : Official Journal of the Movement Disorder Society *18*: 1139–45.

Fonzo, A. Di, Chien, H.F., Socal, M., Giraudo, S., Tassorelli, C., Iliceto, G., et al. (2007). ATP13A2 missense mutations in juvenile parkinsonism and young onset Parkinson disease. Neurology *68*: 1557–62.

Fonzo, A. Di, Dekker, M.C.J., Montagna, P., Baruzzi, A., Yonova, E.H., Correia Guedes, L., et al. (2009). FBXO7 mutations cause autosomal recessive, early-onset parkinsonian-pyramidal syndrome. Neurology *72*: 240–245.

Foo, J.-N., Liany, H., Bei, J.-X., Yu, X.-Q., Liu, J., Au, W.-L., et al. (2013). A rare lysosomal enzyme gene SMPD1 variant (p.R591C) associates with Parkinson's disease. Neurobiology of Aging *34*: 2890.e13–5.

Fountaine, T.M., and Wade-Martins, R. (2007). RNA interference-mediated knockdown of alpha-synuclein protects human dopaminergic neuroblastoma cells from MPP(+) toxicity and reduces dopamine transport. Journal of Neuroscience Research *85*: 351–63.

Freeman, D., Cedillos, R., Choyke, S., Lukic, Z., McGuire, K., Marvin, S., et al. (2013). Alpha-synuclein induces lysosomal rupture and cathepsin dependent reactive oxygen species following endocytosis. PloS One *8*: e62143.

Fusaki, N., Ban, H., Nishiyama, A., Saeki, K., and Hasegawa, M. (2009). Efficient induction of transgene-free human pluripotent stem cells using a vector based on Sendai virus, an RNA virus that does not integrate into the host genome. Proceedings of the Japan Academy. Series B, Physical and Biological Sciences *85*: 348–362.

Futerman, A.H., and Riezman, H. (2005). The ins and outs of sphingolipid synthesis. Trends in Cell Biology *15*: 312–8.

Gandhi, S., Muqit, M.M.K., Stanyer, L., Healy, D.G., Abou-Sleiman, P.M., Hargreaves, I., et al. (2006). PINK1 protein in normal human brain and Parkinson's disease. Brain : a Journal of Neurology *129*: 1720–31.

Gan-Or, Z., Giladi, N., Rozovski, U., Shifrin, C., Rosner, S., Gurevich, T., et al. (2008). Genotype-phenotype correlations between GBA mutations and Parkinson disease risk and onset. Neurology *70*: 2277–2283.

Gan-Or, Z., Ozelius, L.J., Bar-Shira, A., Saunders-Pullman, R., Mirelman, A., Kornreich, R., et al. (2013). The p.L302P mutation in the lysosomal enzyme gene SMPD1 is a risk factor for Parkinson disease. Neurology *80*: 1606–10.

García-Arencibia, M., Hochfeld, W.E., Toh, P.P.C., and Rubinsztein, D.C. (2010). Autophagy, a guardian against neurodegeneration. Seminars in Cell & Developmental Biology *21*: 691–8.

Gegg, M.E., Burke, D., Heales, S.J.R., Cooper, J.M., Hardy, J., Wood, N.W., et al. (2012). Glucocerebrosidase deficiency in substantia nigra of parkinson disease brains. Annals of Neurology *72*: 455–63.

Geisler, S., Holmström, K.M., Treis, A., Skujat, D., Weber, S.S., Fiesel, F.C., et al. (2010). The PINK1/Parkin-mediated mitophagy is compromised by PD-associated mutations. Autophagy *6*: 871–8.

Ginns, E.I., Choudary, P. V, Tsuji, S., Martin, B., Stubblefield, B., Sawyer, J., et al. (1985). Gene mapping and leader polypeptide sequence of human glucocerebrosidase: implications

for Gaucher disease. Proceedings of the National Academy of Sciences of the United States of America *82*: 7101–5.

Gitler, A.D., Chesi, A., Geddie, M.L., Strathearn, K.E., Hamamichi, S., Hill, K.J., et al. (2009). Alpha-synuclein is part of a diverse and highly conserved interaction network that includes PARK9 and manganese toxicity. Nature Genetics *41*: 308–15.

Giussani, P., Tringali, C., Riboni, L., Viani, P., and Venerando, B. (2014). Sphingolipids: key regulators of apoptosis and pivotal players in cancer drug resistance. International Journal of Molecular Sciences *15*: 4356–92.

Goker-Alpan, O., Giasson, B., and Eblan, M. (2006). Glucocerebrosidase mutations are an important risk factor for Lewy body disorders. Neurology *67*: 908–910.

Goker-Alpan, O., Lopez, G., Vithayathil, J., Davis, J., Hallett, M., and Sidransky, E. (2008). The spectrum of parkinsonian manifestations associated with glucocerebrosidase mutations. Archives of Neurology *65*: 1353–7.

Goker-Alpan, O., Schiffmann, R., LaMarca, M.E., Nussbaum, R.L., McInerney-Leo, A., and Sidransky, E. (2004). Parkinsonism among Gaucher disease carriers. Journal of Medical Genetics *41*: 937–940.

Goker-Alpan, O., Stubblefield, B.K., Giasson, B.I., and Sidransky, E. (2010). Glucocerebrosidase is present in α-synuclein inclusions in Lewy body disorders. Acta Neuropathologica *120*: 641–649.

Goldwurm, S., Zini, M., Mariani, L., Tesei, S., Miceli, R., Sironi, F., et al. (2007). Evaluation of LRRK2 G2019S penetrance: relevance for genetic counseling in Parkinson disease. Neurology *68*: 1141–3.

Gómez-Suaga, P., Luzón-Toro, B., Churamani, D., Zhang, L., Bloor-Young, D., Patel, S., et al. (2012). Leucine-rich repeat kinase 2 regulates autophagy through a calcium-dependent pathway involving NAADP. Human Molecular Genetics *21*: 511–25.

González-Del Rincón, M. de L., Monroy Jaramillo, N., Suárez Martínez, A.I., Yescas Gómez, P., Boll Woehrlen, M.C., López López, M., et al. (2013). The L444P GBA mutation is associated with early-onset Parkinson's disease in Mexican Mestizos. Clinical Genetics *84*: 386–7.

Grünewald, A., Arns, B., Seibler, P., Rakovic, A., Münchau, A., Ramirez, A., et al. (2012). ATP13A2 mutations impair mitochondrial function in fibroblasts from patients with Kufor-Rakeb syndrome. Neurobiology of Aging *33*: 1843.e1–7.

Gurdon, J.B. (1962). The Developmental Capacity of Nuclei taken from Intestinal Epithelium Cells of Feeding Tadpoles. J Embryol Exp Morphol *10*: 622–640.

Gusdon, A.M., Zhu, J., Houten, B. Van, and Chu, C.T. (2012). ATP13A2 regulates mitochondrial bioenergetics through macroautophagy. Neurobiology of Disease *45*: 962–72.

Guzman, J.N., Sánchez-Padilla, J., Chan, C.S., and Surmeier, D.J. (2009). Robust pacemaking in substantia nigra dopaminergic neurons. The Journal of Neuroscience : the Official Journal of the Society for Neuroscience *29*: 11011–9.

Halliday, G.M., Holton, J.L., Revesz, T., and Dickson, D.W. (2011). Neuropathology underlying clinical variability in patients with synucleinopathies. Acta Neuropathologica *122*: 187–204.

Halperin, A., Elstein, D., and Zimran, A. (2006). Increased incidence of Parkinson disease among relatives of patients with Gaucher disease. Blood Cells, Molecules & Diseases *36*: 426–8.

Hamza, T.H., Zabetian, C.P., Tenesa, A., Laederach, A., Montimurro, J., Yearout, D., et al. (2010). Common genetic variation in the HLA region is associated with late-onset sporadic Parkinson's disease. Nature Genetics *42*: 781–5.

Hanada, K., Nishijima, M., Kiso, M., Hasegawa, A., Fujita, S., Ogawa, T., et al. (1992). Sphingolipids are essential for the growth of Chinese hamster ovary cells. Restoration of the growth of a mutant defective in sphingoid base biosynthesis by exogenous sphingolipids. The Journal of Biological Chemistry *267*: 23527–33.

Hannun, Y.A. (1996). Functions of ceramide in coordinating cellular responses to stress. Science (New York, N.Y.) *274*: 1855–9.

Hansen, C., Angot, E., Bergström, A.-L., Steiner, J.A., Pieri, L., Paul, G., et al. (2011). α-Synuclein propagates from mouse brain to grafted dopaminergic neurons and seeds aggregation in cultured human cells. The Journal of Clinical Investigation *121*: 715–25.

Hardy, J. (2010). Genetic analysis of pathways to Parkinson disease. Neuron *68*: 201–6.

Hargus, G., Cooper, O., Deleidi, M., Levy, A., Lee, K., Marlow, E., et al. (2010). Differentiated Parkinson patient-derived induced pluripotent stem cells grow in the adult rodent brain and reduce motor asymmetry in Parkinsonian rats. Proceedings of the National Academy of Sciences of the United States of America *107*: 15921–15926.

Hart, L.S., Cunningham, J.T., Datta, T., Dey, S., Tameire, F., Lehman, S.L., et al. (2012). ER stress-mediated autophagy promotes Myc-dependent transformation and tumor growth. The Journal of Clinical Investigation *122*: 4621–34.

Hartfield, E.M., Fernandes, H.J.R., Vowles, J., Cowley, S. a, and Wade-Martins, R. (2012). Cellular reprogramming: a new approach to modelling Parkinson's disease. Biochemical Society Transactions *40*: 1152–7.

Hartfield, E.M., Yamasaki-Mann, M., Ribeiro Fernandes, H.J., Vowles, J., James, W.S., Cowley, S.A., et al. (2014). Physiological Characterisation of Human iPS-Derived Dopaminergic Neurons. PLoS ONE *9*: e87388.

Healy, D.G., Falchi, M., O'Sullivan, S.S., Bonifati, V., Durr, A., Bressman, S., et al. (2008). Phenotype, genotype, and worldwide genetic penetrance of LRRK2-associated Parkinson's disease: a case-control study. Lancet Neurology *7*: 583–90.

Hedrich, K., Djarmati, A., Schäfer, N., Hering, R., Wellenbrock, C., Weiss, P.H., et al. (2004). DJ-1 (PARK7) mutations are less frequent than Parkin (PARK2) mutations in early-onset Parkinson disease. Neurology *62*: 389–94.

Hedrich, K., Marder, K., Harris, J., Kann, M., Lynch, T., Meija-Santana, H., et al. (2002). Evaluation of 50 probands with early-onset Parkinson's disease for Parkin mutations. Neurology *58*: 1239–46.

Hegarty, S. V, Sullivan, A.M., and O'Keeffe, G.W. (2013). Midbrain dopaminergic neurons: a review of the molecular circuitry that regulates their development. Developmental Biology *379*: 123–38.

Higashi, S., Moore, D.J., Yamamoto, R., Minegishi, M., Sato, K., Togo, T., et al. (2009). Abnormal localization of leucine-rich repeat kinase 2 to the endosomal-lysosomal compartment in lewy body disease. Journal of Neuropathology and Experimental Neurology *68*: 994–1005.

Hirsch, E.C., Jenner, P., and Przedborski, S. (2013). Pathogenesis of Parkinson's disease. Movement Disorders : Official Journal of the Movement Disorder Society *28*: 24–30.

Hoepken, H.-H., Gispert, S., Azizov, M., Klinkenberg, M., Ricciardi, F., Kurz, A., et al. (2008). Parkinson patient fibroblasts show increased alpha-synuclein expression. Experimental Neurology *212*: 307–13.

Hoozemans, J.J., Haastert, E.S. van, Eikelenboom, P., Vos, R. a de, Rozemuller, J.M., and Scheper, W. (2007). Activation of the unfolded protein response in Parkinson's disease. Biochem.Biophys.Res.Commun. *354*: 707–711.

Horowitz, M., Wilder, S., Horowitz, Z., Reiner, O., Gelbart, T., and Beutler, E. (1989). The human glucocerebrosidase gene and pseudogene: Structure and evolution. Genomics *4*: 87–96.

Høyer-Hansen, M., and Jäättelä, M. (2007). Connecting endoplasmic reticulum stress to autophagy by unfolded protein response and calcium. Cell Death and Differentiation *14*: 1576–82.

Hruska, K.S., LaMarca, M.E., Scott, C.R., and Sidransky, E. (2008). Gaucher disease: mutation and polymorphism spectrum in the glucocerebrosidase gene (GBA). Human Mutation *29*: 567–83.

Hu, F.-Y., Xi, J., Guo, J., Yu, L.-H., Liu, L., He, X.-H., et al. (2010). Association of the glucocerebrosidase N370S allele with Parkinson's disease in two separate Chinese Han populations of mainland China. European Journal of Neurology : the Official Journal of the European Federation of Neurological Societies *17*: 1476–1478.

Huang, C.-L., Wu-Chou, Y.-H., Lai, S.-C., Chang, H.-C., Yeh, T.-H., Weng, Y.-H., et al. (2011). Contribution of glucocerebrosidase mutation in a large cohort of sporadic Parkinson's disease in Taiwan. European Journal of Neurology : the Official Journal of the European Federation of Neurological Societies *18*: 1227–1232.

Iacovitti, L., Donaldson, A.E., Marshall, C.E., Suon, S., and Yang, M. (2007). A protocol for the differentiation of human embryonic stem cells into dopaminergic neurons using only chemically defined human additives: Studies in vitro and in vivo. Brain Research *1127*: 19–25.

Imaizumi, Y., Okada, Y., Akamatsu, W., Koike, M., Kuzumaki, N., Hayakawa, H., et al. (2012). Mitochondrial dysfunction associated with increased oxidative stress and α-synuclein accumulation in PARK2 iPSC-derived neurons and postmortem brain tissue. Molecular Brain *5*: 35.

Iranzo, A., Tolosa, E., Gelpi, E., Molinuevo, J.L., Valldeoriola, F., Serradell, M., et al. (2013). Neurodegenerative disease status and post-mortem pathology in idiopathic rapid-eye-movement sleep behaviour disorder: an observational cohort study. Lancet Neurology *12*: 443–53.

Iwata, A., Riley, B.E., Johnston, J. a, and Kopito, R.R. (2005). HDAC6 and microtubules are required for autophagic degradation of aggregated huntingtin. The Journal of Biological Chemistry *280*: 40282–40292.

Jamrozik, Z., Lugowska, A., Slawek, J., and Kwiecinski, H. (2010). Glucocerebrosidase mutations p.L444P and p.N370S are not associated with multisystem atrophy, progressive supranuclear palsy and corticobasal degeneration in Polish patients. Journal of Neurology *257*: 459–60.

Jiang, H., Ren, Y., Yuen, E.Y., Zhong, P., Ghaedi, M., Hu, Z., et al. (2012). Parkin controls dopamine utilization in human midbrain dopaminergic neurons derived from induced pluripotent stem cells. Nature Communications *3*: 668.

Kalinderi, K., Bostantjopoulou, S., Paisan-Ruiz, C., Katsarou, Z., Hardy, J., and Fidani, L. (2009). Complete screening for glucocerebrosidase mutations in Parkinson disease patients from Greece. Neuroscience Letters *452*: 87–89.

Kamp, F., Exner, N., Lutz, A.K., Wender, N., Hegermann, J., Brunner, B., et al. (2010). Inhibition of mitochondrial fusion by α-synuclein is rescued by PINK1, Parkin and DJ-1. The EMBO Journal *29*: 3571–89.

Katzenschlager, R., Head, J., Schrag, A., Ben-Shlomo, Y., Evans, A., and Lees, A.J. (2008). Fourteen-year final report of the randomized PDRG-UK trial comparing three initial treatments in PD. Neurology *71*: 474–80.

Kiely, A.P., Asi, Y.T., Kara, E., Limousin, P., Ling, H., Lewis, P., et al. (2013). α-Synucleinopathy associated with G51D SNCA mutation: a link between Parkinson's disease and multiple system atrophy? Acta Neuropathologica *125*: 753–69.

Kim, Y., Park, J., Kim, S., Song, S., Kwon, S.-K., Lee, S.-H., et al. (2008). PINK1 controls mitochondrial localization of Parkin through direct phosphorylation. Biochemical and Biophysical Research Communications *377*: 975–80.

Kirkeby, A., Grealish, S., Wolf, D.A., Nelander, J., Wood, J., Lundblad, M., et al. (2012). Generation of regionally specified neural progenitors and functional neurons from human embryonic stem cells under defined conditions. Cell Reports *1*: 703–14.

Kitada, T., Asakawa, S., Hattori, N., Matsumine, H., Yamamura, Y., Minoshima, S., et al. (1998). Mutations in the parkin gene cause autosomal recessive juvenile parkinsonism. Nature *392*: 605–8.

Kitatani, K., Sheldon, K., Rajagopalan, V., Anelli, V., Jenkins, R.W., Sun, Y., et al. (2009). Involvement of acid beta-glucosidase 1 in the salvage pathway of ceramide formation. The Journal of Biological Chemistry *284*: 12972–8.

Kittappa, R., Chang, W.W., Awatramani, R.B., and McKay, R.D.G. (2007). The foxa2 gene controls the birth and spontaneous degeneration of dopamine neurons in old age. PLoS Biology *5*: e325.

Klein, C., Djarmati, A., Hedrich, K., Schäfer, N., Scaglione, C., Marchese, R., et al. (2005). PINK1, Parkin, and DJ-1 mutations in Italian patients with early-onset parkinsonism. European Journal of Human Genetics : EJHG *13*: 1086–93.

Klein, C., Lohmann-Hedrich, K., Rogaeva, E., Schlossmacher, M.G., and Lang, A.E. (2007). Deciphering the role of heterozygous mutations in genes associated with parkinsonism. Lancet Neurology *6*: 652–62.

Klein, C., and Westenberger, A. (2012). Genetics of Parkinson's disease. Cold Spring Harbor Perspectives in Medicine *2*: a008888.

Klionsky, D.J., Abdalla, F.C., Abeliovich, H., Abraham, R.T., Acevedo-Arozena, A., Adeli, K., et al. (2012). Guidelines for the use and interpretation of assays for monitoring autophagy. Autophagy *8*: 445–544.

Klucken, J., Poehler, A.-M., Ebrahimi-Fakhari, D., Schneider, J., Nuber, S., Rockenstein, E., et al. (2012). Alpha-synuclein aggregation involves a bafilomycin A 1-sensitive autophagy pathway. Autophagy *8*: 754–66.

Kluenemann, H.H., Nutt, J.G., Davis, M.Y., and Bird, T.D. (2013). Parkinsonism syndrome in heterozygotes for Niemann-Pick C1. Journal of the Neurological Sciences *335*: 219–20.

Kong, B., Yang, T., Gu, J.W., Kuang, Y.Q., Cheng, L., Yang, W.T., et al. (2013). The association between lysosomal protein glucocerebrosidase and Parkinson's disease. European Review for Medical and Pharmacological Sciences *17*: 143–51.

Kowal, S.L., Dall, T.M., Chakrabarti, R., Storm, M. V, and Jain, A. (2013). The current and projected economic burden of Parkinson's disease in the United States. Movement Disorders : Official Journal of the Movement Disorder Society *28*: 311–8.

Krebs, C.E., Karkheiran, S., Powell, J.C., Cao, M., Makarov, V., Darvish, H., et al. (2013). The Sac1 domain of SYNJ1 identified mutated in a family with early-onset progressive Parkinsonism with generalized seizures. Human Mutation *34*: 1200–7.

Kriks, S., Shim, J.W., Piao, J., Ganat, Y.M., Wakeman, D.R., Xie, Z., et al. (2011). Dopamine neurons derived from human ES cells efficiently engraft in animal models of Parkinson's disease. Nature *480*: 547–551.

Krüger, R., Kuhn, W., Müller, T., Woitalla, D., Graeber, M., Kösel, S., et al. (1998). Ala30Pro mutation in the gene encoding alpha-synuclein in Parkinson's disease. Nature Genetics *18*: 106–8.

Kumar, K.R., Ramirez, a, Göbel, a, Kresojević, N., Svetel, M., Lohmann, K., et al. (2013). Glucocerebrosidase mutations in a Serbian Parkinson's disease population. European Journal of Neurology *20*: 402–5.

Kurzawa-Akanbi, M., Hanson, P.S., Blain, P.G., Lett, D.J., McKeith, I.G., Chinnery, P.F., et al. (2012). Glucocerebrosidase mutations alter the endoplasmic reticulum and lysosomes in Lewy body disease. Journal of Neurochemistry *123*: 298–309.

Lai, M.I., Wendy-Yeo, W.Y., Ramasamy, R., Nordin, N., Rosli, R., Veerakumarasivam, A., et al. (2011). Advancements in reprogramming strategies for the generation of induced pluripotent stem cells. Journal of Assisted Reproduction and Genetics *28*: 291–301.

Langston, J.W., Ballard, P., Tetrud, J.W., and Irwin, I. (1983). Chronic Parkinsonism in humans due to a product of meperidine-analog synthesis. Science (New York, N.Y.) *219*: 979–80.

Lautier, C., Goldwurm, S., Dürr, A., Giovannone, B., Tsiaras, W.G., Pezzoli, G., et al. (2008). Mutations in the GIGYF2 (TNRC15) gene at the PARK11 locus in familial Parkinson disease. American Journal of Human Genetics *82*: 822–33.

Lee, G., Papapetrou, E.P., Kim, H., Chambers, S.M., Tomishima, M.J., Fasano, C. a, et al. (2009). Modelling pathogenesis and treatment of familial dysautonomia using patient-specific iPSCs. Nature *461*: 402–406.

Lee, H.-J., Cho, E.-D., Lee, K.W., Kim, J.-H., Cho, S.-G., and Lee, S.-J. (2013). Autophagic failure promotes the exocytosis and intercellular transfer of α-synuclein. Experimental & Molecular Medicine *45*: e22.

Lee, Y.-J., Kim, S.-J., and Heo, T.-H. (2011). Protective effect of catechin in type I Gaucher disease cells by reducing endoplasmic reticulum stress. Biochemical and Biophysical Research Communications *413*: 254–258.

Lees, A.J., Hardy, J., and Revesz, T. (2009). Parkinson's disease. Lancet *373*: 2055–66.

Leroy, E., Boyer, R., Auburger, G., Leube, B., Ulm, G., Mezey, E., et al. (1998). The ubiquitin pathway in Parkinson's disease. Nature *395*: 451–2.

Lesage, S., Anheim, M., Condroyer, C., Pollak, P., Durif, F., Dupuits, C., et al. (2011a). Large-scale screening of the Gaucher's disease-related glucocerebrosidase gene in Europeans with Parkinson's disease. Human Molecular Genetics *20*: 202–210.

Lesage, S., Anheim, M., Letournel, F., Bousset, L., Honoré, A., Rozas, N., et al. (2013). G51D α-synuclein mutation causes a novel parkinsonian-pyramidal syndrome. Annals of Neurology *73*: 459–71.

Lesage, S., and Brice, A. (2009). Parkinson's disease: from monogenic forms to genetic susceptibility factors. Human Molecular Genetics *18*: R48–R59.

Lesage, S., Condroyer, C., Hecham, N., Anheim, M., Belarbi, S., Lohman, E., et al. (2011b). Mutations in the glucocerebrosidase gene confer a risk for Parkinson disease in North Africa. Neurology *76*: 301–3.

Li, Y., Sekine, T., Funayama, M., Li, L., Yoshino, H., Nishioka, K., et al. (2014). Clinicogenetic study of GBA mutations in patients with familial Parkinson's disease. Neurobiology of Aging *35*: 935.e3–8.

Lill, C., Roehr, J., and McQueen, M. (2012). Comprehensive research synopsis and systematic meta-analyses in Parkinson's disease genetics: the PDGene database. PLoS Genetics *8*: e1002548.

Lin, C.H., Tan, E.K., Chen, M.L., Tan, L.C., Lim, H.Q., Chen, G.S., et al. (2008). Novel ATP13A2 variant associated with Parkinson disease in Taiwan and Singapore. Neurology *71*: 1727–32.

Liu, G.-H., Qu, J., Suzuki, K., Nivet, E., Li, M., Montserrat, N., et al. (2012a). Progressive degeneration of human neural stem cells caused by pathogenic LRRK2. Nature *491*: 603–7.

Liu, R., Guo, X., Park, Y., Huang, X., Sinha, R., Freedman, N.D., et al. (2012b). Caffeine intake, smoking, and risk of Parkinson disease in men and women. American Journal of Epidemiology *175*: 1200–7.

Lopez, G., and Sidransky, E. (2012). The link between the GBA gene and parkinsonism. The Lancet Neurology *11*: 986–998.

Lübke, T., Lobel, P., and Sleat, D.E. (2009). Proteomics of the lysosome. Biochimica Et Biophysica Acta *1793*: 625–35.

Lücking, C.B., Dürr, A., Bonifati, V., Vaughan, J., Michele, G. De, Gasser, T., et al. (2000). Association between early-onset Parkinson's disease and mutations in the parkin gene. The New England Journal of Medicine *342*: 1560–7.

Lwin, A., Orvisky, E., Goker-Alpan, O., LaMarca, M.E., and Sidransky, E. (2004). Glucocerebrosidase mutations in subjects with parkinsonism. Molecular Genetics and Metabolism *81*: 70–73.

Ma, H.-I., Kim, Y.J., Lee, M.S., Kang, S.Y., Koh, S.-B., Lyoo, C.H., et al. (2012). Association of mutations in the glucocerebrosidase gene with Parkinson disease in a Korean population. Neuroscience Letters *514*: 12–15.

Machaczka, M., Rucinska, M., Skotnicki, A.B., and Jurczak, W. (1999). Parkinson's syndrome preceding clinical manifestation of Gaucher's disease. American Journal of Hematology *61*: 216–7.

MacLeod, D., Dowman, J., Hammond, R., Leete, T., Inoue, K., and Abeliovich, A. (2006). The familial Parkinsonism gene LRRK2 regulates neurite process morphology. Neuron *52*: 587–93.

MacLeod, D.A., Rhinn, H., Kuwahara, T., Zolin, A., Paolo, G. Di, McCabe, B.D., et al. (2013). RAB7L1 interacts with LRRK2 to modify intraneuronal protein sorting and Parkinson's disease risk. Neuron *77*: 425–39.

Mak, S.K., Huang, Y.A., Iranmanesh, S., Vangipuram, M., Sundararajan, R., Nguyen, L., et al. (2012). Small molecules greatly improve conversion of human-induced pluripotent stem cells to the neuronal lineage. Stem Cells International *2012*: 140427.

Mak, S.K., McCormack, A.L., Manning-Bog, A.B., Cuervo, A.M., and Monte, D. a Di (2010). Lysosomal degradation of alpha-synuclein in vivo. The Journal of Biological Chemistry *285*: 13621–9.

Maley, F., Trimble, R.B., Tarentino, A.L., and Plummer, T.H. (1989). Characterization of glycoproteins and their associated oligosaccharides through the use of endoglycosidases. Analytical Biochemistry *180*: 195–204.

Manning-Boğ, A., Schüle, B., and Langston, J. (2009). Alpha-synuclein-glucocerebrosidase interactions in pharmacological Gaucher models: a biological link between Gaucher disease and parkinsonism. Neurotoxicology *30*: 1127–1132.

Manning-Bog, A.B., McCormack, A.L., Li, J., Uversky, V.N., Fink, A.L., and Monte, D.A. Di (2002). The herbicide paraquat causes up-regulation and aggregation of alpha-synuclein in mice: paraquat and alpha-synuclein. The Journal of Biological Chemistry *277*: 1641–4.

Manzoni, C., Mamais, A., Dihanich, S., Abeti, R., Soutar, M.P.M., Plun-Favreau, H., et al. (2013). Inhibition of LRRK2 kinase activity stimulates macroautophagy. Biochimica Et Biophysica Acta *1833*: 2900–10.

Mao, X.-Y., Burgunder, J.-M., Zhang, Z.-J., An, X.-K., Zhang, J.-H., Yang, Y., et al. (2010). Association between GBA L444P mutation and sporadic Parkinson's disease from Mainland China. Neuroscience Letters *469*: 256–259.

Maor, G., Rencus-Lazar, S., Filocamo, M., Steller, H., Segal, D., and Horowitz, M. (2013). Unfolded protein response in Gaucher disease: from human to Drosophila. Orphanet Journal of Rare Diseases *8*: 140.

Marco, E. V De, Annesi, G., Tarantino, P., Rocca, F.E., Provenzano, G., Civitelli, D., et al. (2008). Glucocerebrosidase gene mutations are associated with Parkinson's disease in southern Italy. Mov Disord *23*: 460–3.

Marongiu, R., Ferraris, A., Ialongo, T., Michiorri, S., Soleti, F., Ferrari, F., et al. (2008). PINK1 heterozygous rare variants: prevalence, significance and phenotypic spectrum. Human Mutation *29*: 565.

Martinez-Arias, R. (2001). Sequence Variability of a Human Pseudogene. Genome Research *11*: 1071–1085.

Martinez-Vicente, M., Talloczy, Z., Kaushik, S., Massey, A.C., Mazzulli, J., Mosharov, E. V, et al. (2008). Dopamine-modified alpha-synuclein blocks chaperone-mediated autophagy. The Journal of Clinical Investigation *118*: 777–788.

Mata, I.F., Samii, A., Schneer, S.H., Roberts, J.W., Griffith, A., Leis, B.C., et al. (2008). Glucocerebrosidase gene mutations: a risk factor for Lewy body disorders. Archives of Neurology *65*: 379–382.

Mazzulli, J.R., Xu, Y.-H., Sun, Y., Knight, A.L., McLean, P.J., Caldwell, G.A., et al. (2011). Gaucher disease glucocerebrosidase and α-synuclein form a bidirectional pathogenic loop in synucleinopathies. Cell *146*: 37–52.

Messner, M.C., and Cabot, M.C. (2010). Glucosylceramide in humans. Advances in Experimental Medicine and Biology *688*: 156–64.

Mitsui, J., Mizuta, I., Toyoda, A., Ashida, R., Takahashi, Y., Goto, J., et al. (2009). Mutations for Gaucher disease confer high susceptibility to Parkinson disease. Archives of Neurology *66*: 571–576.

Mizushima, N., Yoshimori, T., and Levine, B. (2010). Methods in mammalian autophagy research. Cell *140*: 313–326.

Monte, D.A. Di (2003). The environment and Parkinson's disease: is the nigrostriatal system preferentially targeted by neurotoxins? Lancet Neurology *2*: 531–8.

Morris, J.F., Omer, S., Davies, E., Wang, E., John, C., Afzal, T., et al. (2006). Lack of annexin 1 results in an increase in corticotroph number in male but not female mice. Journal of Neuroendocrinology *18*: 835–46.

Müller, F.-J., Schuldt, B.M., Williams, R., Mason, D., Altun, G., Papapetrou, E.P., et al. (2011). A bioinformatic assay for pluripotency in human cells. Nature Methods *8*: 315–7.

Nakamura, K., Yoshimura, A., Kaneko, T., Sato, K., and Hara, Y. (2013). ROCK inhibitor Y-27632 maintains the proliferation of confluent human mesenchymal stem cells. Journal of Periodontal Research.

Nalls, M.A., Duran, R., Lopez, G., Kurzawa-Akanbi, M., McKeith, I.G., Chinnery, P.F., et al. (2013). A multicenter study of glucocerebrosidase mutations in dementia with Lewy bodies. JAMA Neurology *70*: 727–35.

Narendra, D., Tanaka, A., Suen, D.-F., and Youle, R.J. (2008). Parkin is recruited selectively to impaired mitochondria and promotes their autophagy. The Journal of Cell Biology *183*: 795–803.

Narendra, D.P., Jin, S.M., Tanaka, A., Suen, D.-F., Gautier, C.A., Shen, J., et al. (2010). PINK1 is selectively stabilized on impaired mitochondria to activate Parkin. PLoS Biology *8*: e1000298.

Neudorfer, O., Giladi, N., Elstein, D., Abrahamov, A., Turezkite, T., Aghai, E., et al. (1996). Occurrence of Parkinson's syndrome in type I Gaucher disease. QJM : Monthly Journal of the Association of Physicians *89*: 691–4.

Neumann, J., Bras, J., Deas, E., O'Sullivan, S.S., Parkkinen, L., Lachmann, R.H., et al. (2009). Glucocerebrosidase mutations in clinical and pathologically proven Parkinson's disease. Brain : a Journal of Neurology *132*: 1783–1794.

Nguyen, H.N., Byers, B., Cord, B., Shcheglovitov, A., Byrne, J., Gujar, P., et al. (2011). LRRK2 mutant iPSC-derived DA neurons demonstrate increased susceptibility to oxidative stress. Cell Stem Cell *8*: 267–280.

Nichols, W.C., Pankratz, N., Marek, D.K., Pauciulo, M.W., Elsaesser, V.E., Halter, C. a, et al. (2009). Mutations in GBA are associated with familial Parkinson disease susceptibility and age at onset. Neurology *72*: 310–316.

Nishimura, K., Sano, M., Ohtaka, M., Furuta, B., Umemura, Y., Nakajima, Y., et al. (2011). Development of defective and persistent Sendai virus vector: a unique gene delivery/expression system ideal for cell reprogramming. The Journal of Biological Chemistry *286*: 4760–4771.

Noreau, A., Rivière, J.-B., Diab, S., Dion, P.A., Panisset, M., Soland, V., et al. (2011). Glucocerebrosidase mutations in a French-Canadian Parkinson's disease cohort. The Canadian Journal of Neurological Sciences. Le Journal Canadien Des Sciences Neurologiques *38*: 772–3.

Nuytemans, K., Theuns, J., Cruts, M., and Broeckhoven, C. Van (2010). Genetic etiology of Parkinson disease associated with mutations in the SNCA, PARK2, PINK1, PARK7, and LRRK2 genes: a mutation update. Human Mutation *31*: 763–80.

Ono, Y., Nakatani, T., Sakamoto, Y., Mizuhara, E., Minaki, Y., Kumai, M., et al. (2007). Differences in neurogenic potential in floor plate cells along an anteroposterior location: midbrain dopaminergic neurons originate from mesencephalic floor plate cells. Development (Cambridge, England) *134*: 3213–25.

Ordonez, M.P., Roberts, E. a, Kidwell, C.U., Yuan, S.H., Plaisted, W.C., and Goldstein, L.S.B. (2012). Disruption and therapeutic rescue of autophagy in a human neuronal model of Niemann Pick type C1. Human Molecular Genetics *21*: 2651–62.

Orenstein, S.J., Kuo, S.-H., Tasset, I., Arias, E., Koga, H., Fernandez-Carasa, I., et al. (2013). Interplay of LRRK2 with chaperone-mediated autophagy. Nature Neuroscience *16*: 394–406.

Orvisky, E., Park, J.K., LaMarca, M.E., Ginns, E.I., Martin, B.M., Tayebi, N., et al. (2002). Glucosylsphingosine accumulation in tissues from patients with Gaucher disease: correlation with phenotype and genotype. Molecular Genetics and Metabolism *76*: 262–70.

Osellame, L.D., Rahim, A. a, Hargreaves, I.P., Gegg, M.E., Richard-Londt, A., Brandner, S., et al. (2013). Mitochondria and quality control defects in a mouse model of Gaucher disease--links to Parkinson's disease. Cell Metabolism *17*: 941–53.

Pacheco, C.D., Kunkel, R., and Lieberman, A.P. (2007). Autophagy in Niemann-Pick C disease is dependent upon Beclin-1 and responsive to lipid trafficking defects. Human Molecular Genetics *16*: 1495–1503.

Paisan-Ruiz, C., Bhatia, K.P., Li, A., Hernandez, D., Davis, M., Wood, N.W., et al. (2009). Characterization of PLA2G6 as a locus for dystonia-parkinsonism. Annals of Neurology *65*: 19–23.

Palacios, N., Gao, X., McCullough, M.L., Schwarzschild, M. a, Shah, R., Gapstur, S., et al. (2012). Caffeine and risk of Parkinson's disease in a large cohort of men and women. Movement Disorders : Official Journal of the Movement Disorder Society *27*: 1276–82.

Panicker, L.M., Miller, D., Park, T.S., Patel, B., Azevedo, J.L., Awad, O., et al. (2012). Induced pluripotent stem cell model recapitulates pathologic hallmarks of Gaucher disease. Proceedings of the National Academy of Sciences of the United States of America *109*: 18054–9.

Pankratz, N., Beecham, G.W., DeStefano, A.L., Dawson, T.M., Doheny, K.F., Factor, S.A., et al. (2012). Meta-analysis of Parkinson's disease: identification of a novel locus, RIT2. Annals of Neurology *71*: 370–84.

Pankratz, N., Wilk, J.B., Latourelle, J.C., DeStefano, A.L., Halter, C., Pugh, E.W., et al. (2009). Genomewide association study for susceptibility genes contributing to familial Parkinson disease. Human Genetics *124*: 593–605.

Park, I., Arora, N., Huo, H., and Maherali, N. (2008). Disease-specific induced pluripotent stem cells. Cell *134*: 877–86.

Park, J., Lee, S.B., Lee, S., Kim, Y., Song, S., Kim, S., et al. (2006). Mitochondrial dysfunction in Drosophila PINK1 mutants is complemented by parkin. Nature *441*: 1157–61.

Pasanen, P., Myllykangas, L., Siitonen, M., Raunio, A., Kaakkola, S., Lyytinen, J., et al. (2014). A novel α-synuclein mutation A53E associated with atypical multiple system atrophy and Parkinson's disease-type pathology. Neurobiology of Aging *35*: 2180.e1–5.

Periquet, M., Latouche, M., Lohmann, E., Rawal, N., Michele, G. De, Ricard, S., et al. (2003). Parkin mutations are frequent in patients with isolated early-onset parkinsonism. Brain : a Journal of Neurology *126*: 1271–8.

Peruzzi, P.P., Lawler, S.E., Senior, S.L., Dmitrieva, N., Edser, P.A.H., Gianni, D., et al. (2009). Physiological transgene regulation and functional complementation of a neurological disease gene deficiency in neurons. Molecular Therapy : the Journal of the American Society of Gene Therapy *17*: 1517–26.

Pissadaki, E.K., and Bolam, J.P. (2013). The energy cost of action potential propagation in dopamine neurons: clues to susceptibility in Parkinson's disease. Frontiers in Computational Neuroscience *7*: 13.

Plowey, E.D., Cherra, S.J., Liu, Y.-J., and Chu, C.T. (2008). Role of autophagy in G2019S-LRRK2-associated neurite shortening in differentiated SH-SY5Y cells. Journal of Neurochemistry *105*: 1048–56.

Polymeropoulos, M.H. (1997). Mutation in the -Synuclein Gene Identified in Families with Parkinson's Disease. Science *276*: 2045–2047.

Qi, Z., Yang, W., Liu, Y., Cui, T., Gao, H., Duan, C., et al. (2011). Loss of PINK1 function decreases PP2A activity and promotes autophagy in dopaminergic cells and a murine model. Neurochemistry International *59*: 572–81.

Qiao, L., Hamamichi, S., Caldwell, K.A., Caldwell, G.A., Yacoubian, T.A., Wilson, S., et al. (2008). Lysosomal enzyme cathepsin D protects against alpha-synuclein aggregation and toxicity. Molecular Brain *1*: 17.

Quadri, M., Fang, M., Picillo, M., Olgiati, S., Breedveld, G.J., Graafland, J., et al. (2013). Mutation in the SYNJ1 gene associated with autosomal recessive, early-onset Parkinsonism. Human Mutation *34*: 1208–15.

Rakovic, A., Shurkewitsch, K., Seibler, P., Grünewald, A., Zanon, A., Hagenah, J., et al. (2013). Phosphatase and tensin homolog (PTEN)-induced putative kinase 1 (PINK1)-dependent ubiquitination of endogenous Parkin attenuates mitophagy: study in human primary fibroblasts and induced pluripotent stem cell-derived neurons. The Journal of Biological Chemistry *288*: 2223–37.

Ramirez, A., Heimbach, A., Gründemann, J., Stiller, B., Hampshire, D., Cid, L.P., et al. (2006). Hereditary parkinsonism with dementia is caused by mutations in ATP13A2, encoding a lysosomal type 5 P-type ATPase. Nature Genetics *38*: 1184–91.

Reczek, D., Schwake, M., Schröder, J., Hughes, H., Blanz, J., Jin, X., et al. (2007). LIMP-2 is a receptor for lysosomal mannose-6-phosphate-independent targeting of beta-glucocerebrosidase. Cell *131*: 770–783.

Reinhardt, P., Schmid, B., Burbulla, L.F., Schöndorf, D.C., Wagner, L., Glatza, M., et al. (2013). Genetic correction of a LRRK2 mutation in human iPSCs links parkinsonian neurodegeneration to ERK-dependent changes in gene expression. Cell Stem Cell *12*: 354–67.

Reyes, S., Fu, Y., Double, K., Thompson, L., Kirik, D., Paxinos, G., et al. (2012). GIRK2 expression in dopamine neurons of the substantia nigra and ventral tegmental area. The Journal of Comparative Neurology *520*: 2591–607.

Rigat, B., and Mahuran, D. (2009). Diltiazem, a L-type Ca 2+ channel blocker, also acts as a pharmacological chaperone in Gaucher patient cells. Molecular Genetics and Metabolism *96*: 225–232.

Rodriguez-Oroz, M.C., Jahanshahi, M., Krack, P., Litvan, I., Macias, R., Bezard, E., et al. (2009). Initial clinical manifestations of Parkinson's disease: features and pathophysiological mechanisms. Lancet Neurology *8*: 1128–39.

Rodríguez-Pascau, L., Gort, L., Schuchman, E.H., Vilageliu, L., Grinberg, D., and Chabás, A. (2009). Identification and characterization of SMPD1 mutations causing Niemann-Pick types A and B in Spanish patients. Human Mutation *30*: 1117–22.

Ron, I., and Horowitz, M. (2005). ER retention and degradation as the molecular basis underlying Gaucher disease heterogeneity. Human Molecular Genetics *14*: 2387–2398.

Ross, G.W., Abbott, R.D., Petrovitch, H., Morens, D.M., Grandinetti, A., Tung, K.H., et al. Association of coffee and caffeine intake with the risk of Parkinson disease. JAMA : the Journal of the American Medical Association *283*: 2674–9.

Rungsiwiwut, R., Manolertthewan, C., Numchaisrika, P., Ahnonkitpanit, V., Virutamasen, P., Techakumphu, M., et al. (2013). The ROCK inhibitor Y-26732 enhances the survival and proliferation of human embryonic stem cell-derived neural progenitor cells upon dissociation. Cells, Tissues, Organs *198*: 127–38.

Sadhukhan, T., Biswas, A., Das, S.K., Ray, K., and Ray, J. (2012). DJ-1 variants in Indian Parkinson's disease patients. Disease Markers *33*: 127–35.

Saito, Y., Suzuki, K., Hulette, C.M., and Murayama, S. (2004). Aberrant phosphorylation of alpha-synuclein in human Niemann-Pick type C1 disease. Journal of Neuropathology and Experimental Neurology *63*: 323–8.

Sánchez-Danés, A., Richaud-Patin, Y., Carballo-Carbajal, I., Jiménez-Delgado, S., Caig, C., Mora, S., et al. (2012). Disease-specific phenotypes in dopamine neurons from human iPS-based models of genetic and sporadic Parkinson's disease. EMBO Molecular Medicine *4*: 380–95.

Sardi, S., and Clarke, J. (2011). CNS expression of glucocerebrosidase corrects α-synuclein pathology and memory in a mouse model of Gaucher-related synucleinopathy. Proceedings of the … *108*: 12101–12106.

Sardi, S.P., Clarke, J., Kinnecom, C., Tamsett, T.J., Li, L., Stanek, L.M., et al. (2011). CNS expression of glucocerebrosidase corrects alpha-synuclein pathology and memory in a mouse model of Gaucher-related synucleinopathy. Proceedings of the National Academy of Sciences of the United States of America *108*: 12101–6.

Satake, W., Nakabayashi, Y., Mizuta, I., Hirota, Y., Ito, C., Kubo, M., et al. (2009). Genome-wide association study identifies common variants at four loci as genetic risk factors for Parkinson's disease. Nature Genetics *41*: 1303–7.

Sato, C., Morgan, A., Lang, A.E., Salehi-Rad, S., Kawarai, T., Meng, Y., et al. (2005). Analysis of the glucocerebrosidase gene in Parkinson's disease. Movement Disorders : Official Journal of the Movement Disorder Society *20*: 367–370.

Saunders-Pullman, R., Hagenah, J., Dhawan, V., Stanley, K., Pastores, G., Sathe, S., et al. (2010). Gaucher disease ascertained through a Parkinson's center: imaging and clinical characterization. Movement Disorders : Official Journal of the Movement Disorder Society *25*: 1364–72.

Schapansky, J., Nardozzi, J.D., Felizia, F., and Lavoie, M.J. (2014). Membrane recruitment of endogenous LRRK2 precedes its potent regulation of autophagy. Human Molecular Genetics.

Schenck, C.H., Boeve, B.F., and Mahowald, M.W. (2013). Delayed emergence of a parkinsonian disorder or dementia in 81% of older men initially diagnosed with idiopathic rapid eye movement sleep behavior disorder: a 16-year update on a previously reported series. Sleep Medicine *14*: 744–8.

Schmitz, M., Alfalah, M., Aerts, J.M.F.G., Naim, H.Y., and Zimmer, K.-P. (2005). Impaired trafficking of mutants of lysosomal glucocerebrosidase in Gaucher's disease. The International Journal of Biochemistry & Cell Biology *37*: 2310–2320.

Schulze, H., and Sandhoff, K. (2011). Lysosomal lipid storage diseases. Cold Spring Harbor Perspectives in Biology *3*:

Segarane, B., Li, A., Paudel, R., Scholz, S., Neumann, J., Lees, A., et al. (2009). Glucocerebrosidase mutations in 108 neuropathologically confirmed cases of multiple system atrophy. Neurology *72*: 1185–6.

Seibler, P., Graziotto, J., Jeong, H., Simunovic, F., Klein, C., and Krainc, D. (2011). Mitochondrial Parkin recruitment is impaired in neurons derived from mutant PINK1 induced pluripotent stem cells. The Journal of Neuroscience : the Official Journal of the Society for Neuroscience *31*: 5970–6.

Setó-Salvia, N., Pagonabarraga, J., Houlden, H., Pascual-Sedano, B., Dols-Icardo, O., Tucci, A., et al. (2012). Glucocerebrosidase mutations confer a greater risk of dementia during Parkinson's disease course. Movement Disorders : Official Journal of the Movement Disorder Society *27*: 393–9.

Sevlever, D., Jiang, P., and Yen, S.-H.C. (2008). Cathepsin D is the main lysosomal enzyme involved in the degradation of alpha-synuclein and generation of its carboxy-terminally truncated species. Biochemistry *47*: 9678–87.

Shimura, H., Hattori, N., Kubo, S. i, Mizuno, Y., Asakawa, S., Minoshima, S., et al. (2000). Familial Parkinson disease gene product, parkin, is a ubiquitin-protein ligase. Nature Genetics *25*: 302–5.

Shulman, J.M., Jager, P.L. De, and Feany, M.B. (2011). Parkinson's disease: genetics and pathogenesis. Annual Review of Pathology *6*: 193–222.

Sidransky, E., and Lopez, G. (2012). The link between the GBA gene and parkinsonism. The Lancet Neurology *11*: 986–998.

Sidransky, E., Nalls, M.A., Aasly, J.O., Aharon-Peretz, J., Annesi, G., Barbosa, E.R., et al. (2009). Multicenter analysis of glucocerebrosidase mutations in Parkinson's disease. The New England Journal of Medicine *361*: 1651–61.

Sillence, D.J., Puri, V., Marks, D.L., Butters, T.D., Dwek, R. a, Pagano, R.E., et al. (2002). Glucosylceramide modulates membrane traffic along the endocytic pathway. Journal of Lipid Research *43*: 1837–1845.

Simon, H.H., Saueressig, H., Wurst, W., Goulding, M.D., and O'Leary, D.D.M. (2001). Fate of Midbrain Dopaminergic Neurons Controlled by the Engrailed Genes. J. Neurosci. *21*: 3126–3134.

Simón-Sánchez, J., Schulte, C., Bras, J.M., Sharma, M., Gibbs, J.R., Berg, D., et al. (2009). Genome-wide association study reveals genetic risk underlying Parkinson's disease. Nature Genetics *41*: 1308–12.

Smidt, M.P., Schaick, H.S. van, Lanctôt, C., Tremblay, J.J., Cox, J.J., Kleij, A.A. van der, et al. (1997). A homeodomain gene Ptx3 has highly restricted brain expression in mesencephalic dopaminergic neurons. Proceedings of the National Academy of Sciences of the United States of America *94*: 13305–10.

Soldner, F., Hockemeyer, D., Beard, C., and Gao, Q. (2009). Parkinson's disease patient-derived induced pluripotent stem cells free of viral reprogramming factors. Cell *136*: 964–977.

Soldner, F., Laganière, J., Cheng, A.W., Hockemeyer, D., Gao, Q., Alagappan, R., et al. (2011). Generation of Isogenic Pluripotent Stem Cells Differing Exclusively at Two Early Onset Parkinson Point Mutations. Cell *146*: 318–331.

Song, W., Wang, F., Savini, M., Ake, A., Ronza, A. di, Sardiello, M., et al. (2013). TFEB regulates lysosomal proteostasis. Human Molecular Genetics *22*: 1994–2009.

Soper, J.H., Kehm, V., Burd, C.G., Bankaitis, V.A., and Lee, V.M.-Y. (2011). Aggregation of α-synuclein in S. cerevisiae is associated with defects in endosomal trafficking and phospholipid biosynthesis. Journal of Molecular Neuroscience : MN *43*: 391–405.

Spillantini, M.G., Schmidt, M.L., Lee, V.M., Trojanowski, J.Q., Jakes, R., and Goedert, M. (1997). Alpha-synuclein in Lewy bodies. Nature *388*: 839–40.

Spitz, M., Rozenberg, R., Pereira, L.D.V., and Reis Barbosa, E. (2008). Association between Parkinson's disease and glucocerebrosidase mutations in Brazil. Parkinsonism & Related Disorders *14*: 58–62.

Stadtfeld, M., Nagaya, M., Utikal, J., Weir, G., and Hochedlinger, K. (2008). Induced pluripotent stem cells generated without viral integration. Science (New York, N.Y.) *322*: 945–949.

Strauss, K.M., Martins, L.M., Plun-Favreau, H., Marx, F.P., Kautzmann, S., Berg, D., et al. (2005). Loss of function mutations in the gene encoding Omi/HtrA2 in Parkinson's disease. Human Molecular Genetics *14*: 2099–111.

Studer, L. (2012). Derivation of dopaminergic neurons from pluripotent stem cells. Progress in Brain Research *200*: 243–63.

Su, Y.-C., and Qi, X. (2013). Inhibition of excessive mitochondrial fission reduced aberrant autophagy and neuronal damage caused by LRRK2 G2019S mutation. Human Molecular Genetics *22*: 4545–61.

Sugita, M., Izuno, T., Tatemichi, M., and Otahara, Y. (2001). Meta-analysis for epidemiologic studies on the relationship between smoking and Parkinson's disease. Journal of Epidemiology / Japan Epidemiological Association *11*: 87–94.

Sun, M., Latourelle, J.C., Wooten, G.F., Lew, M.F., Klein, C., Shill, H.A., et al. (2006). Influence of heterozygosity for parkin mutation on onset age in familial Parkinson disease: the GenePD study. Archives of Neurology *63*: 826–32.

Sun, Q.-Y., Guo, J.-F., Wang, L., Yu, R.-H., Zuo, X., Yao, L.-Y., et al. (2010). Glucocerebrosidase gene L444P mutation is a risk factor for Parkinson's disease in Chinese population. Movement Disorders : Official Journal of the Movement Disorder Society *25*: 1005–1011.

Sun, Y., Ran, H., Liou, B., Quinn, B., and Zamzow, M. (2011). Isofagomine in vivo effects in a neuronopathic Gaucher disease mouse. PloS One *6*: e19037.

Surguchov, A. (2013). Parkinson's disease: Is there a light at the end of a tunnel? Advances in Parkinson's Disease *02*: 116–117.

Swan, M., and Saunders-Pullman, R. (2013). The association between ß-glucocerebrosidase mutations and parkinsonism. Current Neurology and Neuroscience Reports *13*: 368.

Takahashi, K., Tanabe, K., Ohnuki, M., Narita, M., Ichisaka, T., Tomoda, K., et al. (2007). Induction of Pluripotent Stem Cells from Adult Human Fibroblasts by Defined Factors. Cell *131*: 861–872.

Takahashi, K., and Yamanaka, S. (2006). Induction of pluripotent stem cells from mouse embryonic and adult fibroblast cultures by defined factors. Cell *126*: 663–76.

Tan, E.-K., Tong, J., Fook-Chong, S., Yih, Y., Wong, M.-C., Pavanni, R., et al. (2007). Glucocerebrosidase mutations and risk of Parkinson disease in Chinese patients. Archives of Neurology *64*: 1056–8.

Tanner, C.M., Goldman, S.M., Aston, D.A., Ottman, R., Ellenberg, J., Mayeux, R., et al. (2002). Smoking and Parkinson's disease in twins. Neurology *58*: 581–588.

Tayebi, N., Callahan, M., Madike, V., Stubblefield, B.K., Orvisky, E., Krasnewich, D., et al. (2001). Gaucher disease and parkinsonism: a phenotypic and genotypic characterization. Molecular Genetics and Metabolism *73*: 313–21.

Tayebi, N., Stubblefield, B.K., Park, J.K., Orvisky, E., Walker, J.M., LaMarca, M.E., et al. (2003a). Reciprocal and nonreciprocal recombination at the glucocerebrosidase gene region:

implications for complexity in Gaucher disease. American Journal of Human Genetics *72*: 519–34.

Tayebi, N., Walker, J., Stubblefield, B., Orvisky, E., LaMarca, M.E., Wong, K., et al. (2003b). Gaucher disease with parkinsonian manifestations: does glucocerebrosidase deficiency contribute to a vulnerability to parkinsonism? Molecular Genetics and Metabolism *79*: 104–9.

Thatava, T., Kudva, Y.C., Edukulla, R., Squillace, K., Lamo, J.G. De, Khan, Y.K., et al. (2013). Intrapatient variations in type 1 diabetes-specific iPS cell differentiation into insulin-producing cells. Molecular Therapy : the Journal of the American Society of Gene Therapy *21*: 228–39.

Theka, I., Caiazzo, M., Dvoretskova, E., Leo, D., Ungaro, F., Curreli, S., et al. (2013). Rapid generation of functional dopaminergic neurons from human induced pluripotent stem cells through a single-step procedure using cell lineage transcription factors. Stem Cells Translational Medicine *2*: 473–9.

Thomas, K.J., McCoy, M.K., Blackinton, J., Beilina, A., Brug, M. van der, Sandebring, A., et al. (2011). DJ-1 acts in parallel to the PINK1/parkin pathway to control mitochondrial function and autophagy. Human Molecular Genetics *20*: 40–50.

Tiscornia, G., Vivas, E.L., Matalonga, L., Berniakovich, I., Barragán Monasterio, M., Eguizábal, C., et al. (2013). Neuronopathic Gaucher's disease: induced pluripotent stem cells for disease modelling and testing chaperone activity of small compounds. Human Molecular Genetics *22*: 633–45.

Tofaris, G.K. (2012). Lysosome-dependent pathways as a unifying theme in Parkinson's disease. Movement Disorders : Official Journal of the Movement Disorder Society *27*: 1364–9.

Toft, M., Pielsticker, L., Ross, O. a, Aasly, J.O., and Farrer, M.J. (2006). Glucocerebrosidase gene mutations and Parkinson disease in the Norwegian population. Neurology *66*: 415–417.

Tong, Y., Yamaguchi, H., Giaime, E., Boyle, S., Kopan, R., Kelleher, R.J., et al. (2010). Loss of leucine-rich repeat kinase 2 causes impairment of protein degradation pathways, accumulation of alpha-synuclein, and apoptotic cell death in aged mice. Proceedings of the National Academy of Sciences of the United States of America *107*: 9879–9884.

Tresse, E., Krainc, D., Taylor, J.P., Mazzulli, J.R., and Usenovic, M. (2012). Deficiency of ATP13A2 Leads to Lysosomal Dysfunction, -Synuclein Accumulation, and Neurotoxicity. Journal of Neuroscience *32*: 4240–4246.

Trinh, J., and Farrer, M. (2013). Advances in the genetics of Parkinson disease. Nature Reviews. Neurology *9*: 445–54.

Tsuang, D., Leverenz, J., and Lopez, O. (2012). GBA mutations increase risk for Lewy body disease with and without Alzheimer disease pathology. Neurology *79*: 1944–50.

Tsuji, S., Choudary, P. V, Martin, B.M., Stubblefield, B.K., Mayor, J.A., Barranger, J.A., et al. (1987). A mutation in the human glucocerebrosidase gene in neuronopathic Gaucher's disease. The New England Journal of Medicine *316*: 570–5.

Tsuji, S., Martin, B.M., Barranger, J.A., Stubblefield, B.K., LaMarca, M.E., and Ginns, E.I. (1988). Genetic heterogeneity in type 1 Gaucher disease: multiple genotypes in Ashkenazic and non-Ashkenazic individuals. Proceedings of the National Academy of Sciences of the United States of America *85*: 2349–52.

Ugolino, J., Fang, S., Kubisch, C., and Monteiro, M.J. (2011). Mutant Atp13a2 proteins involved in parkinsonism are degraded by ER-associated degradation and sensitize cells to ER-stress induced cell death. Human Molecular Genetics *20*: 3565–3577.

Uversky, V.N., Li, J., Bower, K., and Fink, A.L. (2002). Synergistic effects of pesticides and metals on the fibrillation of a-synuclein: implications for Parkinson's disease. NeuroToxicology *23*: 527–536.

Uversky, V.N., Li, J., and Fink, A.L. (2001a). Metal-triggered structural transformations, aggregation, and fibrillation of human alpha-synuclein. A possible molecular NK between Parkinson's disease and heavy metal exposure. The Journal of Biological Chemistry *276*: 44284–44296.

Uversky, V.N., Li, J., and Fink, A.L. (2001b). Pesticides directly accelerate the rate of α-synuclein fibril formation: A possible factor in Parkinson's disease. FEBS Letters *500*: 105–108.

Valente, E.M., Abou-Sleiman, P.M., Caputo, V., Muqit, M.M.K., Harvey, K., Gispert, S., et al. (2004). Hereditary early-onset Parkinson's disease caused by mutations in PINK1. Science (New York, N.Y.) *304*: 1158–60.

Velayati, A., DePaolo, J., Gupta, N., Choi, J.H., Moaven, N., Westbroek, W., et al. (2011). A mutation in SCARB2 is a modifier in Gaucher disease. Human Mutation *32*: 1232–8.

Vierbuchen, T., Ostermeier, A., Pang, Z.P., Kokubu, Y., Südhof, T.C., and Wernig, M. (2010). Direct conversion of fibroblasts to functional neurons by defined factors. Nature *463*: 1035–1041.

Vilariño-Güell, C., Rajput, A., Milnerwood, A.J., Shah, B., Szu-Tu, C., Trinh, J., et al. (2014). DNAJC13 mutations in Parkinson disease. Human Molecular Genetics *23*: 1794–801.

Vilariño-Güell, C., Wider, C., Ross, O.A., Dachsel, J.C., Kachergus, J.M., Lincoln, S.J., et al. (2011). VPS35 mutations in Parkinson disease. American Journal of Human Genetics *89*: 162–7.

Vitner, E.B., Dekel, H., Zigdon, H., Shachar, T., Farfel-Becker, T., Eilam, R., et al. (2010). Altered expression and distribution of cathepsins in neuronopathic forms of Gaucher disease and in other sphingolipidoses. Human Molecular Genetics *19*: 3583–90.

Vives-Bauza, C., Zhou, C., Huang, Y., Cui, M., Vries, R.L.A. de, Kim, J., et al. (2010). PINK1-dependent recruitment of Parkin to mitochondria in mitophagy. Proceedings of the National Academy of Sciences of the United States of America *107*: 378–83.

Wang, F., and Segatori, L. (2013). Remodeling the Proteostasis Network to Rescue Glucocerebrosidase Variants by Inhibiting ER-Associated Degradation and Enhancing ER Folding. PloS One *8*: e61418.

Wang, F., Song, W., Brancati, G., and Segatori, L. (2011). Inhibition of endoplasmic reticulum-associated degradation rescues native folding in loss of function protein misfolding diseases. Journal of Biological Chemistry *286*: 43454–43464.

Wang, Y., Liu, L., Xiong, J., Zhang, X., Chen, Z., Yu, L., et al. (2012). Glucocerebrosidase L444P mutation confers genetic risk for Parkinson's disease in central China. Behavioral and Brain Functions : BBF *8*: 57.

Watanabe, K., Ueno, M., Kamiya, D., Nishiyama, A., Matsumura, M., Wataya, T., et al. (2007). A ROCK inhibitor permits survival of dissociated human embryonic stem cells. Nature Biotechnology *25*: 681–6.

Webb, J.L., Ravikumar, B., Atkins, J., Skepper, J.N., and Rubinsztein, D.C. (2003). Alpha-Synuclein is degraded by both autophagy and the proteasome. The Journal of Biological Chemistry *278*: 25009–13.

Wei, H., Kim, S.-J., Zhang, Z., Tsai, P.-C., Wisniewski, K.E., and Mukherjee, A.B. (2008). ER and oxidative stresses are common mediators of apoptosis in both neurodegenerative and non-neurodegenerative lysosomal storage disorders and are alleviated by chemical chaperones. Human Molecular Genetics *17*: 469–77.

Wei, R.R., Hughes, H., Boucher, S., Bird, J.J., Guziewicz, N., Patten, S.M. Van, et al. (2011). X-ray and biochemical analysis of N370S mutant human acid β-glucosidase. The Journal of Biological Chemistry *286*: 299–308.

West, A., Periquet, M., Lincoln, S., Lücking, C.B., Nicholl, D., Bonifati, V., et al. (2002). Complex relationship between Parkin mutations and Parkinson disease. American Journal of Medical Genetics *114*: 584–91.

Westbroek, W., Gustafson, A.M., and Sidransky, E. (2011). Exploring the link between glucocerebrosidase mutations and parkinsonism. Trends in Molecular Medicine *17*: 485–493.

Wilgenburg, B. van, Browne, C., Vowles, J., and Cowley, S.A. (2013). Efficient, long term production of monocyte-derived macrophages from human pluripotent stem cells under partly-defined and fully-defined conditions. PloS One *8*: e71098.

Wilmut, I., Schnieke, A.E., McWhir, J., Kind, A.J., and Campbell, K.H. (1997). Viable offspring derived from fetal and adult mammalian cells. Nature *385*: 810–3.

Winder-Rhodes, S., Evans, J., and Ban, M. (2013). Glucocerebrosidase mutations influence the natural history of Parkinson's disease in a community-based incident cohort. Brain *136*: 392–9.

Winfield, S.L., Tayebi, N., Martin, B.M., Ginns, E.I., and Sidransky, E. (1997). Identification of three additional genes contiguous to the glucocerebrosidase locus on chromosome 1q21: implications for Gaucher disease. Genome Research *7*: 1020–6.

Winslow, A.R., Chen, C.-W., Corrochano, S., Acevedo-Arozena, A., Gordon, D.E., Peden, A. a, et al. (2010). α-Synuclein impairs macroautophagy: implications for Parkinson's disease. The Journal of Cell Biology *190*: 1023–37.

Wirdefeldt, K., Adami, H.-O., Cole, P., Trichopoulos, D., and Mandel, J. (2011). Epidemiology and etiology of Parkinson's disease: a review of the evidence. European Journal of Epidemiology *26 Suppl 1*: S1–58.

Wu, Y.-R., Chen, C.-M., Chao, C.-Y., Ro, L.-S., Lyu, R.-K., Chang, K.-H., et al. (2007). Glucocerebrosidase gene mutation is a risk factor for early onset of Parkinson disease among Taiwanese. Journal of Neurology, Neurosurgery & Psychiatry *78*: 977–979.

Xi, J., Liu, Y., Liu, H., Chen, H., Emborg, M., and Zhang, S. (2012). Specification of midbrain dopamine neurons from primate pluripotent stem cells. Stem Cells *30*: 1655–1663.

Xilouri, M., Vogiatzi, T., Vekrellis, K., Park, D., and Stefanis, L. (2009). Abberant alpha-synuclein confers toxicity to neurons in part through inhibition of chaperone-mediated autophagy. PloS One *4*: e5515.

Xu, Y.-H., Quinn, B., Witte, D., and Grabowski, G. a. (2003). Viable Mouse Models of Acid β-Glucosidase Deficiency. The American Journal of Pathology *163*: 2093–2101.

Xu, Y.H., Sun, Y., Ran, H., Quinn, B., Witte, D., and Grabowski, G.A. (2011). Accumulation and distribution of α-synuclein and ubiquitin in the CNS of Gaucher disease mouse models. Molecular Genetics and Metabolism *102*: 436–47.

Yagi, T., Ito, D., Okada, Y., Akamatsu, W., Nihei, Y., Yoshizaki, T., et al. (2011). Modeling familial Alzheimer's disease with induced pluripotent stem cells. Human Molecular Genetics *20*: 4530–9.

Yakubov, E., Rechavi, G., Rozenblatt, S., and Givol, D. (2010). Reprogramming of human fibroblasts to pluripotent stem cells using mRNA of four transcription factors. Biochemical and Biophysical Research Communications *394*: 189–193.

Yap, T.L., Gruschus, J.M., Velayati, A., Westbroek, W., Goldin, E., Moaven, N., et al. (2011). Alpha-synuclein interacts with Glucocerebrosidase providing a molecular link between Parkinson and Gaucher diseases. The Journal of Biological Chemistry *286*: 28080–8.

Yelamanchili, S. V, Chaudhuri, A.D., Flynn, C.T., and Fox, H.S. (2011). Upregulation of cathepsin D in the caudate nucleus of primates with experimental parkinsonism. Molecular Neurodegeneration *6*: 52.

Yorimitsu, T., Nair, U., Yang, Z., and Klionsky, D.J. (2006). Endoplasmic reticulum stress triggers autophagy. The Journal of Biological Chemistry *281*: 30299–304.

Yu, J., Hu, K., Smuga-Otto, K., Tian, S., Stewart, R., Slukvin, I.I., et al. (2009a). Human induced pluripotent stem cells free of vector and transgene sequences. Science (New York, N.Y.) *324*: 797–801.

Yu, J., Vodyanik, M., Smuga-Otto, K., Antosiewicz-Bourget, J., Frane, J.L., Tian, S., et al. (2007). Induced pluripotent stem cell lines derived from human somatic cells. Science *318*: 1917 – 1920.

Yu, W.H., Dorado, B., Figueroa, H.Y., Wang, L., Planel, E., Cookson, M.R., et al. (2009b). Metabolic activity determines efficacy of macroautophagic clearance of pathological oligomeric alpha-synuclein. The American Journal of Pathology *175*: 736–47.

Yu, Z., Liu, M., Fu, P., Xie, M., Wang, W., and Luo, X. (2012). ROCK inhibition with Y27632 promotes the proliferation and cell cycle progression of cultured astrocyte from spinal cord. Neurochemistry International *61*: 1114–20.

Yusa, K., Rad, R., Takeda, J., and Bradley, A. (2009). Generation of transgene-free induced pluripotent mouse stem cells by the piggyBac transposon. Nature Methods *6*: 363–369.

Zabetian, C.P., Hutter, C.M., Factor, S.A., Nutt, J.G., Higgins, D.S., Griffith, A., et al. (2007). Association analysis of MAPT H1 haplotype and subhaplotypes in Parkinson's disease. Annals of Neurology *62*: 137–44.

Zachos, C., Blanz, J., Saftig, P., and Schwake, M. (2012). A critical histidine residue within LIMP-2 mediates pH sensitive binding to its ligand β-glucocerebrosidase. Traffic (Copenhagen, Denmark) *13*: 1113–23.

Zampieri, S., Bembi, B., Rosso, N., Filocamo, M., and Dardis, A. (2012). Treatment of Human Fibroblasts Carrying NPC1 Missense Mutations with MG132 Leads to an Improvement of Intracellular Cholesterol Trafficking. JIMD Reports *2*: 59–69.

Zarranz, J.J., Alegre, J., Gómez-Esteban, J.C., Lezcano, E., Ros, R., Ampuero, I., et al. (2004). The new mutation, E46K, of alpha-synuclein causes Parkinson and Lewy body dementia. Annals of Neurology *55*: 164–73.

Zetterström, R.H. (1997). Dopamine Neuron Agenesis in Nurr1-Deficient Mice. Science *276*: 248–250.

Zhang, X., Bao, Q.-Q., Zhuang, X.-S., Gan, S.-R., Zhao, D., Liu, Y., et al. (2012). Association of Common Variants in the Glucocerebrosidase Gene with High Susceptibility to Parkinson's Disease among Chinese. The Chinese Journal of Physiology *55*: 398–404.

Zhu, J.-H., Guo, F., Shelburne, J., Watkins, S., and Chu, C.T. (2003). Localization of phosphorylated ERK/MAP kinases to mitochondria and autophagosomes in Lewy body diseases. Brain Pathology (Zurich, Switzerland) *13*: 473–81.

Zhu, J.-H., Horbinski, C., Guo, F., Watkins, S., Uchiyama, Y., and Chu, C.T. (2007). Regulation of autophagy by extracellular signal-regulated protein kinases during 1-methyl-4-phenylpyridinium-induced cell death. The American Journal of Pathology *170*: 75–86.

Ziegler, S.G., Eblan, M.J., Gutti, U., Hruska, K.S., Stubblefield, B.K., Goker-Alpan, O., et al. (2007). Glucocerebrosidase mutations in Chinese subjects from Taiwan with sporadic Parkinson disease. Molecular Genetics and Metabolism *91*: 195–200.

Zimprich, A., Benet-Pagès, A., Struhal, W., Graf, E., Eck, S.H., Offman, M.N., et al. (2011). A mutation in VPS35, encoding a subunit of the retromer complex, causes late-onset Parkinson disease. American Journal of Human Genetics *89*: 168–175.